



Review of Devonian-Carboniferous Boundary sections in the Rhenish Slate Mountains (Germany)

R. Thomas Becker¹ · Sven Hartenfels² · Sandra I. Kaiser³

Received: 1 April 2020 / Revised: 29 September 2020 / Accepted: 1 October 2020 / Published online: 25 March 2021
© The Author(s) 2020

Abstract

Thirty Devonian-Carboniferous Boundary sections of the Rhenish Slate Mountains and adjacent subsurface areas are reviewed with respect to litho-, event, conodont, ammonoid, sequence, and chemostratigraphy. In the interval from the base of the uppermost Famennian (Wocklum Beds, Wocklumian) to the base of the middle Tournaisian (base Lower Alum Shale), 11 conodont and 16 ammonoid (sub)zones are distinguished. The terminology of the Hangenberg Crisis Interval is refined, with an overall regressive Crisis Prelude below the main Hangenberg Extinction, which defines the base of the transgressive Lower Crisis Interval (Hangenberg Black Shale). The glacigenic and regressive Middle Crisis Interval (Hangenberg Shale/Sandstone) is followed by the overall transgressive Upper Crisis Interval that can be subdivided into three parts (I to III) with the help of conodont stratigraphy (upper *costatus-kockeli* Interregnum = upper ckI, *Protognathodus kockeli* Zone, and lower part of *Siphonodella* (*Eosiphonodella*) *sulcata* s.l./*Pr. kuehni* Zone). *Protognathodus kockeli* includes currently a wide range of forms, which variabilities and precise ranges need to be established before a precise GSSP level should be selected. Returning to its original definition, the former Upper *duplicata* Zone is re-named as *Siphonodella* (*S.*) *mehli* Zone. It replaces the *S. (S.) jii* Zone, which is hampered by taxonomic complications. The *S. (S.) quadruplicata* Zone of Ji (1985) is hardly supported by Rhenish data. The entry of typical *S. (S.) lobata* (M1) characterises an upper subdivision (subzone) of the *S. (S.) sandbergi* Zone; the new *S. (S.) lobata* M2 enters much earlier within the *S. (S.) mehli* Zone. The ammonoid-defined base of the Wocklum-Stufe (Upper Devonian = UD VI) begins with the *Linguaclymenia similis* Zone (UD VI-A₁). The oldest *S. (Eosiphonodella)* enter within the *Muessenia bisulcata* Zone (UD VI-A₂). The traditional *Parawocklumeria paradoxa* Zone of Schindewolf (1937) is divided into successive *P. paprothae* (VI-C₁), *P. paradoxa* (VI-C₂), and *Mayneoceras nucleus* (VI-C₃) Subzones. In the lower Tournaisian (Lower Carboniferous = LC I), the *Gattendorfia subinvoluta* Zone is subdivided into *G. subinvoluta* (LC I-A₂) and “*Eocanites*” *nodosus* (LC I-A₃) Subzones. The *Paprothites dorsoplanus* Zone (LC I-B) can be divided into *Pap. dorsoplanus* (LC I-B₁) and *Paragattendorfia sphaeroides* (LC I-B₂) Subzones. Potential subdivisions of the *Pseudarrietites westfalicus* (LC I-C) and *Parag. patens* Zones (LC I-D) are less distinctive. The unfossiliferous or argillaceous upper part of the Hangenberg Limestone and the overlying Lower Alum Shale Event Interval remain regionally unzoned for ammonoids.

Keywords Rhenish Massif · Devonian-Carboniferous Boundary · Lithostratigraphy · Biostratigraphy · Hangenberg Crisis · Carbon isotopes

This article is a contribution to the special issue “Global review of the Devonian-Carboniferous Boundary”

✉ R. Thomas Becker
rbecker@uni-muenster.de

Sven Hartenfels
shartenf@uni-koeln.de

Sandra I. Kaiser
dr.sandra.kaiser@gmail.com; sandra.kaiser@smns-bw.de

¹ Institut für Geologie und Paläontologie, Westfälische Wilhelms-Universität, Corrensstr. 24, 48149 Münster, Germany

² Institut für Geologie und Mineralogie, Universität zu Köln, Zülpicher Straße 49a, 50674 Cologne, Germany

³ Staatliches Museum für Naturkunde Stuttgart, Rosenstein 1, 70191 Stuttgart, Germany

Introduction

The Rhenish Slate Mountains, especially the northern and eastern Sauerland in the east of the river Rhine, are the most important of the classical regions for the study of the Devonian-Carboniferous Boundary (DCB) and of the global mass extinction interval that is now known as Hangenberg Crisis (e.g. Kaiser et al. 2015). Following a proposal by Paeckelmann and Schindewolf (published in 1937), the DCB type section was defined during the Second Heerlen Congress in 1935 in a railway cut near Oberrödinghausen. This was the first international chronostratigraphic boundary that was established at all. Unfortunately, it had to be discarded when a hiatus was discovered right at the chosen boundary level (Alberti et al. 1974). During the following search for a new stratotype, many old and new lateral sections were investigated in detail. Results were published in a series of monographs, review papers, and field guidebooks. Important summaries are, for example, Stoppel (1977), Paproth and Streel (1982, 1984), Paproth (1986), Paproth et al. (1986b), Clausen et al. (1989a), Streel et al. 1993, Becker et al. (1993), Korn et al. (1994a), Korn (2002), Hartenfels et al. (2016), and Becker et al. (2016b). There is a flood of individual papers (e.g. many contributions by D. Korn, F.W. Luppold, and co-authors), which are fully referenced in the individual section descriptions. These form the fundament of our review, which includes a smaller amount of unpublished information. Since research is ongoing, this paper will be completed soon by forthcoming publications. For example, a new study will provide details of the currently best Rhenish DCB section at the Borkewehr near Wocklum (northern Sauerland). A palaeogeographical overview was given by Paproth et al. (1986a), with recent updates by Koltonik et al. (2018).

For details concerning the global, first order Hangenberg Crisis or mass extinction, the reader is referred to the review by Kaiser et al. (2015). Becker et al. (2016a) summarised the DCB bio- and event stratigraphy, with the Rhenish succession as a sort of “standard reference” for global correlations. This approach is elaborated here by the introduction of a new formal subdivision and nomenclature for the distinctive intervals of the Hangenberg Crisis. We supply a summary of Rhenish DCB conodont and ammonoid zones, with new subzones, and the evidence they are based on. Due to the considerable number of Rhenish DCB sections and the wealth of literature, our review will exploit the extensive published evidence by quoting for each section all relevant papers, and by focusing on the staged entries (FADs, local FODs) and disappearances (LADs/local LODs) of stratigraphically relevant taxa and rare/unusual taxon occurrences. For detailed data on sedimentology and the complete faunal records, the reader should survey the quoted papers. In the section discussions, we emphasise aspects that are of especial importance for the current

DCB revision and selection of a future GSSP level and section. Since significant parts of the reviewed information have previously been published in German, our paper aims to recycle the incredibly rich Rhenish DCB record for a wide international audience.

Abbreviations and repository

DCB = Devonian-Carboniferous Boundary, FAD/FOD = first appearance (global) and occurrence (local) datum, LAD/LOD = last appearance (global) and occurrence (local) datum, LC = Lower Carboniferous, Tn = Tournaisian, UD = Upper Devonian; for the ammonoid zonal key see Becker (1996) and Fig. 1.

Lithostratigraphic units: HBS = Hangenberg Black Shale, HS = Hangenberg Shale, HSS = Hangenberg Sandstone, LAS = Lower Alum Shale (= Kahlenberg Formation).

Sequence stratigraphy: LST = Lowstand System Tract, TST = Transgressive System Tract, HST = Highstand System Tract, FSST = Falling Stage System Tract.

Conodont genera/subgenera: *Bi.* = *Bispaphodus*, *Br.* = *Branmehla*, *Eo.* = *Eosiphonodella*, *Neo.* = *Neopolygnathus*, *Pa.* = *Palmatolepis*, *Po.* = *Polygnathus*, *Pr.* = *Protognathodus*, *Ps.* = *Pseudopolygnathus*, *S.* = *Siphonodella*, *Sc.* = *Scaliognathus*.

Ammonoid genera/subgenera: *Ac.* = *Acutimitoceras*, *B.* = *Balvia*, *C.* = *Cymaclymenia*, *Cost.* = *Costimitoceras*, *Cyrt.* = *Cyrtoclymenia*, *Eff.* = *Effenbergia*, *Eoc.* = *Eocanites*, *Epi.* = *Epiwocklumeria*, *F.* = *Finiclymenia*, *G.* = *Gattendorfia*, *Gl.* = *Globimitoceras*, *H.* = *Hasselbachia*, *K.* = *Kalloclymenia*, *Kamp.* = *Kamptoclymenia*, *Kaz.* = *Kazakhstania*, *Ken.* = *Kenseyoceras*, *Kos.* = *Kosmoclymenia*, *L.* = *Linguaclymenia*, *Liss.* = *Lissoclymenia*, *M.* = *Muessenbiaergia*, *May.* = *Mayneoceras*, *Mim.* = *Mimimitoceras*, *N.* = *Nicimitoceras*, *P.* = *Parawocklumeria*, *Pap.* = *Paprothites*, *Parag.* = *Paragattendorfia*, *Post.* = *Postclymenia*, *Pseud.* = *Pseudarietites*, *R.* = *Rectimitoceras*, *Sph.* = *Sphenoclymenia*, *St.* = *Stockumites*, *Str.* = *Streeliceras*, *Tria.* = *Triacylmenia*, *V.* = *Voehringerites*, *W.* = *Wocklumeria*, *Wey.* = *Weyerella*.

SMNS = Staatliches Museum für Naturkunde Stuttgart (figured conodonts). All ammonoids, collection numbers B6C.54.1 to B6C.54.11, are deposited in the Geomuseum of the WWU at Münster.

Conodont biostratigraphy (Fig. 1)

The DCB conodont stratigraphy has been reviewed by Becker et al. (2016a), with subsequent nomenclatural changes by Spalletta et al. (2017) and with a discussion in Söte et al. (2017). The pelagic facies zonation of the Sauerland cannot be applied to the shallow-water

	chrono.	conodonts	key	ammonoids	lithostratigraphy	events / crisis
CARBONIFEROUS	lower Tournaisian Balvian, LC I	<i>S. (S.) crenulata</i>	II-A	[no record]	Lower Alum Shale	Lower Alum Shale Event
		<i>S. (S.) lobata M1</i>	I-E			
		(quad.)	I-D	<i>[Ps. serratus] Paragattendorfia patens</i>		
		<i>S. (S.) sandbergi</i>	I-C	<i>Pseudarietites westfalicus</i>	Hangenberg Limestone	post-Crisis Interval
		[<i>S. (S.) cf. wilbertii</i>] <i>S. (S.) mehlri</i> [<i>S. (S.) carinthiaca</i>]	I-B2	<i>Paragattendorfia sphaerooides</i>		
		<i>S. (S.) duplicata</i>	I-B1	<i>Paprothites dorsoplanus</i>		
		<i>S. (S.) bransoni</i>	I-A3	[<i>Voehringerites peracutus</i>] "Eocanites" nodosus		
		<i>S. (Eo.) sulcata</i> <i>Pr. kuehni</i>	I-A2	<i>Gattendorfia subinvoluta</i>		
		<i>Pr. kockeli</i>	I-A1	[<i>Ac. (St.) stockumense</i>] [<i>Ac. (Streeliceras) carinatum</i>] [<i>Post. nigra</i>]	upper Stockum Limestone lower basal	III
		<i>Bi. costatus -</i> <i>Pr. kockeli</i> Interregnum (ckl)	VI-F	<i>Ac. (Stockumites) prorsum</i> <i>Ac. (St.) cf. procedens</i>		II Upper
			VI-E	<i>Postclymenia evoluta</i>	Hangenberg Shale	I
			VI-D2	<i>Epiwocklumeria applanata</i>		II Middle
			VI-D1	<i>Wocklumeria denckmanni</i>		I
			VI-C3	<i>Mayneoceras nucleus</i>	Hangenberg Blackshale	Hangenberg Crisis
			VI-C2	<i>Parawocklumeria paradoxa</i>		Lower EVENT
			VI-C1	<i>Parawocklumeria paprothae</i> [<i>Kamptoclymenia endogona</i>]		†
			VI-B	<i>Effenbergia lens</i>		II
			VI-A2	[<i>M. parundulata</i>] <i>Muessenbiaergia bisulcata</i>		Prelude
			VI-A1	[<i>Kalloclymenia subarmata</i>] [<i>Sphenoclymenia erinacea</i>] [<i>Muessenbiaergia sublaevis</i>] <i>Linguaclymenia similis</i>		
						pre-Crisis Interval
DEVONIAN	uppermost Famennian Wocklumerian, UD VI				Wocklumeria Limestone	

Fig. 1 Correlation of chrono-, litho- bio-, and event stratigraphy around the Devonian-Carboniferous Boundary, showing both zonal index taxa (in bold) and important auxiliary marker species [in brackets]. The ammonoid zonal key follows, with further subdivision, the scheme of Becker

(1996); m.T. = middle Tournaisian, (quad.) = approximate level of former *Siphonodella* (*S.*) *quadruplicata* Zone, SLBS = Stockum Level Black Shales, sdst. = sandstone. s.l. = sensu lato (in a wide taxonomic sense) For (sub)generic abbreviations see main text

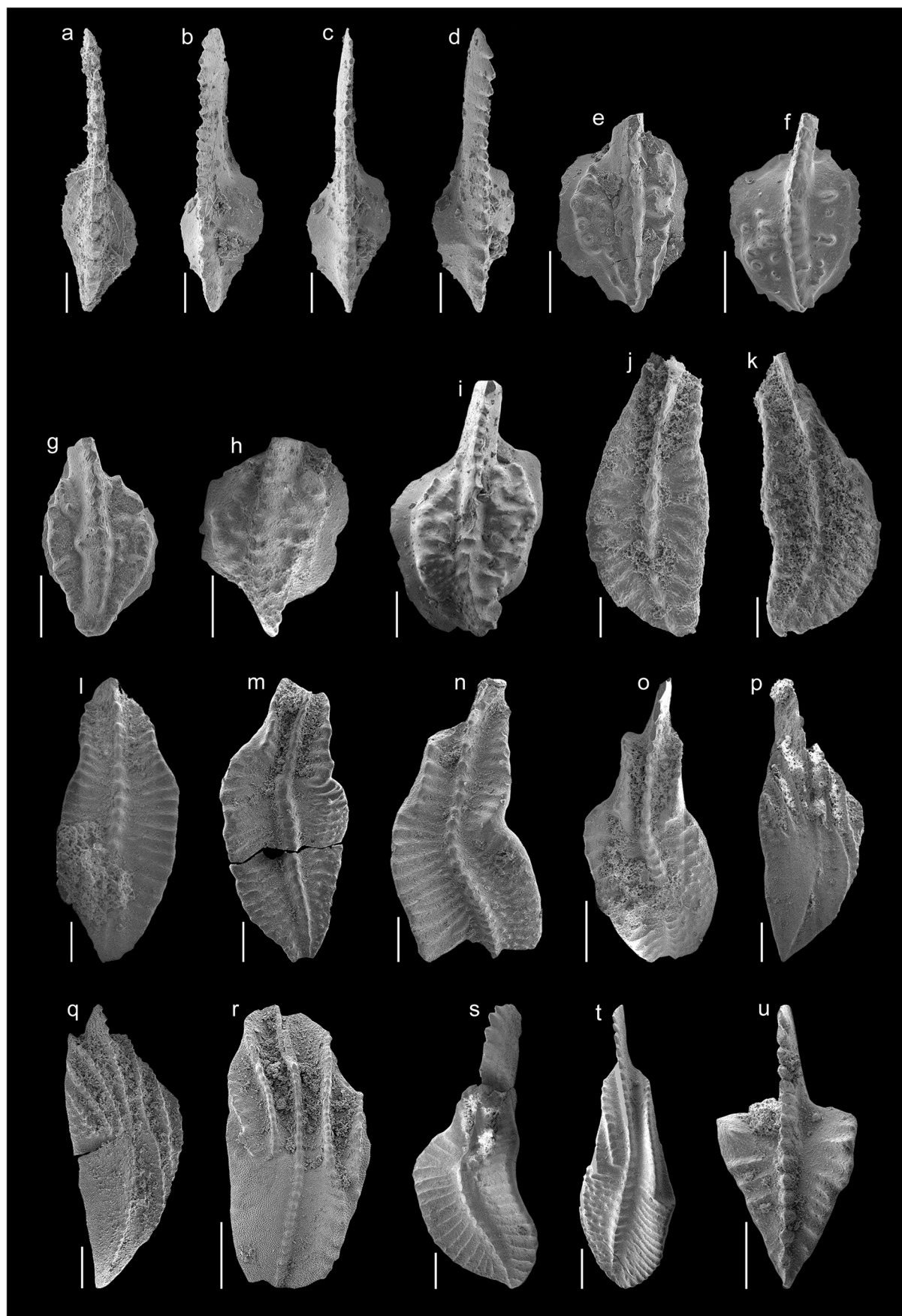


Fig. 2 Some lower Tournaisian conodonts from the Rhenish Massif (northern Sauerland); all kept in the Staatliches Museum für Naturkunde Stuttgart (SMNS); scale bars = 0.2 mm. **a** *Protognathodus cf. meischneri*, specimen with narrow platform, Hangenberg, Bed 8, ?*Siphonodella (Eosiphonodella) bransoni* Zone, SMNS 70394/1; **b–d** *Pr. collinsoni*, Hangenberg, Bed 8, SMNS 70394/2; **e–g** *Protognathodus* sp., three specimens with atypical ornament transitional between *Pr. kockeli* and *Pr. kuehni*, Oberrödinghausen Railway Cut (ORC), Bed 4b, lower part of *S. (S.) duplicata* Zone, SMNS 70394/3–5; **h** *Pr. kockeli*, transitional towards *Pr. kuehni*, ORC, Bed 6b, *S. (Eo.) sulcata* s.l./*Pr. kuehni* Zone, SMNS 70393/1–9 (Kaiser et al. 2017, fig. 10.9); **i** *Pr. kuehni*, Oese, Bed 4b, basal *S. (Eo.) sulcata* s.l./*Pr. kuehni* Zone, SMNS 70393/1–14 (Kaiser et al. 2017, fig. 10.14); **j, k** *S. (Eo.) sulcata* s.l., anterior platform with a slight trend towards *S. (Eo.) bransoni*, Drever, Bed 12, *S. (Eo.) sulcata* s.l./*Pr. kuehni* Zone, SMNS 70394/6–7; **l** *S. (Eo.) bransoni*, ORC, Bed 5b, *S. (Eo.) bransoni* Zone, SMNS 70393/1–2 (Kaiser et al. 2017, fig. 10.2); **m, n** *S. (S.) duplicata*, ORC, Beds 4b (SMNS 70394/8) and 4a (SMNS 70391/1–3, Kaiser et al. 2017, fig. 10.3), *S. (S.) duplicata* Zone; **o** *S. (S.) carinthiaca*, Oese, Kaiser-Bed 21 = Bed Q = Bed 31, upper part of *S. (S.) mehli* Zone, SMNS 70393/1–11; **p–r** *S. (S.) belkai* M1, ORC Beds 3c2 (SMNS 70393/1–19, Kaiser et al. 2017, fig. 12.2, upper *S. (S.) mehli* Zone), ORC Bed 2b (SMNS 70393/1–8, Kaiser et al. 2017, fig. 12.1), *S. (S.) sandbergi* Zone, and ORC 2a (SMNS 70393/1–21, Kaiser et al. 2017, fig. 12.7, *S. (S.) sandbergi* Zone with *S. (S.) quadruplicata*); **s** *S. (S.) lobata* M2, ORC, Bed 3c2, upper *S. (S.) mehli* Zone, SMNS 70393/1–6 (Kaiser et al. 2017, fig. 10.6); **t** *S. (S.) quadruplicata*, morphotype with short, secondary rostral ridge only on the inner side, ORC, Bed 1b, top *S. (S.) sandbergi* Subzone, SMNS 70393/1–4 (Kaiser et al. 2017, fig. 10.4); **u** *Pseudopolygnathus triangulus* *triangulus*, ORC, Bed 2b, *S. (S.) sandbergi* Subzone, SMNS 70393/1–7 (Kaiser et al. 2017, fig. 10.8).

limestones of the Aachen and Velbert regions, which are, unfortunately, mostly very poor in conodonts. The zone definitions and terminology used here follow, with one exception at the main Hangenberg Extinction, the FADs of name-giving index species. The upper boundaries of zones/subzones are automatically defined by the base of the next higher zone/subzone. Besides the defining index species, there are other marker species, which have their FADs within given zones, but not necessarily precisely at the same level as the index species. For the literature of given reference beds, see the individual section descriptions. Examples of marker conodonts are given in Fig. 2.

Bispatherodus ultimus ultimus Zone (Becker et al. 2016a; Hartenfels and Becker 2016)

Synonyms: Lower part of Middle *costatus* Zone of Ziegler (1962) and Klapper and Ziegler (1979), Upper *expansa* Zone of Ziegler and Sandberg (1984b), lower part of *Bi. ultimus* Zone of Corradini et al. (2016).

Reference sections: Hasselbachtal (Beds -20S to 17S), Oese (Nowak-Beds 180b–186b), Oberrödinghausen (Schindewolf-Beds 23–18), Dasberg (Beds 0a-b), Reigern Quarry (Beds 5–

22, Söte et al. 2017), Müsingenberg (Beds 85–56), Effenberg (Bed 19 and higher), Eulenspiegel (Beds 5–10).

Other marker species: *Palmatolepis gracilis gonioclymeniae*, *Ps. marburgensis trigonicus*, *Br. suprema*.

Discussion: Since *Bi. ultimus* includes three subspecies with different stratigraphic ranges, the generalised *Bi. ultimus* Zone of Corradini et al. (2016) and Spalletta et al. (2017) had to be refined. It is important to note that their *Bi. ultimus* Zone embraced also a much longer time interval, until the base of the *Pr. kockeli* Zone (Becker et al. 2016a; Söte et al. 2017).

In the Rio Boreado section of the Carnic Alps, *Bi. ultimus ultimus*, *Pa. gracilis gonioclymeniae*, and *Ps. marburgensis trigonicus* enter synchronously (Kaiser et al. 2009). In other Carnic Alps sections and in the Rhenish Massif, the situation is much more complex. *Pseudopolygnathus marburgensis trigonicus* seems to enter first (base of Wocklum Limestone at Oberrödinghausen, Schindewolf-Bed 23, Bed 181b of Sacher 2016; Sample 11 of Eickhoff 1973), followed by *Pa. gracilis gonioclymeniae* and *Br. suprema* at the level of “*Sphenoclymenia*” cf. *brevispina* (Oberrödinghausen, Schindewolf-Bed 22, Kürschner et al. 1993; Bed 185b of Sacher 2016), and then by the name-giving zonal species (Müsingenberg, Bed 80, Luppold et al. 1994; Oberrödinghausen, Schindewolf-Bed 20 = Bed 191b of Sacher 2016). It is well possible that more detailed sampling will change this picture. Currently, it is not clear whether the Rio Boreado or Rhenish patterns represent better the FADs of the three marker species.

The oldest Rhenish *Pr. meischneri*, which is the oldest member of *Protognathodus*, occurs at Oberrödinghausen in Bed 20 (Kürschner et al. 1993), slightly below the first *Kalloclymenia*. The taxon is much too rare in the Wocklum Limestone to have biostratigraphical significance. As outlined by Tragelehn (2010), Becker et al. (2013), and Söte et al. (2017), there are early relatives of *Siphonodella*, which represent two different genera. These “siphonodelloids” have *Polygnathus*-type upper platforms, for example as in *Po. inornatus* and *Po. symmetricus*, but non-polygnathid, extended basal cavities. The group requires detailed taxonomic treatment (see Tragelehn 2010; Becker et al. 2013). Both the *Po. inornatus-symmetricus* Group (see Corradini et al. 2016) and the “siphonodelloids” enter above the base of the *Bi. ultimus ultimus* Zone and specific forms may enable a future subdivision.

Siphonodella (Eosiphonodella) praesulcata s.l. Zone (Sandberg et al. 1978)

Synonyms: Lower *praesulcata* and basal Middle *praesulcata* Zones (below main Hangenberg Extinction) of Ziegler and Sandberg (1984a), upper part of extended *Bi. ultimus* Zone, but below the main Hangenberg Extinction, of Corradini et al. (2016).

Reference sections: Hasselbachtal (Beds 18S–114N), Oese (Nowak-Beds 187b–228a), Oberrödinghausen (Schindewolf-

Beds 17–1, Kürschner et al. 1993), Wocklum (Beds -3b to -1b), Reigern Quarry (Beds 24–39, Söte et al. 2017), Müssenberg (Beds 55–4, Luppold et al. 1994), Eulenspiegel (Beds 11–15).

Discussion: Kaiser and Corradini (2011) showed the vague distinction between *S. (Eo.) praesulcata* and *sulcata* and the rather subjective past identifications of both taxa by different authors. The holotype of *S. (Eo.) praesulcata* comes in the Lick Creek type section of Montana from a level above Hangenberg Shale/Sandstone equivalents (= Units 4 and lower 5 of the Middle Sappington Formation, LN Zone, Di Pasquo et al. 2016), therefore from the Upper Crisis Interval (oolites at the top of Unit 5; Rice et al. 2017). As noted by Becker et al. (2016a), the FOD of any *S. (Eosiphonodella)* is currently used within the Wocklum Limestone to recognise the base of the *S. (Eo.) praesulcata* Zone in a wide sense (s.l.). This vagueness, however, does not necessarily require that the zone has to be abandoned, as proposed by Corradini et al. (2016). Kaiser et al. (2009) showed that it can be recognised in all sections that they studied in the Carnic Alps, Graz Palaeozoic, and the Pyrenees. Söte et al. (2017) documented that early *S. (Eosiphonodella)* can easily be found in Wocklum Limestone successions that are not very rich in conodonts (Reigern Quarry, Hachen). The taxonomy of pre-Crisis siphonodellids requires an intensive revision (e.g. Tragelehn 2010; Becker et al. 2013). Such a reassessment will eventually lead to a refined zone defined by the FAD of the oldest *S. (Eosiphonodella)* species.

Subdivision: In the Müssenberg type section, *Bi. muessenbergensis* appears high in the *S. (Eo.) praesulcata* Zone (Bed 18, Luppold et al. 1994), at the level of the *May. nucleus* Subzone (UD VI-C₃). This may provide a correlation level within the poorly calcareous “Wocklum Beds” of Stockum (Bed 172, Clausen et al. 1994). The oldest known *Pr. collinsoni* of the Rhenish Massif was listed together with various pre-Crisis palmatolepids, bispathodids, and *Ps. marburgensis trigonicus* from Seiler, Section I (Sample 1, Clausen et al. 1989a). This corresponds to an occurrence at the top of the *S. (Eo.) praesulcata* Zone at Grüne Schneid in the Carnic Alps (e.g. Kaiser et al. 2006; Corradini et al. 2017; Schönlaub 2018). Unfortunately, the species is too rare to be used as a zonal index form.

Bispathodus costatus-Protognathodus kockeli Interregnum (ckI, Kaiser et al. 2009)

Synonyms: Main part (above the noted conodont extinction) of the Middle *praesulcata* Zone sensu Ziegler and Sandberg (1984a).

Reference sections: Dreher (Beds 94–97); conodont-free Hangenberg Black Shale to Hangenberg Sandstone of other sections.

Discussion: Since the LOD of *Pa. gracilis gonioclymeniae* varies widely between sections, and even between different sampling campaigns of the same section, Kaiser et al. (2009) discarded the Middle *praesulcata* Zone and replaced it by the ckI, which was defined by the synchronous LOD of many taxa, such as *Bi. costatus*, *Bi. ultimus ultimus*, *Ps. marburgensis trigonicus*, *Pa. gracilis gracilis*, *Pa. gracilis expansa*, and *Pa. gracilis sigmoidalis*. Whilst these do not re-occur in the Upper and post-Crisis Intervals of calm pelagic carbonate platform settings (Kaiser et al. 2009), reworking and downslope transport at seamounts, or stratigraphic leak due to the bioturbation of extremely condensed successions, may lead to post-crisis occurrences, always in very low numbers, including various Rhenish sections. Their reworked nature has been questioned by several authors but the assumption of a survival without recovery and without a new spread into the easily accessible, stable platform settings is more unlikely.

In the Rhenish Massif, the ckI is mostly represented by siliciclastics that have not yielded any conodonts so far. Therefore, the regional ckI conodont record is very poor, with the exception of some limestone nodules from near its top at Dreher (Bed 97, Korn et al. 1994b). They yielded an assemblage with *Pr. meischneri*, *Pr. collinsoni*, and *Neo. communis communis*, which are common in ckI faunas of many other regions (see compilation in Becker et al. 2016a, p. 363). Since there are no newcomers in such faunas on a global scale, it is currently not possible to replace the ckI by a FAD-based zone.

Several attempts to retrieve conodonts from weathered Hangenberg Black Shale failed. So far, no conodonts have been observed on black shale bedding surfaces. It is theoretically possible that some victim taxa survived into the conodont-poor Lower Crisis Interval, similar as postclymeniids did among the ammonoids (see Corradini and Spalletta 2018).

Protognathodus kockeli Zone (Kaiser et al. 2009)

Synonyms: Upper *praesulcata* Zone of Ziegler and Sandberg (1984a), lower part of extended *Pr. kockeli* Zone in Corradini et al. (2016).

Reference sections: Neu-Moresnet (Reissner 1990), Oese (Bed A, Kaiser-Beds 3–4a, Korn-Beds 1–3), Apricke (Beds 39–37), Effenberg (3 cm calcareous shale with *Guerichia* to ca. Bed 18c), Hangenberg (Sample I of Luppold et al. 1994), Dreher (Beds 100 and 1), Wocklum (Beds ?3–5), Stockum (Beds 108–105), Eulenspiegel (Bed 21), Scharfenberg (Beds 1–3).

Other marker species: *Polygathus purus subplanus* (e.g. Dreher, Bed 1), *Po. purus purus* (Apricke, Bed 1H; Wocklum, Bed 4b), *Neo. communis dentatus* (Stockum, Bed 105). The type Stockum Limestone (Bed 103, upper part of *Pr. kockeli* Zone) yielded taxa that are not known from other localities, such as *Po. marginvolutus*, *Neo. communis* cf.

carina, *Ps. nodomarginatus*, and *Ps. cf. fusiformis* (Clausen et al. 1994). A post-Crisis spread of pseudopolygnathids is more characteristic for the basal Hangenberg Limestone of other sections (see Scharfenberg).

Discussion: The precise use of the zone for a future DCB GSSP definition is hampered by a wide and variable definition of the species, which is based on intraspecific variability and rapid evolution of *Protognathodus* in the early recovery phase of the global Hangenberg Crisis. The types of *Pr. kockeli* come from the Wocklum or Borkewehr section, which is currently under re-study (Becker et al. 2016a; Becker and Hartenfels 2017; Hartenfels et al. 2017a, b; Hartenfels and Becker 2019). The holotype and figured paratypes of Bischoff (1957) represent advanced forms with either two rows of nodes on each platform side or incipient second rows (consisting of two nodes only) on one or both sides. In the first limestones above the Hangenberg Sandstone, there are much simpler forms, partly with only one row of nodes on one side and with at least three nodes defining a row. “Double-rowed” forms sensu Kaiser et al. (2019) possess a row of nodes on each platform side. Intermediates from *Pr. collinsoni* display at least on one side two nodes that are arranged in parallel to the carina. Complexly ornamented *collinsoni* variants possess many randomly distributed nodes. There are also *Pr. kockeli* morphotypes that are intermediate towards *Pr. kuehni*, (Figs 2e–h), which is characterised by transverse ridges. The total *Protognathodus* variability of the Stockum Limestone is even higher and includes aberrant morphotypes (e.g. specimens identified as *Pr. praedelicatus*, *Pr. cordiformis*, *Protognathodus* sp. A and B in Luppold et al. 1994). Kaiser et al. (2019) showed that platform shape (e.g. asymmetry) and blade curvature are less useful to define specific *Protognathodus* morphotypes but these features require further evaluations (Kaiser and Hubmann, this vol.). The precise succession of morphotypes and their ontogeny and variability have to be worked out before protognathodids can be used as a DCB GSSP criterion.

Polygnathus purus purus enters at Wocklum in the second bed of the *Pr. kockeli* Zone (Bed 4b, Hartenfels et al. 2017a). However, Kaiser (2009) noted a much earlier occurrence in the Montagne Noire, from Bed 70 (lower ckl) of the current DCB GSSP at La Serre, which is the bed just above the supposed HBS equivalent (Bed 69; see Feist et al. 2020). Supposed pre-Crisis occurrences reported by Corradini et al. (2003) have not been illustrated. Close relatives of *Po. purus purus* characterised by a more anterior position of the basal pit were described from the upper ckl of southern Morocco (Becker et al. 2013) and identified as *Po. cf. purus purus*. They suggest that it is possible to distinguish very early and typical forms of the subspecies.

Siphonodella (Eosiphonodella) sulcata s.l./*Protognathodus kuehni* Zone (Kaiser et al. 2009)

Synonyms: Higher part of the extended *Pr. kockeli* Zone in the scheme of Corradini et al. (2016).

Reference sections: Hasselbachtal (Beds 84N–81N), Oese (Beds B–E = Kaiser-Beds 4b–8 = Korn-Beds 4–11), Apricke (Beds 6H–10H = 36–35), Oberrödinghausen (Beds 6A–5c, Voges-Samples 1–3), Effenberg (ca. Beds 18d–l), Hangenberg (Sample II of Luppold et al. 1994), Müsselfeld (Beds 3a–3B), Stockum (Beds 100–97, especially Unit Alb-C-c, Sample 330 of Alberti et al. 1974), Dreher (Beds 3–4), Eulenspiegel (Bed 22), Scharfenberg (Beds 4–5).

Other index species: At Stockum, Bed 100 yielded *Ps. fusiformis* (Clausen et al. 1994). The alternative shallow-water siphonodellids of South China (e.g. *S. (Eo.) homosimplex*, *S. (Eo.) semichatovae*) have not yet been found in Rhenish sections. The same applies to *Clydagnathus-Patognathus* faunas that appear in the basal Tournaisian of Russian and Chinese sections (e.g. Becker et al. 2016a; Zhuravlev et al. 2018).

Discussion: Kaiser and Corradini (2011) documented the currently subjective identification of *S. (Eo.) sulcata* in many papers. Many specimens do not conform to the type North American lost specimen, which came from the basal Tournaisian Henryville Bed within the Ellsworth Member of the New Albany Shale (Evans et al. 2013). Until further revision, curved and ribbed basal Carboniferous siphonodellids are referred to as *S. (Eo.) sulcata* s.l. Following Kaiser and Corradini (2011), it is their Morphotype 5 that has the best potential to define a refined *S. (Eo.) sulcata* Zone. A joint *S. (Eo.) sulcata* s.l./*Pr. kuehni* occurrence in the top Stockum Limestone at Seiler, Section I (Bed 5), resulted in a first close alignment of both FADs (Clausen et al. 1989a). Based on direct co-occurrences in the Graz Palaeozoic and Carnic Alps, Kaiser et al. (2019) confirmed the usefulness of (typical) *Pr. kuehni* as an alternative index species for the *S. (Eo.) sulcata* (s.l.) Zone. This is especially important for the majority of sections, where siphonodellids are absent in the Upper Crisis Interval (Stockum Limestone and equivalents, see compilation of Kaiser et al. 2015, tab. 5). It results in a combined *S. (Eo.) sulcata* s.l./*Pr. kuehni* Zone that ranges from Upper Crisis Interval III into the basal post-crisis time (basal Hangenberg Limestone). However, revisions of *Protognathodus* taxonomy, especially of the complex *Pr. kockeli-kuehni* transition (see Kaiser et al. 2019), have to consider the fact that the types of *Pr. kuehni* are not from the *S. (Eo.) sulcata* s.l./*Pr. kuehni* Zone, but from the younger *S. (S.) duplicata* Zone at Seiler, Trench 2.

Siphonodella (Eosiphonodella) bransoni Zone (Ji 1985)

Synonyms: Lower *duplicata* Zone of Sandberg et al. (1978).

Reference sections: Hasselbachtal (Beds 72H–70H), Oese (Beds F–I = Kaiser-Beds 9–12 = Korn-Beds 12–17), Apricke (Beds 13H/14H = 33), Oberrödinghausen (Bed 5b and Kürschner-Bed 4), Seiler, Section II (Bed 10), Dreher (Bed 5), ?Stockum (Unit Alb-C-e = Bed 95), Scharfenberg (Bed 6), Eulenspiegel (Bed 23).

Discussion: Ji (1985) re-named *S. duplicata* M1 as *S. (Eo.) bransoni*. As discussed below, it is possible that *Ps. triangulus inaequalis* enters within the *S. (Eo.) bransoni* Zone.

Siphonodella (Siphonodella) duplicata Zone (Ji 1985)

Synonyms: Possibly the *triangulus inaequalis* Zone of Voges (1960).

Reference sections: Hasselbachtal (Beds 69H–65H), Oese (Kaiser-Bed 13), Oberrödinghausen (Beds 4a–4b), Kaiser et al. 2017; Kürschner-Beds 5–6), Seiler, Section 0 (Bed 3), Section II (Beds 11–12), Section III (Beds 4–6), Stockum (Unit Alb-D, Samples 315–316), Scharfenberg (Bed 7).

Other marker species: Possibly *Pseudopolygnathus triangulus inaequalis* (e.g. Seiler, Section 0, Bed 3, Hasselbachtal, Bed 69H, Oberrödinghausen, Bed 4 = Sample 5, Voges 1959), *S. (S.) lobata* M2 (Oberrödinghausen, Bed 4 = Sample 5, Voges 1959).

Discussion: The lowest range of *Ps. triangulus inaequalis* requires further data. Without specific information, Ziegler (1971) placed the base of the “*triangulus inaequalis* Zone” at Oese between Beds F and G, which is well below the locally oldest *S. (S.) duplicata* in Bed J. The entry of early relatives of *S. (Eo.) isosticha* (e.g. at Hasselbachtal from Bed 65H on) requires also further work.

Siphonodella (S.) mehli Zone (nom. nov.)

Synonyms: Upper *duplicata* Zone of Sandberg et al. (1978), *jii* Zone of Becker et al. (2016a), *triangula triangula* Zone of Voges (1959, 1960).

Reference sections: Hasselbachtal (Beds 63H–45H), Seiler, Section 0 (Bed 4 with *S. (S.) mehli*, *S. (S.) cooperi*, and *S. (S.) carinthiaca*, Beds 5–6), Section II (Bed 13 with *S. (S.) mehli* and *S. (S.) carinthiaca*, Beds 14–16), Section III (Bed 6 with *Ps. triangulus triangulus*, Bed 7 with *S. (S.) mehli*, *S. (S.) carinthiaca*, and *S. (S.) cooperi*; Clausen et al. 1989a), Oese (?Kaiser-Bed 14 with *S. (S.) duplicata* and *S. (S.) cf. wilberti*, Kaiser-Bed 17 with *S. (S.) carinthiaca* and *S. (S.) belkai* M1, Kaiser-Bed 21 with *S. (S.) carinthiaca*, *S. (S.) cf. wilberti*, and *S. (S.) lobata* M2, Kaiser-Bed 22 with *S. (S.) obsoleta*, Oberrödinghausen (?Bed 3e, Beds 3d–3b = Ziegler-Beds ?9–13 with *S. (S.) belkai* M2, *S. (S.) cf. wilberti*, *S. (S.) lobata* M2, and *S. (S.) obsoleta*; Korn and Weyer 2003; Kaiser 2005; Kaiser et al. 2017; Kürschner-Beds 8–12), Müssenberg (Bed 0 with *S. (S.) carinthiaca* and *Ps. triangulus triangulus*), Stockum (Unit Alb-D, Sample 918), Dreher (Beds 6/7 with *S. (S.) carinthiaca* and *S. (S.) cooperi*, Beds 8/9 with *S. (S.) mehli* and “*S. duplicata* sensu Hass” (= *S. (S.) cf. wilberti*), Scharfenberg (?Beds 8–9 with *S. (S.) cf. wilberti*, Beds 10–11 with *S. (S.) mehli* and *S. (S.) carinthiaca*), Eulenspiegel (Bed 24 with *S. (S.) mehli*, *S. (S.) carinthiaca*, and *S. (S.) cf. wilberti*).

Other marker species: *S. (S.) carinthiaca* (Hasselbachtal, Beds 59H–47H; Seiler, Section 0/Beds 4–5, Section II, Beds 13–14, Clausen et al. 1989a; Oese, Bed 21, Kaiser et al. 2017; new records from Borkewehr), *S. (S.) cooperi* (= M2; Hasselbachtal, Bed 65H; Seiler, Section 0/Bed 4, Clausen et al. 1989a), *Ps. triangulus triangulus* (Hasselbachtal, Beds 49H–47H), Dreher, Beds 6–7; Seiler, Section 0, Beds 4–5).

Discussion: Sandberg et al. (1978) based their Upper *duplicata* Zone on the FAD of *S. cooperi* M1, which was re-named by Ji (1985) as *S. (S.) mehli*. Ji (1985), by contrast, used the FAD of *S. duplicata* sensu Hass, which he re-named as *S. (S.) hassi*, to define a supposedly corresponding *hassi* Zone. Becker et al. (2016a) recognised that *S. (S.) hassi* Ji 1985 is an invalid junior homonym of *S. cooperi hassi* Thompson and Fellows 1970, and, consequently, re-named *S. duplicata* sensu Hass as *S. (S.) jii*, with two originals of *S. duplicata* var. A of Hass (1959) as type specimens. The adult USNM 115140, the original of Hass (1959, pl. 49, fig. 18), is here selected as the lectotype. The species re-naming resulted in a name change from *hassi* Zone to *jii* Zone. Zhuravlev and Plotitsyn (2018) re-illustrated the types of *S. (S.) jii* and showed the presence of incipient second rostral ridges, at least on the inner anterior platform. In this respect, the morphology of the *jii* lectotype is less advanced than in typical adult *S. (S.) quadruplicata* (see Zhuravlev and Plotitsyn 2018: fig. 3). The specimen can be regarded as an early morphotype (M2) of *S. (S.) quadruplicata*. The second, smaller specimen (Hass 1959, pl. 49, fig. 17) fits well into an ontogenetic series of *S. (S.) quadruplicata* from the Polar Urals. Chinese specimens of “*S. (S.) hassi*” do not display incipient secondary rostra, apparently throughout ontogeny. They may be assigned to *S. (S.) wilberti* Bardasheva Bardashev, Weddige and Ziegler, 2004 described from the middle Tournaisian of Tadzhikistan. The *wilberti* holotype is characterised by a peculiar, undulating and serrate outer platform corner, which could be a pathological feature. Until the variability of *S. (S.) wilberti* is better known, we suggest to name specimens of “*S. (S.) hassi* sensu Ji 1985” as *S. (S.) cf. wilberti*. Although representatives from the Rhenish Massif have never been illustrated, we preliminary extend this assignment to previously reported Rhenish “*S. duplicata* sensu Hass”. We are aware that some of these specimens may be identical with *S. (S.) jii* sensu its lectotype (= *S. (S.) quadruplicata* M2). This has to be clarified by the revision of specimens and the study and illustration of additional faunas.

In order to avoid these taxonomic complications, the *jii* Zone of Becker et al. (2016a) is replaced by the re-named *S. (S.) mehli* Zone, returning to the original definition of the Upper *duplicata* Zone by Sandberg et al. (1978). However, it is unfortunate that *S. (S.) mehli* (= *cooperi* M1) is relatively rare in several sections of the Rhenish Massif.

Subdivision: Sandberg et al. (1978) suggested that *S. (S.) carinthiaca* and *S. (S.) cooperi* s. str. (=Morph 2) enter later than *S. (S.) mehli* (=*S. cooperi* M1). Published faunas from Rhenish sections do not provide any support. As explained below, the FAD of *S. (S.) quadruplicata* occurs in several sections in the *S. (S.) mehli* Zone or even before (e.g. Seiler Trench 2, Bed 14, Koch et al. 1970), well before the entry of *S. (S.) sandbergi* or *S. (S.) lobata*. Currently, it is unclear whether all or only some of these records refer to the early M2 in the sense of the *S. (S.) jii* lectotype.

Sandberg et al. (1978) showed that the FAD of *S. (S.) obsoleta* lies near the top of the Upper *duplicata* Zone (e.g. Oese, Kaiser-Bed 22b = R; Seiler sections, compare range in Ji 1985). The species occurs at Oberrödinghausen well below the base of the *sandbergi* Zone (Bed 3d₂ = Voges 1959, Sample 6) and jointly with the first *S. (S.) belkai* M2 (Kaiser et al. 2017). The FADs of both taxa mark in the Rhenish Massif a position in higher parts of the *S. (S.) mehli* Zone but currently we refrain from proposing a new subzone.

Since Voges (1959), various authors correlated the *triangulus triangulus* Zone with a high level in the Hangenberg Limestone (e.g. Ziegler 1971). However, there is evidence from several sections (Drewer, Seiler sections) that the index species may enter much lower, around the base of the *S. (S.) mehli* Zone. For example, Koch et al. (1970) recorded *Ps. triangulus triangulus* at Seiler Trench 2 from Bed 13, below the FAD of *S. (S.) obsoleta*. Ziegler (1971) marked at Oese the base of the *triangulus triangulus* Zone at the base of Bed M, within the range of *Paprothites* (Korn and Weyer 2003). A possibly even earlier record was listed by Luppold et al. (1994) from Müssenberg (Bed 1). Eickhoff (1973) noted at Oberrödinghausen a joint entry of *Ps. triangulus inaequalis* and *Ps. triangulus triangulus* in his Sample 3, correlated with Sample 5 of Voges (1959), which is in the *S. (S.) duplicata* Zone. More precision of the *Ps. triangulus* ssp.-siphonodellid correlation is required.

Siphonodella (Siphonodella) sandbergi Zone (Sandberg et al. 1978)

Reference sections: Oberrödinghausen (Beds 2b–1a, Kaiser 2005; Kürschner-Sample 13), Stockum (Unit Alb-D, Samples 921, 919).

Other marker species: *Siphonodella (Eo.) cf. isosticha* (Oberrödinghausen, Bed 1b, Ziegler 1971; Seiler, Section 0, Bed 10, Clausen et al. 1989a).

Discussion: *Siphonodella (S.) sandbergi* is rather rare in the Rhenish Massif and, therefore, its zone is difficult to recognise apart from Oberrödinghausen and Stockum. In several sections, *S. (S.) quadruplicata*, possibly M2, was reported to enter jointly with “*S. duplicata* sensu Hass” (= *S. (S.) cf. wilberti*; e.g. Drewer, Bed 9), below (Seiler, Trench 2, Bed 14) or with the first *S. (S.) obsoleta* (Seiler, Section III, Bed 8,

Section 0, Bed 6), or with *S. (S.) cooperi* (M2, Seiler, Section II, Beds 15–16), in all cases without any evidence for *S. (S.) sandbergi* (compare early *?quadruplicata* records at Stockum, Groos-Uffenorde and Uffenorde 1974). This questions the *quadruplicata* Zone of Ji (1985), which he established for an upper subdivision of the *sandbergi* Zone. *Siphonodella (S.) quadruplicata* occurs commonly in higher parts of the *S. (S.) sandbergi* Zone of some sections (e.g. at Scharfenberg, Beds 13–14, Clausen et al. 1989a, and at Oberrödinghausen, Kaiser 2005; Kaiser et al. 2017). It may be possible to separate typical/late (M1) and early morphotypes (M2) but this requires a better documentation. Currently we hesitate to recognise a *S. (S.) quadruplicata* Zone (better subzone) in the top Hangenberg Limestone of the Rhenish Massif. The *S. (S.) sandbergi/quadruplicata* range relationships are not much clearer in the Montagne Noire (Kaiser et al. 2009; Feist et al. 2020: with *S. (S.) quadruplicata* entering before *S. (S.) sandbergi* at Col de Puech de la Suque) or in the Carnic Alps (e.g. Kronhofgraben, Kaiser et al. 2006). The *S. (S.) quadruplicata* Zone also has not been recognised in the recent review of Chinese Carboniferous conodont zones by Hu et al. (2019).

Subdivision: Sandberg et al. (1978) suggested that the entry of *S. (S.) lobata* could be used to separate an upper subzone. This is supported by records from the top Hangenberg Limestone of Apricke (Bed 34H = 16), Oberrödinghausen (Bed 1a = Voges 1959, Sample 11), Seiler (all sections), Drewer (Bed 12), Stockum (Unit Alb-D, Sample 353), and Scharfenberg (Beds 12–14, Clausen et al. 1989a). Voges (1959, pl. 35, figs. 35, 36, 38) illustrated typical specimens that share with the North American holotype an anterior direction of the side lobe marked by a secondary carina. This form is here called Morph 1. Other specimens (e.g. Voges 1959, pl. 35, fig. 39) and especially older representatives (Ji et al. 1989, pl. 14, figs. 3–4, basal *sandbergi* Zone; Kaiser et al. 2017, figs. 10.6 and 10.13, “*jii* Zone”) have a more incipient platform lobe directed to the side, which lacks on the oral surface a secondary carina. These are assigned to our new Morph 2. Only *S. (S.) lobata* M1 indicates the upper *S. (S.) sandbergi* Zone or *S. (S.) lobata* M1 Subzone. The base of the *S. (S.) crenulata* Zone forms the top of the new subzone. For associated siphonodellids and other conodonts, see the range charts in Sandberg et al. (1978), Clausen et al. (1989a), and Ji (1985).

Ammonoid biostratigraphy (Fig. 1)

The DCB ammonoid biostratigraphy has been reviewed by Becker et al. (2016a), who emphasised parallel zonations based on successive members of the Prionoceratidae,

Kosmoclymeniidae, other clymeniid groups, and, in the lower Tournaisian, early prolecanitids. A different approach was followed by Klein and Korn (2016), who used three quantitative methods (unitary associations, ranking and scaling, constrained optimisation) to correlate Rhenish records (reference sections Müssenberg 1 for the upper/uppermost Famennian, Oberrödinghausen Railway Cut for the lower Tournaisian) and to establish composite ranges. These, however, differ from each other and the correlation obviously did not consider other stratigraphic markers, such as conodonts and metabentonites. The Rhenish Slate Mountains yielded on a global scale the most detailed DCB ammonoid record. Several ammonoid subzones are based on the detailed classical studies by Schindewolf (1937) and Vöhringer (1960). Subsequent studies and revisions added many precise data and taxa (e.g. Korn 1981a, b, 1984, 1988a, 1988b, 1991, 1992a, b, 1993, 1994, 2000; Becker 1988, 1996, 2000; Clausen et al. 1989a, b; Korn and Luppold 1987; Luppold et al. 1994; Korn et al. 1994b; Korn and Weyer 2003; Korn and Vöhringer 2004; Ebbighausen and Korn 2007; Becker et al. 2016a) but in general supported the originally established faunal sequence. The current knowledge of Rhenish DCB ammonoid zones/subzones, with all units (apart from the *Post. evoluta* Zone) named after the FAD of its index species, is from base to top (for reference section literature, see section descriptions):

Linguaclymenia similis Zone (Becker et al. 2002, UD VI-A₁)

Synonyms: *Muessenia sublaevis* Zone (Korn 2000).

Other marker species: *Muessenia sublaevis* (Müssenberg, Bed 90; Dasberg, Bed L), “*Mim.*” *liratum* (Müssenberg, Bed 90), “*Mim.*” *geminum* (Hasselbachtal, Bed 1S; Dasberg, Bed K), *Kos. undulata* (Müssenberg, Bed 90), *Rodachia dorsocostata* (Müssenberg, Bed 90), *C. semistriata* (Effenberg, Figs. 5i–j), *Cyrto. plicata* (Müssenberg, Bed 90), *Cyrto. lateseptata* (Hasselbachtal, Bed 1, ?= *Cyrto. campanulata*), “*Sph.*” *brevispina* (cf. Oberrödinghausen, Schindewolf-Bed 22; Effenberg, Bed 17), “*Sph.*” *erinacea* (Dasberg, Bed 0a = L), *R. quadripartitum* (Hasselbachtal, Bed 2).

Reference sections: Müssenberg (Beds 90–68), Hasselbachtal (3 m below Bed 0 to Bed 12), Oberrödinghausen (Schindewolf-Beds 23-ca. 19), Dasberg trench (Korn and Luppold 1987, base of Bed 0b; Clausen and Korn 2008, Beds L–J), Effenberg (kosmoclymeniid coquinas, Hartenfels et al. 2016).

Discussion: Schindewolf (1937) proposed to use the entry of *Kalloclymenia* (s.l., at his time including various sphenoclymeniids and *Finichlymenia*) to define the base of the Wocklum Beds and a *Kalloclymenia*-Wocklumeria-Stufe. However, in his type section in the Oberrödinghausen Railway Cut, bed-by-bed collecting started with Bed 23, from which he recorded “*Oxyclymenia bisulcata*”. At his time, such an identification referred to kosmoclymeniids with marked

ventrolateral furrows, which included, among others, forms now assigned to *Linguaclymenia*, especially *L. similis* (see synonymy list in Korn and Price 1987). Therefore, it can be assumed that Schindewolf’s section began locally with the FOD of *Linguaclymenia*. The first “*Kalloclymenia*”, in fact “*Sph.*” cf. *brevispina*, commenced one bed higher, which led to the term *K. subarmata*-*K. brevispina* Zone. Korn and Luppold (1987) subdivided the zone and defined their “Lower subarmata Zone” by the entry of “*Sph.*” *brevispina*, stimulated by new records of that species from Dasberg and Effenberg. However, in the subsequent review of “*Sph.*” *brevispina* by Price and Korn (1989), the Dasberg specimens were re-assigned to a new species, “*Sph.*” *erinacea* (see also Clausen and Korn 2008). This showed that several “sphenoclymeniids” enter in the basal Wocklum Beds. The phrase “*Sphenoclymenia*” refers to the distinction of moderately large forms with narrowly rounded venter from the poorly known, giant-sized, oxyconic-type species of the genus, *Sph. maxima*.

At Müssenberg (Korn 1993; Klein and Korn 2016), *M. sublaevis* and *L. similis* enter jointly in Bed 90. This was obviously the base for a re-definition of the Wocklum-Stufe by the FAD of *M. sublaevis* (Korn 2000), although “*Sph.*” *brevispina* enters at Müssenberg five beds higher. Because kosmoclymeniids are more common than “sphenoclymeniids”, we accept Korn’s slight extension of the *Wocklumeria*-Stufe but give preference to *L. similis* as the main index species. It is very distinctive and more easily recognisable than *M. sublaevis* in poorly preserved faunas without shell, even as small fragment. In addition, its zone can be traced widely, for example to Morocco (Becker et al. 2002). A joint FAD of *L. similis* and *M. sublaevis* was also shown at Dasberg (Clausen and Korn 2008).

Subdivision: Hartenfels and Becker (2016) re-habilitated *Kalloclymenia* (s.str.) as a marker genus for the lower Wocklumian. It enters at Oberrödinghausen (Schindewolf-Bed 19: *K. cf. uhligi*), Müssenberg (Bed 78: *K. subarmata*), and Hasselbachtal (Bed 2: *K. pessoides*) well above the base of the *L. similis* Zone (compare ranges in Klein and Korn 2016). However, Korn and Luppold (1987) noted a *Kalloclymenia* sp. from the second bed of the Wocklum Limestone at Dasberg.

Muessenia galeata enters in higher parts of the zone (Dasberg, Bed K; Hasselbachtal, Bed 12, Becker 1996; see RASC plot of Klein and Korn 2016: fig. 11).

Conodont correlation: The entries of *L. similis* and *M. sublaevis* pre-date at Müssenberg the FODs of any of the three main marker conodonts for the *Bi. ultimus ultimus* Zone. “*Sphenoclymenia*” *brevispina* begins jointly with *Ps. marburgensis trigonicus* (Bed 85), *K. subarmata* (in Bed 78) slightly above the FODs of *Bi. ultimus ultimus* (= *ziegleri ziegleri*) and *Pa. gracilis gonioclymeniae* (Bed 80, Luppold et al. 1994). At Effenberg “*Sph.*” *brevispina* occurs in Bed 17 below *Pa. gracilis gonioclymeniae* (Bed 19); the

local first *K. subarmata* was recorded from well above it (Bed 23). In the Dasberg trench, *K. subarmata* was also found above (Bed 0b) the oldest *Pa. gracilis gonioclymeniae* (Bed 0a; Korn and Luppold 1987). At Oberrödinghausen, Bed 23 of the basal Wocklum Limestone yielded *Ps. marburgensis trigonicus* (Sacher 2016), Bed 22 with “*Sph.*” cf. *brevispina* produced *Pa. gracilis gonioclymeniae* and *Br. suprema* (Kürschner et al. 1993), and Bed 20, below the oldest *Kalloclymenia* (in Bed 19), *Bi. ultimus ultimus*.

The complete evidence is a mosaic from these different sections. It suggests that the base of the *Bi. ultimus ultimus* Zone, if defined by either of the three main markers, lies close to the base of the *L. similis* Zone. *Bispathodus ultimus ultimus*, the proposed index fossil for the definition of a formal uppermost Famennian substage, however, does not display consistent FODs in individual sections and partly very long delays. Its oldest regional occurrence post-dates the oldest “*Sph.*” *brevispina*. This suggests that *Bi. ultimus ultimus* was ecologically sensitive in pelagic facies.

Muessenbiaergia bisulcata Zone (Korn 2000; UD VI-A₂)

Synonyms: Upper *subarmata* Zone, lower part (Korn and Luppold 1987).

Reference sections: Müssenberg (Beds 67–39), Hasselbachtal (Beds 14–31), Effenberg (“Bed 93d” with *M. parundulata*), Reigern Quarry (ca. Beds 10b–21), Dasberg trenches (Beds I–G).

Other marker species: *Muessenbiaergia parundulata* (Müssenberg, Bed 67), “*C.*” *barbara* (Oberrödinghausen, Schindewolf-Bed 16), “*Cyrto.*” *tetragona* (Oberrödinghausen, Schindewolf-Bed 18).

Conodont correlation: Based on the Müssenberg section (Clausen et al. 1989b), the base of the *M. bisulcata* Zone (Bed 67) lies well below the FAD (Bed 55) of *S. (Eosiphonodella)*.

Effenbergia lens Zone (UD VI-B)

Reference sections: Müssenberg (Beds 38–35), Hasselbachtal (Beds 32–43), Oese (within Becker-package 4, Nowak-Bed 210l), Oberrödinghausen (Schindewolf-Beds 15–11 with “*Prionoceras* n. sp. IV”), Reigern Quarry (?Beds 27–28, Price 1982).

Other marker species: The FODs of several species are known from middle (*Mim. trizonatum*, Oese, within Nowak-Bed 210, Dasberg, Bed E) to upper parts of the zone: *Eff. minutula* (Oese, Nowak-Bed 210j, Dasberg, Bed D), *M. ademmeri* (Dasberg Bed D), *Kos. schindewolfi* (Oberrödinghausen, Schindewolf-Bed 12; Dasberg, Bed D), *C. cf. sudetica* (Oberrödinghausen, Sacher-Bed 204b), *Soliclymenia solariooides* (Dasberg, Bed D), and *Gl. glaucopis* (Dasberg, Bed D; Oese, Nowak-Bed 210l).

Discussion: Already Korn (1992a) and Luppold et al. (1994) recognised the level of *Eff. lens* and *Eff. minutula* as an upper subdivision of their “Late *K. subarmata* Zone” but the zone

was not formally named until Korn (2000). It can be followed to southern Morocco (Becker et al. 2002).

Conodont correlation: Based on the Müssenberg section (Clausen et al. 1989b), the base of the *Eff. lens* Zone (Bed 38) lies well above the FAD (Bed 55) of *S. (Eosiphonodella)*. This is supported by less detailed data from Oese (Nowak 2008).

Parawocklumeria paprothae Zone and Subzone (Clausen et al. 1989a; UD VI-C₁)

Synonyms: *Kamptoclymenia endogona* Zone (or Subzone; Schindewolf 1937).

Reference sections: Müssenberg (Beds 34–26), Hasselbachtal (ca. Beds 44–63), Oberrödinghausen (Schindewolf-Beds 10–7), Dasberg (Beds B–A).

Other marker species: *Parawocklumeria patens* (Müssenberg, Bed 34; Dasberg, Bed B), *P. distorta* (Oberrödinghausen, Schindewolf-Bed 10; Dasberg, Bed A), *Kamp. endogona* (Müssenberg, Bed 34; Dasberg, Bed A), *Kamp. trigona* (Müssenberg, Bed 34; Dasberg, Bed A), *Tria. triangularis* (Oberrödinghausen, Schindewolf-Bed 10), *M. ?xenostriata* (Hasselbachtal, Beds 46–49, above the LOD of *Eff. lens*), *Eff. falk* (Müssenberg, Bed 34; Dasberg, Bed B), *B. globularis* (Müssenberg, Bed 34), *Ken. rostratum* (= *biforme*; Dasberg, Bed B).

Subdivision: Somewhat above the zonal base (e.g. Müssenberg, Bed 29; Dasberg, Bed A), the distinctive *Liss. wocklumeri* enters.

Discussion: It is a matter of personal preferences to separate this level as a full zone or as a lower subzone (applied here) of the longer interval characterised by *Parawocklumeria* faunas before the onset of *Wocklumeria*. Since *Kamptogona* tends to be rare, the more common *P. paprothae* (see Becker 2000) is given preference as the index taxon.

Conodont correlation: The *P. paprothae* Subzone lies entirely within the *S. (Eo.) praesulcata* s.l. Zone.

Parawocklumeria paradoxa Subzone (Schindewolf 1937, UD VI-C₂)

Reference sections: Müssenberg (Beds 25–20), Hasselbachtal (Beds 64–ca. 83cN), Oese (Becker-package 2), ?Oberrödinghausen (parts of Schindewolf-Beds 7–6).

Other marker species: “*Mimimitoceras*” *lentum* (Müssenberg, Bed 25, Klein and Korn 2016).

Conodont correlation: The *P. paradoxa* Subzone lies entirely within the *S. (Eo.) praesulcata* s.l. Zone.

Mayneoceras nucleus Subzone (Becker et al. 2002, UD VI-C₃)

Reference sections: Müssenberg (Beds 19–14), Hasselbachtal (Beds 84N–91N), Oese (Nowak-Beds 225b–226d), Oberrödinghausen (main Schindewolf-Bed 6).



Fig. 3 Examples for DCB ammonoids from the eastern Rhenish Massif; scale bar = 5 mm. **a, b** *Wocklumeria denckmanni*, adult specimen, Dreher, Bed 93 (UD VI-D₂), leg. 2019, lateral and ventral views, B6C.54.1, $\times 1.5$; **c, d** *W. denckmanni*, rather compressed middle-sized specimen with triangular constrictions, Hasselbachthal, loose (UD VI-D), lateral and ventral views, B6C.54.2; $\times 1.7$; **e, f** *Parawocklumeria paradoxa*, Hasselbachthal, Bed 103N (UD VI-D₁), lateral and ventral views, B6C.54.3, $\times 1.7$; **g, h** *Mayneoceras sinuconstrictum*, Oese, collected from debris (UD VI-C/D), first record for the Rhenish Massif, lateral and ventral views, B6C.54.4, $\times 3$; **i, j** *Cymaclymenia semistriata*, Effenberg, loose (UD VI), lateral and ventral views, more compressed than *C. cf. sudetica*, B6C.54.5, $\times 1.5$; **k** *Postclymenia cf. evoluta*, squashed, Oese, HBS, B6C.54.6, $\times 1$; **l, m** *Gattendorfia subinvoluta*, specimen with rursiradiate constrictions (unlike the type material), Oberrödinghausen Railway Cut, Bed 5 (LC I-A₃), lateral and ventral views, B6C.54.7, $\times 1.5$; **n, o** *Paraggattendorfia cf. sphaeroides*, new rather involute variant of the species with relatively high whorls, Oberrödinghausen Railway Cut, level unclear, lateral and adoral views, B6C.54.8, $\times 2$; **p, q** “G.” *costata*, topotype, Oberrödinghausen Railway Cut, Bed 2 (lower LC I-D), lateral and ventral views showing the strongly concavoconvex ornament (unlike the ornament in typical gattendorfiids), B6C.54.9, $\times 1.5$; **r, s** fragmentary *Acutimitoceras (Streeliceras) heterolobatum*, Dreher, collected from debris, lateral and ventral views showing typical sutures with short, slightly pouched ventral lobes, new local record, B6C.54.10, $\times 1$

Other marker species: *Finiclymenia wocklumensis* (Müssenberg, Bed 17; Oese, cf. Nowak-Bed 225b), *Postglatziella carinata* (Müssenberg, Bed 17), possibly *May. sinuconstrictum* (Oese, Figs. 5g–h).

Conodont correlation: The *May. nucleus* Subzone lies entirely within the *S. (Eo.) praesulcata* s.l. Zone.

Discussion: Successive FADs of *P. paradoxa* and *May. nucleus* were confirmed by quantitative analyses of Klein and Korn (2016). Contemporary faunas with *Finiclymenia* and *May. nucleus* occur also in North Africa (Becker et al. 2002: section Lambidia).

Wocklumeria denckmanni Zone and Subzone (Schindewolf 1937, UD VI-D₁)

Reference sections: Hasselbachthal (Beds 92N–112N; Figs. 5c–d), Oese (Korn-Bed 2, Becker-package 1, Nowak-Beds 226e–227c), Apricke (Beds 3–2), Oberrödinghausen (Schindewolf-Beds 5–2), Wocklum (Bed 3), Müssenberg (Beds 13–ca. 6), Dreher (Beds 91b–c), Grimminghausen (*Wocklumeria* record of Weber 1934).

Other marker species: *Wocklumeria sphaeroides* (Dreher, Bed 91b, Becker et al. 2016b), *C. nephroides* (Bilstein, Korn 1981a). In siliciclastic facies, *Post. evoluta* occurs. Its type level is at the top of the subzone at Dreher but its full and possibly lower range is currently unknown in the neritic sections of the Bergisches Land.

Discussion: The morphometric study of Ebbighausen and Korn (2007) showed that Rhenish wocklumeriids differ from the *W. sphaeroides* type population of Thuringia. Therefore, the long

disused name *W. denckmanni* was revived for the typical Sauerland representatives. However, *sphaeroides*-type specimens, without marked triangular stage and with early rotund whorls, do occur in the Rhenish Massif. Due to a high variability of relative whorl and umbilical width, *W. aperta* Schindewolf, 1937 and *W. plana* Schindewolf, 1937 were placed by Ebbighausen and Korn (2007) in synonymy of *W. denckmanni*. Both names can be used to characterise intra-specific morphotypes (e.g. Fig. 3a–d), which distributions in space and time need further considerations.

Conodont correlation: The *W. denckmanni* Subzone lies entirely within the *S. (Eo.) praesulcata* s.l. Zone.

Epiwocklumeria applanata Subzone (Schindewolf 1937, UD VI-C₂)

Reference sections: Hasselbachthal (Beds 113aN–114N), Oberrödinghausen (Schindewolf-Bed 1), Dreher (Beds 93a–c, with the last *W. denckmanni*, Figs. 5a–b), Wocklum (ca. Beds –2 to –1).

Conodont correlation: The *Epi. applanata* Subzone lies at the top of the *S. (Eo.) praesulcata* s.l. Zone, within the former Upper *costatus* Zone sensu Ziegler (1962). It equals the basal part of the Middle *praesulcata* Zone sensu Ziegler and Sandberg (1984b).

Postclymenia evoluta Zone (Schindewolf 1937, UD VI-E)

Reference sections: Lintorf area (Diepenbrock Anticline, Paul 1938a), Cromford (Beds 22–23) and adjacent localities, Scharpenhaus (Beds 2–3, Paul 1939a, p. 676), Hefel (Bed 1), Riescheid, Am Haken Brickwork Quarry, Mirker Hain, ?B224 building site near Aprath (pyritic Bed 05/30, with *Acutimitoceras* sp. but without conodont record), Hasselbachthal (Bed 115N), Apricke (Bed 42), Oberrödinghausen (Sacher-Bed 225), Oese (Nowak-Bed 229; Fig. 3k), Dreher (Bed 94), Vingerhoets 93 Well (1716–1720 m).

Discussion: The zonal base is defined by the LAD of all ammonoid taxa (especially of *Wocklumeria*, *Epiwocklumeria*, *Parawocklumeria*, *Finiclymenia*, *Lissoclymenia*, *Cyrtoclymenia*, N. Gen. aff. *Cyrtoclymenia* (“*Pricella homoeomorph*”), the “*Cyrtoclymenia*” tetragona Group, *Mayneoceras*, *Kenseyoceras*, *Balvia*, *Sporadoceras*, and *Ebbighausenites*) apart from *Postclymenia*, NOT by the *Post. evoluta* FAD (Becker 1988). The term *P. evoluta* Zone was chosen, because there is hardly any other ammonoid apart from postclymeniids in the HBS. The poor preservation of postclymeniids in the Hangenberg Black Shale requires a careful taxonomic approach (Zhang et al. 2019). Therefore, such specimens should be identified as *Post. cf. evoluta* (Fig. 3k). Currently, there is no proof that *Post. nigra* occurs in the typical (lower) Hangenberg Black Shale or Lower Crisis Interval. Therefore, it is not recognised as an alternative zonal index

(compare the zonation of Korn 2000). In Section WJ at Brewer, *Post. nigra* even overlaps with *Pr. kockeli*.

The rare prionoceratids from the Hangenberg Black Shale are too poorly preserved for a reliable identification. Paul (1937b, p. 751) mentioned a large-sized “*Imitoceras*” from Velbert, which, unfortunately, was never described or illustrated. Based on the discovery of very early *Ac. (Stockumites)* sp. in Hangenberg Black Shale equivalents of southern Morocco (Klug et al. 2016), the presence of the genus at this level in the Rhenish Massif is possible, too. Very restricted evidence comes from a pyritic and septarian-rich marl with *Ac. (Stockumites)* sp. at the B224 building site (Bed 05/30, Korn 1992b), which overlay as a deepening unit oncoid-bearing neritic strata but which correlation with the Hangenberg Black Shale level is very tentative.

Conodont correlation: The base of the *Post. evoluta* Zone correlates with the base of the *ckI*.

Acutimitoceras (Stockumites) prorsum Zone (UD I-F to LC I-A₁)

Reference sections: B224 building site near Aprath (Bed 06/1), Am Haken Brickwork Quarry (pyritic black shale), Hasselbachtal (Beds 85H–81H), Apricke (Bed 2H), Oberrödinghausen (Hangenberg Shale, Sacher-Beds 226a–b), Wocklum (Beds 2–5b), Effenberg (Beds 18b–c), Stockum (Beds 103 and 100), Brewer (Bed 95 = Hangenberg Sandstone, Beds 97–100 = Stockum Level Black Shale, Beds 1 and 1/2 = 13d = Lower Stockum Limestone, Bed 2 = 13c = ?Upper Stockum Limestone).

Other marker species: *Acutimitoceras (St.) cf. procedens*, *Ac. (St.) subbilobatum* (auct.), *Ac. (St.) intermedium* (auct.), *Ac. (St.) aff. antecedens*, *Ac. (St.) kleinerae*, *Ac. (St.) stockumense*, *Ac. (Str.) caesari*, *Ac. (Str.) carinatum*.

Discussion, subdivision, and conodont correlation: Specimens from the Hangenberg Shale/Sandstone are squashed, which makes their precise identification arbitrary. Therefore, it is difficult to establish a species succession within the total, relatively long interval. Based on the litho- and event stratigraphy in combination with conodont and/or spore data, there are currently five successive goniatite levels within the zone (marking the current knowledge of staged entries in bold):

1. Basal part (Middle Crisis Interval I, basal UD VI-F, lower Hangenberg Shale)

***Ac. (Stockumites)* sp.** (?intermediate from *Mimimitoceras*, with still relatively low whorls) and *Postclymenia* sp. from 42 cm above the base of the Hangenberg Shale at Oberrödinghausen (Becker et al. 2016a).

2. Lower part (Middle Crisis Interval II, main UD VI-F, upper part of Hangenberg Shale/Hangenberg Sandstone):

Ac. (St.) cf. procedens and ***Ac. (St.) aff. antecedens*** (as evolve as in the *prorsum* Group) from ca. 3.8 m above the base (= 2.2 m below top) of the Hangenberg Shale at Oberrödinghausen (Becker et al. 2016a).

Ac. (St.) cf. subbilobatum (auct.) from 1.1 m below the top of the Hangenberg Shale at Oberrödinghausen (Luppold et al. 1994).

Ac. (St.) cf. procedens from 25 cm below the top of the Hangenberg Shale at Oberrödinghausen (Paproth and Strel 1970; *Imitoceras (Prionoceras?)* sp., pl. 24, figs. 1a–1b).

Ac. (St.) cf. procedens (e.g. Becker et al. 2016a: fig. 6.3) and ***Ac. (St.) prorsum* Group** (see Korn et al. 1994: fig. 18I) in the Hangenberg Sandstone (Bed 95) at Brewer.

3. Middle part (Upper Crisis Interval I, upper UD VI-F, basal Stockum Limestone and shale equivalents still without *Pr. kockeli*, *ckI*)

Post. nigra and *Post. evoluta* from limestones nodules in the lower part of the Stockum Level Black Shale (Bed 97) at Brewer (Korn 1991; Korn et al. 1994b).

4. Upper part (Upper Crisis Interval II, UD VI-F/LC I-A₁, depending on the future GSSP position, Lower Stockum Limestone and equivalents with *Pr. kockeli*)

Ac. (St.) subbilobatum (auct.) and *Ac. (Stockumites)* sp. (including *Ac. (St.) cf. prorsum* of Becker 1988 and *Ac. acutum* of Korn 1993 and Luppold et al. 1994) from the dark-grey, calcareous top of the Hangenberg Shale (Stockum Level Black Shale) at Hasselbachtal (Bed 85).

Post. nigra, *Post. evoluta*, ***Ac. (St.) intermedium*** (auct.), and *Ac. (St.) cf. prorsum* from limestone nodules in the upper part of the Stockum Level Black Shale (Bed 100) at Brewer (Korn 1991; Korn et al. 1994b).

Ac. (Str.) carinatum in the Lower Stockum Limestone (Beds 1 and 1/2) at Brewer (Korn et al. 1994b; Becker et al. 2016b).

Ac. (Str.) carinatum, ***Ac. (Str.) caesari***, and ***Ac. (St.) kleinerae*** in the probable Lower Stockum Limestone of section Steinberg Brook (B224 building site, Korn 1992b).

Ac. (Str.) cf. carinatum and *Ac. (Stockumites)* sp. in Bed 2H (38; Lower Stockum Limestone) at Apricke.

Unspecified acutimitoceratid assemblage of Effenberg (Beds 18b–c).

Ac. (St.) prorsum, ***Ac. (St.) stockumense***, *Ac. (St.) subbilobatum* (auct.), *Ac. (St.) intermedium* (auct.), *Ac. (St.) kleinerae*, *Ac. (Str.) carinatum*, and *Ac. (Str.) caesari* from the type Stockum Limestone (Bed 103, upper part of *Pr. kockeli* Zone) of Stockum (Schmidt 1924a; Korn 1984, 1994).

5. Uppermost part (Upper Crisis Interval III, LC I-A₁, Upper Stockum Limestone with *Pr. kuehni*):

Abundant juvenile acutimitocerids from the Upper Stockum Limestone (Bed 100) at Stockum (*Pr. kuehni* recorded by Alberti et al. 1974; Sample 330).

Ac. (St.) intermedium (auct.), *Ac. (St.) subbilobatum* (auct.), *Ac. (St.) kleinerae*, and *Ac. (Str.) carinatum* from the lower part of the Upper Stockum Limestone (Bed 3a) at Müssenberg (Korn 1993; Luppold et al. 1994).

Ac. (St.) stockumense, *Ac. (St.) procedens*, *Ac. (St.) kleinerae*, *Ac. (St.) intermedium* (auct.), *Ac. (St.) subbilobatum* (auct.), and *Ac. (Str.) carinatum* from the upper part of the Upper Stockum Limestone (Bed 3A) at Müssenberg (Luppold et al. 1984; Korn 1993).

Ac. (St.) intermedium (auct.) and the youngest Rhenish clymeniid, *C. striata*, from the top of the Stockum Limestone at Müssenberg (Luppold et al. 1984; Korn 1989, 1993).

This summary suggests that *Ac. (Str.) carinatum*, *Ac. (Str.) caesari*, *Ac. (St.) kleinerae*, and *Ac. (St.) stockumense* may have potential for a future subdivision of the *Ac. (St.) prorsum* Zone. However, this is based on combined evidence, not on a locality with a faunal sequence. Therefore, we regard the current knowledge as too premature to propose subzones. The type level of the poorly known *Ac. (St.) infracarbonicum* (Paeckelmann, 1913) in the former Am Haken Brickwork Quarry of the Wuppertal region probably falls in the Upper Crisis Interval but cannot be placed with any precision. The taxonomic identity of Rhenish *Ac. (St.) subbilobatum* and *Ac. (St.) intermedium* with the types from Franconia requires modern studies of ontogenetic morphometry.

Gattendorfia subinvoluta Zone and Subzone (Vöhringer 1960, LC I-A₂)

Synonym: *Acutimitoceras (Acutimitoceras) acutum* Zone (Vöhringer 1960).

Reference sections: Oberrödinghausen (Beds 6b–6a), Hasselbachtal (Beds 80H–73H), Müssenberg (Bed 3C–2), Dreher (Bed 3).

Other marker species: *Acutimitoceras (A.) acutum* (Oberrödinghausen, Bed 6), *Wey. reticula* (Oberrödinghausen, Bed 6), “G.” *costata* (Hasselbachtal, Bed 80, Korn and Weyer 2003), *G. involuta* (Oberrödinghausen, new record from the upper part of Bed 6), *H. sphaeroidalis* (Oberrödinghausen, Bed 6), *Ac. (St.) undulatum* (Oberrödinghausen, Bed 6), *Ac. (St.) antecedens* (Oberrödinghausen, Bed 6), *Ac. (St.) convexum* (Oberrödinghausen, Bed 6), “Mim.” *simile* (Hasselbachtal, cf. Bed 80).

Discussion: As noted in the taxonomic appendix, there are morphological differences between the types of *G. subinvoluta* from Franconia and assumed Rhenish representatives of the species. This may reflect the biogeographic separation by a narrow oceanic system.

Conodont correlation: The base of the zone falls in the ca. middle part of the *S. (Eo.) sulcata* s.l./*Pr. kuehni* Zone (Hasselbachtal, Bed 80; Dreher, Bed 3a).

“*Eocanites*” *nodosus* Subzone (new, LC I-A₃)

Reference sections: Oberrödinghausen Railway Cut (Beds 5c–5a), Hasselbachtal (Beds 72H–ca. 62H), Müssenberg (Bed 1), Dreher (Beds 3a–5a).

Other markers: *Voehringerites peracutus* (Oberrödinghausen, Beds 5c–5a2, Becker and Weyer 2004; Hasselbachtal, Bed 72H), *Ac. (Str.) heterolobatum* (Oberrödinghausen, Bed 5), *N. trochiforme* (Oberrödinghausen, Bed 5), *N. subacre* (Oberrödinghausen, Bed 5), “Wey.” *concava* (Oberrödinghausen, Bed 5).

Discussion: The “*Eoc.*” *nodosus* Group differs in its square, rectangular to sulcate cross-sections clearly from the typical, younger *Eoc. supradevonicus* Group, which is characterised by well-rounded whorls. This should be used for a distinction at generic level.

Conodont correlation: At Dreher (Bed 3a), the oldest *Eocanites* sp. pre-dates the FAD of *S. (Eo.) bransoni*. At Hasselbachtal, *V. peracutus* and “*Eoc.*” *nodosus* occur in the lower part of the *S. (Eo.) bransoni* Zone. At Oberrödinghausen, *V. peracutus* is recorded from the top of the *S. (Eo.) sulcata* s.l./*Pr. kuehni* to the lower *S. (Eo.) bransoni* Zone (Becker and Weyer 2004). Much younger (level with *Ps. triangulus triangulus*) is the supposed *V. peracutus* from Müssenberg (Bed 1, Luppold et al. 1994), which likely affinities with the Karagandoceratidae have been raised by Korn and Weyer (2003, p. 99) and Becker and Weyer (2004, p. 29).

Paprothites dorsoplanus Zone and Subzone (Vöhringer 1960, LC I-B₁)

Reference sections: Oberrödinghausen Railway Cut (Beds 4b–4a), Hasselbachtal (Beds ?59H–58H).

Other marker species: *Globimitoceras globiforme* (Oberrödinghausen, Bed 4), *H. multisulcata* (Oberrödinghausen, Bed 4), “*Mim.*” *exile* (Oberrödinghausen, Bed 4).

Conodont correlation: At Hasselbachtal and Oberrödinghausen, the base of the zone corresponds closely to the base of the *S. (S.) duplicata* Zone.

Paragattendorfia sphaeroides Subzone (new, LC I-B₂)

Reference sections: Oberrödinghausen Railway Cut (Beds 3e–3d₁), Hasselbachtal (Beds 57H–51H, see Korn and Weyer 2003), Oese (Korn-Beds 22–27 = Kaiser-Beds 16–19).

Other marker species: *Costimitoceras ornatum* (Oberrödinghausen, Bed 3e), *H. gracilis* (Oberrödinghausen, Bed 3d; Hasselbachtal, Bed 57H), *Wey. molaris* (Oberrödinghausen, Bed 3e; Hasselbachtal, Bed 57H), *Pap. raricostatus*

(Oberrödinghausen, Bed 3d), *Pap. ruzhencevi* (Hasselbachatal, Bed 57H), *Paragattendorfia* n. sp. II of Korn and Weyer (2003; Oese, Korn-Bed 22 between Beds L and M).

Discussion: It is possible that *Parag. sphaerooides* Weyer, 1972 is a junior synonym of the poorly known type species of the genus, *Parag. humilis* Schindewolf, 1924. If this is confirmed, the subzone name will have to be changed. An involute variant with slightly higher whorls than in typical specimens, *Parag. cf. sphaerooides*, is illustrated in Fig. 3n–o.

Conodont correlation: At Oberrödinghausen, the zonal base lies in Bed 3e below the FOD of several indicators of the higher *S. (S.) mehli* Zone (in Bed 3d2 = Voges-Sample 10 = Ziegler-Bed 10), such as *S. (S.) cf. wilberti*, *S. (S.) lobata* M1, *S. (S.) belkai* M2, and *S. (S.) obsoleta*. The Hasselbachatal record from Bed 57H post-dates the first *S. (S.) cooperi* (M2), which indicates a position above the base of the *S. (S.) mehli* Zone. At Oese, the *Paprothites-Paragattendorfia* fauna (Korn-Bed 22 = Kaiser-Bed 16) is not well dated by conodonts. *Siphonodella (S.) belkai* M1, an indicator for the *S. (S.) mehli* Zone, was recorded by Kaiser et al. (2017) from just above (Kaiser-Bed 17).

Pseudarietites westfalicus Zone (Vöhringer 1960, LC I-C)

Reference sections: Oberrödinghausen Railway Cut (Beds 3c₂–3a), Hasselbachatal (Bed 49H), Oese (Korn-Beds 28 to ca. 33 or higher), Dreher (Bed 10).

Other marker species: *Pseudarietites subtilis* (Oberrödinghausen, Bed 3c; cf. Oese, Korn-Bed 28), *Eoc. brevis* (Oberrödinghausen, Bed 3c), *Eoc. tener* (Oberrödinghausen, Bed 3c), *Eoc. spiratissimus* (Oberrödinghausen, Bed 3c).

Subdivision: At Oberrödinghausen, a range of taxa enter somewhat higher in the zone, which may enable the separation of an upper or *G. crassa* Subzone (Beds 3b–3a, LC I-C₂). Characteristic at this higher level are *Kaz. evoluta*, *N. acre*, *Ac. (St.) depressum*, and *Pseud. carinatus* (here transferred from *Eocanites* because of its concave ribs, keel, and *Pseudarietites*-type sutures). An entry of *Kaz. evoluta* above the oldest *Pseudarietites* is also known from Oese (Korn and Weyer 2003, Korn-Bed 30). *Pseudarietites planissimus* occurs at Oberrödinghausen near the top of the *westfalicus* Zone (see Korn 2006). A fauna with *G. crassa* has also been mentioned from the Attendorn-Elspe Syncline (Weber 1934).

Conodont correlation: At Oberrödinghausen, the base of the zone lies in the middle between the FODs of *S. (S.) obsoleta* and *Ps. triangulus triangulus*, ca. in middle to higher parts of the *S. (S.) mehli* Zone. The zonal occurrences at Hasselbachatal and Oese belong also to this time interval. The levels with *Kaz. evoluta* at Oberrödinghausen and Oese are still within the same conodont zone.

Paragattendorfia patens Zone (LC I-D)

Reference sections: Oberrödinghausen Railway Cut (Beds 2b–1a), Oese (Korn-Beds 36–38).

Other marker species: *Eocanites supradevonicus* (Oberrödinghausen, Bed 2; Oese, Bed S = Korn-Bed 36, Kullmann in Becker et al. 1993). Korn and Weyer (2003), however, noted an *Eoc. cf. supradevonicus* already lower at Hasselbachatal (Bed 51H), in association with the last local *Paprothites* (top LC I-B). Following Korn (2006, fig. 2), *Paralytoceras crispum* enters at Oberrödinghausen at the base of the *patens* Zone.

Subdivision: The entries of *Eoc. planus* and *Pseud. serratus* in Bed 1 of Oberrödinghausen can possibly be used to define an upper subzone. However, since the type level is relatively poor in fauna (Vöhringer 1960), additional data are needed. Korn (1988a) described an isolated corresponding faunule with *Pseud. cf. serratus* from Hoppecke in the eastern Sauerland.

Conodont correlation: At Oberrödinghausen, the base of the zone slightly post-dates the base of the *S. (S.) sandbergi* Zone (Bed 3a, Korn and Weyer 2003). In the absence of index conodonts, the beds with *Eoc. supradevonicus* at Oese cannot be correlated with precision. The entry of *Pseud. serratus* in the upper part of the *Parag. patens* Zone pre-dates at Oberrödinghausen the FOD of *S. (S.) lobata* M1 (in Bed 1a = Ziegler Bed 17 = Voges Sample 11).

LC I-E

North African goniaticite successions (eastern Anti-Atlas: Ebbighausen and Bockwinkel 2007, southern Algeria: Ebbighausen et al. 2004) showed the existence of a fifth lower Tournaisian zone (LC I-E) with the index genus *Kahlacanites* below the Lower Alum Shale Event Interval at the base of the middle Tournaisian (basal Tn 2 of classical substage subdivision). There are no corresponding goniaticite faunas from any European section. However, the top of the Rhenish Hangenberg Limestone is marked by a variably thick unfossiliferous shale unit. This should be regarded as an equivalent of the Gondwana *Kahlacanites* interval and may represent a long time interval.

Event stratigraphy (Fig. 1)

Kaiser et al. (2015) and Becker et al. (2016a) introduced informally a new terminology and subdivision of the extended Hangenberg Crisis Interval, which is formalised and refined here. Using lithostratigraphic units of the northern Rhenish Massif as examples/reference, the new scheme will add

precision to global correlation and provide distinctive, unequivocal terms to be used during the ongoing GSSP search. Refined information from other regions may lead to the recognition of further event stratigraphical units. The subdivision of the Hangenberg Crisis Interval in the Rhenish Massif (from base to top) is as follows:

Crisis Prelude (initial regressive interval)

- Part I. Dreher Sandstone with *Post. evoluta* or increasing condensation and macrofossil accumulation in the upper Wocklum Limestone, top *W. denckmanni* Subzone (UD VI-D₁); supposed equivalents in the neritic facies of the Velbert Anticline (see Paul 1937a, 1939a).
- Part II. Top Wocklum Limestone with *Epi. applanata* (UD VI-D₂) and diverse pre-extinction faunas.

Lower Crisis Interval (transgressive and climatic warming interval)

- Part I. Hangenberg Mass Extinction (base UD VI-E, base ckl) with the sudden onset of anoxia/euxinia (local pyrite lags).
- Part II. Hangenberg Black Shale with restricted *Post. cf. evoluta* Fauna, basal LN Zone; supposed oxic equivalents with rich benthic fauna in the Velbert region (see sections of Paul 1939a).

Middle Crisis Interval (glacial regressive interval)

- Part I. Hangenberg Shale (greenish-grey) with basal *Ac. (Stockumites)* fauna (base UD VI-F).

- Sequence boundary -

- Part II. Hangenberg Sandstone, Seiler Conglomerate or lateral upper parts of the Hangenberg Shale, oolithic or neritic limestones, with *Pr. meischneri* and *Pr. collinsoni* (middle ckl), lower *Ac. (Stockumites)* faunas (middle UD VI-F).

Upper Crisis Interval (initial post-glacial transgressive interval)

- Part I. Basal Stockum Limestones (first limestones above Hangenberg Sandstone) or Stockum Level Black Shales (partly marly or with limestone nodules), still only with *Pr. meischneri* and *Pr. collinsoni* (upper ckl), middle *Ac. (Stockumites)* faunas (upper UD VI-F).

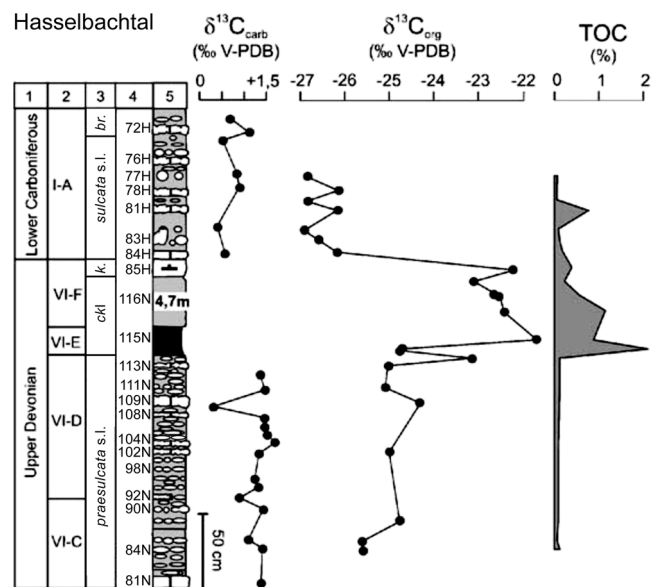


Fig. 4 Top-Devonian to basal Tournaisian carbon isotope values from carbonate ($\delta^{13}\text{C}_{\text{carb}}$) and organic matter ($\delta^{13}\text{C}_{\text{org}}$) at Hasselbachatal, showing the marked positive excursion of the second starting in the Hangenberg Black Shale (basal ckl) and lasting into the marly Stockum Level Black Shale (ca. *Protognathodus kockeli* Zone) of Bed 85N (extracted and modified from Kaiser et al. 2006, fig. 6C, with simplified lithology of limestone nodules and nodular limestone in white, shale and siltstone in grey, black shale = Bed 115N, and dark-grey marl = Bed 85H). 1 = chronostratigraphy, 2 = ammonoid zonal key after Becker (1996), 3 = conodont zonation, 4 = bed numbers, 5 = lithology, TOC = total organic carbon.

Part II. Lower Stockum Limestones with *Pr. kockeli* (s.l.) or Stockum Level Black Shale (e.g. calcareous black shale of Hasselbachatal) with upper *Ac. (Stockumites)* faunas, locally with subdivisions. Slightly higher follows the LN/VI Zone boundary, the main terrestrial extinction level, possibly also the main extinction level in neritic facies, which lies above the *Pr. kockeli* FAD.

Part III. Upper Stockum Limestones with *Pr. kuehni* and uppermost *Ac. (Stockumites)* faunas (current LC I-A₁); *S. (Eo.) sulcata* s.l. may be rarely present; locally with encrinites or turbidites (subdivisions) at the base.

(local parasequence boundary)

Post-Crisis Interval

Basal part: Basal Hangenberg Limestone, overlap of *S. (Eo.) sulcata* s.l. and *G. subinvoluta* (LC I-A₂) Zones.

Main part: Main Hangenberg Limestone, *S. (S.) bransoni* to *S. (S.) sandbergi* zones, *Pap. dorsoplatus* to *Parag. patens* Zones (LC I-B to D).

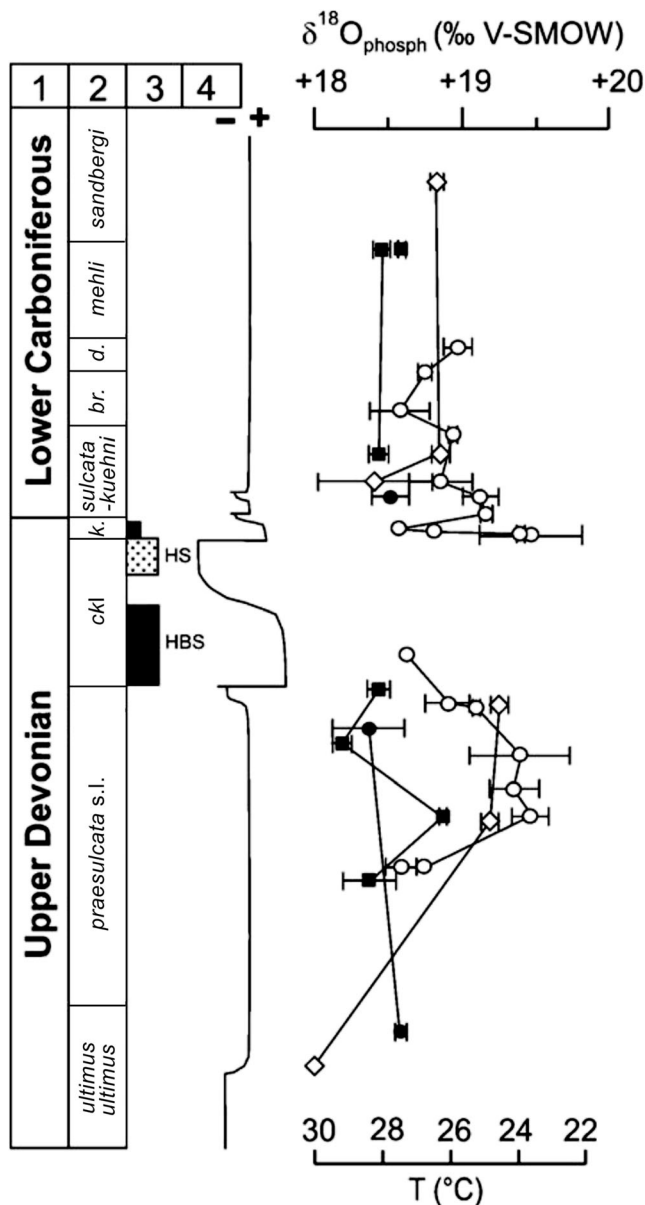


Fig. 5 Pelagic sea surface palaeotemperatures (black dots and squares) calculated from oxygen isotope values of conodont phosphate from the uppermost Famennian and basal Tournaisian of Hasselbachtal (dots) and the Oberrödinghausen Railway Cut (squares), extracted and modified from Kaiser et al. (2006, fig. 7). 1 chronostratigraphy, 2 conodont zonation (compare Fig. 1 to understand abbreviations), 3 marker units, 4 sea-level curve; HBS Hangenberg Black Shale, HS Hangenberg Shale/Sandstone.

Stable isotope stratigraphy

In the Rhenish Massif, DCB carbon and oxygen stable isotope analyses were conducted bed-by-bed at Hasselbachtal (Figs. 4, 5), Oberrödinghausen (Fig. 5), and Oese (Kaiser 2005; Kaiser et al. 2006). Carbon isotopes of micrites ($\delta^{13}\text{C}_{\text{carb}}$) and of sedimentary organic matter ($\delta^{13}\text{C}_{\text{org}}$) were used to reconstruct variations in the carbon isotope composition of the oceanic dissolved inorganic carbon pool. During

marine anoxia, global black shale deposition (HBS), and enhanced organic carbon burial, a pronounced positive carbon isotope excursion (CIE) could be recorded at Hasselbachtal (Fig. 4). The CIE is well correlated with a CIE measured in black shales at Kronhofgraben (Carnic Alps), in continuous pelagic limestone successions at Grüne Schneid (Carnic Alps), as well as with positive peaks measured in several other distant regions worldwide (see review in Kaiser et al. 2015). Thus, carbon isotopes can be used as a chemostratigraphic tool to record the level of the anoxic Lower Crisis Interval (HBS) even when there are locally no black shales.

Conodont apatite is used for the analyses of $\delta^{18}\text{O}_{\text{phosph}}$ because it has a high preservation potential of the primary isotopic signature and is considered to be unaffected by diagenesis. The oxygen isotopic composition of biogenic phosphate is dependent on temperature and composition of ambient seawater, and can be therefore used as a proxy for estimating sea-surface temperatures and salinity changes. The high abundance and high morphological diversity of conodonts provides a detailed bio- and chemostratigraphic resolution and the correlation of sections from different palaeogeographical realms. In this respect, the oxygen isotope values measured from Hasselbachtal, Oese, and Oberrödinghausen (Fig. 5) are similar to values from other sections in Spain (Pyrenees) and France (Montagne Noire). Slightly decreasing values from the *Bi. ultimus ultimus* Zone to the lower Tournaisian indicate a minor warming during the corresponding time span, if there was no influence of palaeosalinity, and without details for the intervening Hangenberg Crisis Interval. In the Rhenish Massif, no conodonts were available from the *ckl*. Records of a cooling episode, probably time-equivalent to the regressive Middle Crisis Interval, were observed in equivalent successions of the Carnic Alps (Kaiser et al. 2006).

Sequence stratigraphy

The successions of the Rhenish Massif have been used as a reference for DCB sequence stratigraphy (Van Steenwinkel 1993; Bless et al. 1993; Kaiser et al. 2011, 2015). A gradual shallowing upwards of the depositional environments is evident in the upper part of the Wocklum Limestone by increasing condensation (reduced sedimentation rates), a consequently strongly increasing fossil content, and by the return of shallow pelagic taxa, such as large-eyed trilobites or tabulate corals (Becker et al. 2016b). This highstand episode was followed by the local “Drewer Sandstone” (Crisis Prelude I, Fig. 1), which can be regarded as a lowstand deposit and its base represents a (para)sequence boundary. In the neritic realm of the eastern Velbert Anticline (Fig. 6), there are correlative pre-Crisis oolites and sandy beds, changing laterally (Wuppertal region) into red shales, marls, and limestones (Am Haken Brickwork Quarry). In several Sauerland sections (Dasberg, Reigern, Kattensiepen), the upper part of the

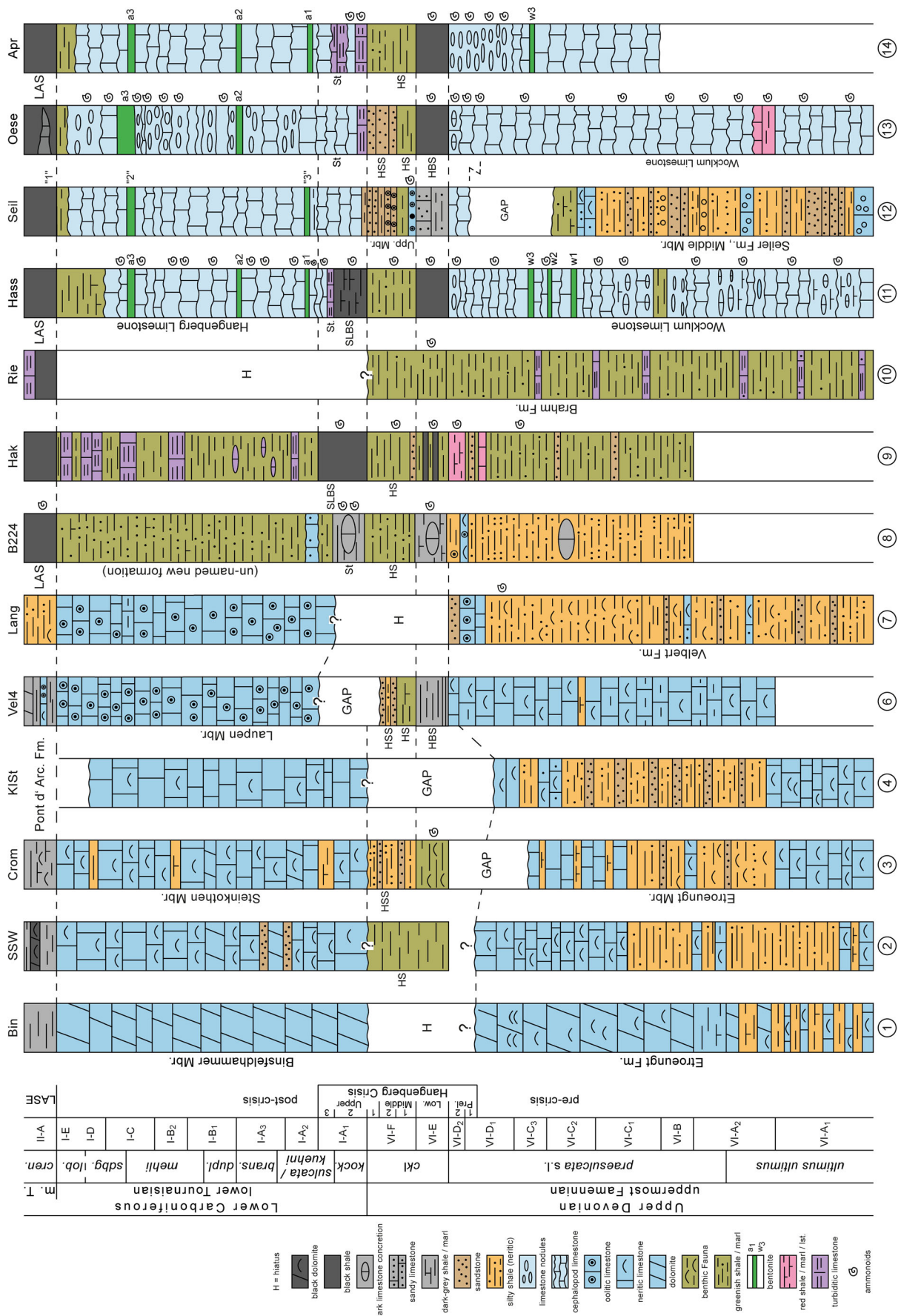
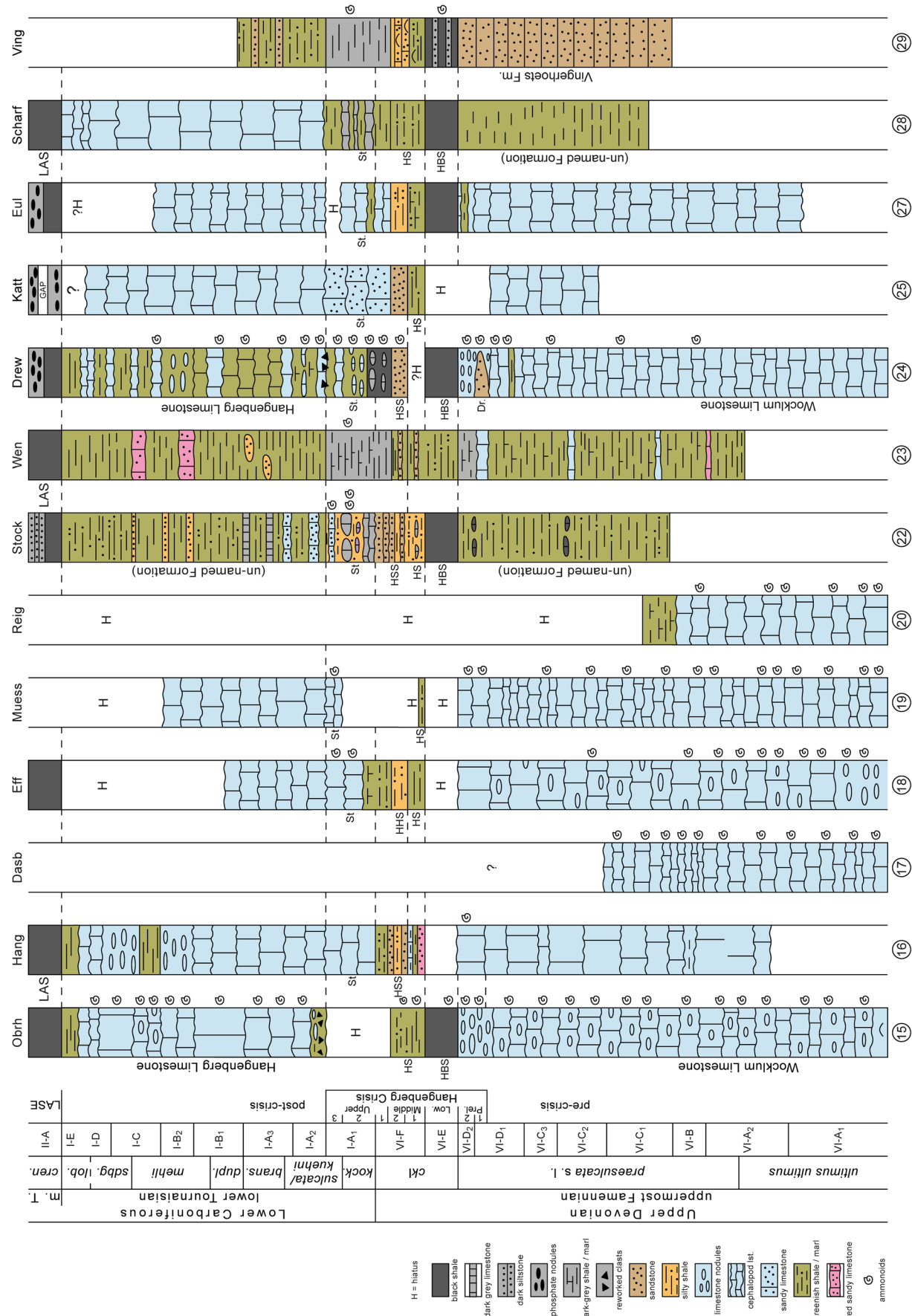


Fig. 6 Summary of facies developments in DCB sections of the Aachen, Velbert, and Wuppertal to Hennei regions. *Bin* Binsfeldhammer, *SSW* Stüchtel-Stittard Well, *Crom* Ratingen-Cromford, *K/St* Klein-Steinkothen, *Vel* Velbert 4 Well, *Lang* Langenhorst, *B224* B224 section near Aprath, *Hak* former Am Haken Brickwork Quarry, *Rie* Riescheid, *Hass* Hasselbachthal, *Oese* B7 road cut at Hennei-Oese, *Apr*-Hennei-Apricke, *HBS* Hangenberg Black Shale, *HSS* Hangenberg Sandstone, *S* Stockum Limestone, *SLBS* Stockum Level Black Shale, *Upp. Mbr.* Upper Member (of Seiler Formation), *LAS* Lower Alum Shale, *LASE* Lower Alum Shale Event, “1” to “3” = correlation levels sensu Clausen et al. (1989a); ammonoid zonal key (e.g. VI-B, I-C) as explained in the text, *ckl costatus-kockei* Interregnum, *kock kockeli*, *transsoni*



◀ Fig. 7 Summary of facies developments in DCB sections of the Sauerland and northern subsurface (section numbering as in the text). *Obrh* Oberrhödinghausen Railway Cut, *Hang* Hangenberg, *Dash* Dasberg, *Eff* Effenberg, *Muess* Müssenberg, *Reig* Reigern Quarry near Hachen, *Stock* Stockum Trenches (mostly Trench II), *Wen* section E of Weninghausen, *Drew* Provincial Quarry Drewer, *Katt* Kattensiepen Quarry, *Eul* Eulenspiegel, *Scharf* Scharfenberg, *Ving* Vingerhoets 93 Well near Oelde. For other abbreviations, see Fig. 6.

Wocklumian falls in a time of current-induced non-deposition (Fig. 7). The shallowing at the “Drewer Sandstone” level can be recognised in many parts of the world and represents a global pre-Crisis sea-level drop (Kaiser et al. 2011, 2015), possibly related to an initial glacial cooling.

The Hangenberg Black Shale and its less anoxic, grey to greenish equivalents in western sections (Cromford, Velbert 4 Well, B224 near Aprath; Fig. 6) represent a sudden transgressive episode and phase of maximum flooding, defining the Lower Crisis Interval. The pyrite-enriched, often sharp base of the black shales suggests an anoxic marine flooding surface at the base of a TST, which is the level of the main Hangenberg Extinction, at least in the pelagic realm. The transgressive nature of the HBS is underlined by sections, where greenish, dark-grey, or black (hemi)pelagic shales, often with *Post. cf. evoluta*, overly shallow-water strata, such as neritic limestones (Cromford, Velbert 4 Well, Fig. 6), oncoidal siltstones (B224 near Aprath, Fig. 6), or sandstones (Vingerhoets 93 Well, Fig. 7). Similar patterns can be seen on other continents (Kaiser et al. 2015; Zhang et al. 2019).

The gradual change from the HBS to greenish and silty shale marks the slowing of sea-level rise to beginning sea-level fall and regression. The Hangenberg Shale is a pelagic highstand deposit (FSST) still low in the LN miospore Zone (Middle Crisis Interval I).

A subsequent main lowstand phase (LST) is represented by the locally increasing influx of coarser clastic sediments, the Hangenberg Sandstone, and its equivalents, such as siltstones (Drewer, Borkewehr) or thick, re-sedimented oolithic conglomerates and siliciclastics of the Seiler area (Fig. 7). A sequence boundary is placed at the base of the sandstones, conglomerates, or reworked oolites. The latter represents basin floor fans and incised valley fills above marine unconformities (e.g. Van Steenwinkel 1993). Herbig (2016) used the Hangenberg Sandstone base to define his Sequence 1. Both in the western realm (Aachen region: Binsfeldhammer, Velbert Anticline: Langenhorst; Fig. 6) and in the deeper facies of the Sauerland (Müssenberg, Kattensiepen, Drewer; Fig. 7), the sea-level fall caused gaps due to erosion and/or non-deposition. The partly much thicker HSS equivalent clastic deposits of other regions and continents correspond with a maximum lowstand (LST) in the higher LN miospore Zone and upper *cI* (Middle Crisis Interval II).

In the eastern Rhenish Massif, the Upper Crisis Interval (DCB interval) is characterised by a return to carbonate

sedimentation and condensed, fully pelagic conditions. This transgressive (TST) interval is characterised by the polyphase Stockum Limestone deposits, including some turbiditic limestones (Hasselbachatal, Oese, Apricke; Fig. 7), or by partially correlative, pyritic, or organic-rich Stockum Level Black Shales (SLBS, Am Haken Brickwork Quarry, Hasselbachatal; Figs. 6, 7), sometimes with embedded, fossiliferous limestone nodules (B224 near Aprath, Drewer). For the precise DCB positioning and correlation, it is important to realise that the first limestone level above the HS/HSS is locally of variable age (Fig. 7), from the top *cI* with *Pr. collinsoni* (Drewer, ?Eulenspiegel; Upper Crisis Interval I), to the *Pr. kockeli* (Oese, Apricke, Hangenberg, Stockum; Upper Crisis Interval II) or even *S. (Eo.) sulcata* s.l./*Pr. kuehni* Zone (Hasselbachatal; Upper Crisis Interval III). In the neritic Ardennes and Aachen region (western Rhenish Massif), the shallow-water limestones of the basal Hastière Formation begin with the *Pr. kockeli* Zone. But at the Velbert Anticline, the lack of conodonts prevents the precise dating of the basal Steinkothen and oolithic Laupen Members. Locally, there is evidence for a minor sea-level fall separating Lower and Upper Stockum Limestones (Lower and Upper *Protognathodus* levels, Upper Crisis Intervals II and III; Fig. 7), or marls with *Ac. (Stockumites)* faunas and the latter (Hasselbachatal; Fig. 6). It caused the minor unconformity in the Oberrhödinghausen Railway Cut, which disqualified it as DCB stratotype. A slightly younger reworking phase may lie at the base of the Hangenberg Limestone (Drewer), within the *S. (Eo.) sulcata* s.l./*Pr. kuehni* Zone; it marks the end of the Upper Crisis Interval.

The polyphase top-Devonian to basal Tournaisian (basal Mississippian) transgression (Sequence 1 of Herbig 2016) is well expressed on a global scale (Kaiser et al. 2015). The Hangenberg Limestone represents a highstand interval (HST), in which the fossil content becomes gradually sparser, changing eventually into a shaly interval. The sharp base of the anoxic to euxinic, basal middle Tournaisian Lower Alum Shale (LAS) represents the very sudden onset of a second Lower Carboniferous TST (base of Sequence 2 of Herbig 2016). It is equally distinctive in the western neritic realm, where it is expressed by the less anoxic and partly fossiliferous Pont d’Arcole Formation that drowned the Hastière Formation carbonate platform (Fig. 6).

Trace element geochemistry, magnetic susceptibility, and cyclostratigraphy

Trace element geochemistry and gamma ray spectroscopy (CGR values) are important tools to reconstruct changes of detrital discharge, redox conditions (U/Th), and palaeoproductivity around the DCB. Magnetic susceptibility (MS) logging provides insights into changes of sedimentation and condensation.

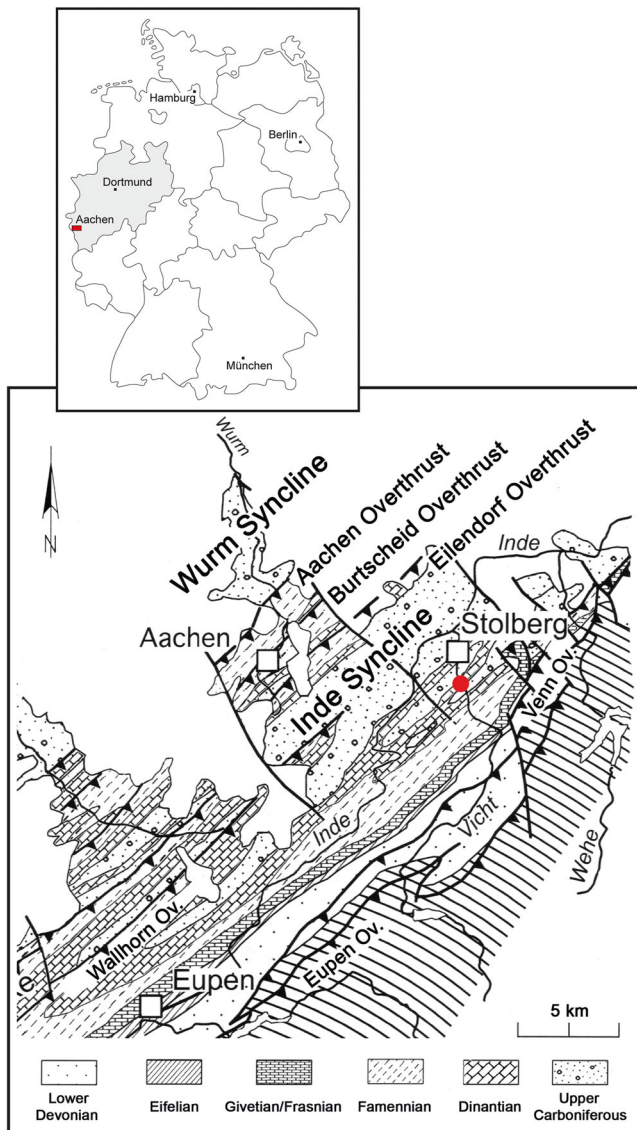


Fig. 8 Geographic location of the Binsfeldhammer DCB section in the Aachen region of the western Rhenish Massif (extracted and re-drawn from Walter 2010, fig. 14)

tation, especially in relation to sea-level change. These methods, therefore, complement litho- and sequence stratigraphy. In addition, they are most useful to delineate cyclostratigraphic patterns, which are strongly expressed in the Wocklum and Hangenberg Limestones. For refined cyclostratigraphic correlations, it will be most important to tie each cycle to precise bed numberings and the biostratigraphical scales (see Korn and Weyer 2003). Kumpan et al. (2015), Becker et al. (2016b), and Hartenfels et al. (2017a, b) provided relevant data for four Rhenish DCB sections: Oese, Oberrödinghausen, Dreher, and Borkewehr. They support the general interpretations of sedimentary environment, microfacies, palaeoecology, sea-level changes, and event patterns as summarised by Kaiser et al. (2015).

Section descriptions

Aachen region and Niederrhein

In terms of sedimentation and lithostratigraphy, the DCB transition of the Aachen region continues the shallow-water setting of the eastern Ardennes. The Belgian formation terminology (e.g. Bultynck and Dejonghe 2002; Poty et al. 2002) can be largely adopted. The term Dolhain Formation, used for equivalents of the Etroeungt Formation in the Vesdre Nappe of Belgium (e.g. Bultynck and Dejonghe 2002), has not yet been accepted on the German side (e.g. Ammer and Herbig 2006; Kasig and Reissner 2008). Currently, the only moderately good DCB outcrop is at Binsfeldhammer in the Burgholz Syncline.

Binsfeldhammer (Fig. 6)

Location: Slope of the road cut branching off from the Volberg-Vicht road towards Hastenrath, west of the middle/upper Tournaisian Binsfeldhammer Quarry, at r 2 516 900, h 5 624 800 on topographic sheet 5203 Stolberg (Fig. 8).

Literature: Paul (1937a: type locality of *Syringopora (Vaughanites) flabelliformis*), unpublished Ph.D. Thesis by Reissner (1990), Kasig and Reissner (2008: section log), Ammer and Herbig (2006: type section of the Binsfeldhammer Subformation = Member). For more literature, see the review by Becker and Weber (2016).

Summary of succession:

Pont d'Arcole Formation (previously “*peracuta* Shale” or “Zwischenschiefer”): Unfossiliferous dark shales, with the major deepening of the Lower Alum Shale Event at the base; middle Tournaisian.

Hastière Formation, Binsfeldhammer Member: Ca. 3.5 m of cross-bedded dolomites with rare syringoporid corals above the last level with stromatoporoids; with *Pr. kockeli* in the lower part and *S. (S.) duplicata* in the higher part in the lateral Neu-Moresnet section (Reissner 1990). Age: *Pr. kockeli* Zone (Upper Crisis Interval) to top of lower Tournaisian. Our new sampling at Binsfeldhammer did not produce any conodonts.

- unconformity -

Etroeungt Formation (= Dolhain Formation):

Upper part: Thick-bedded dolomites with numerous relict structures of stromatoporids (indet.), the youngest known from the Rhenish Massif, rugose and syringoporid corals. Repeated sampling did not produce conodonts.

Lower to middle parts: Calcareous shales, thin-bedded limestones and thin- to thick-bedded dolomites with brachiopods, corals, stromatoporids, and foraminifers. *Quasiendothyra kobeitusana*, the index species of the DFZ 7 and for the uppermost Famennian, begins ca. 9 m below the top of the formation.

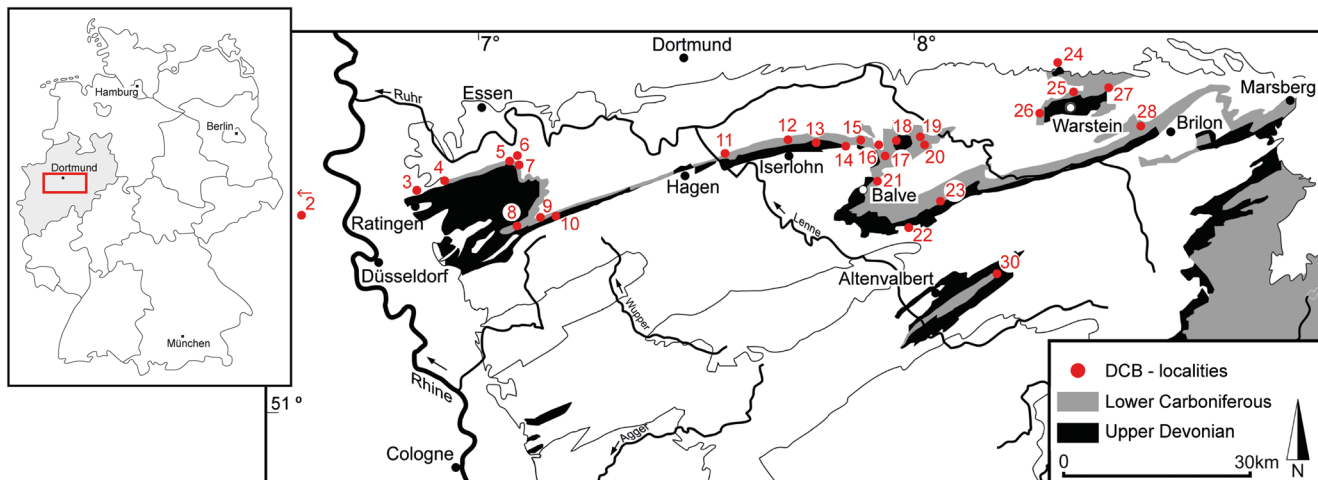


Fig. 9 Geographic location of DCB sections in the Bergisches Land (Velbert Anticline and Wuppertal area) and Sauerland (section numbering as in the text). 2 Süchteln-Sittard Well, 3 Ratingen-Cromford, 4 Klein-Steinkothen, 5 Hefel, 6 Velbert 4 Well, 7 Langenhorst, 8 B224 near Aprath, 9 Am Haken Brickwork Quarry, 10 Riescheid, 11 Hasselbachthal, 12 Seiler N of Iserlohn, 13 Oese, 14 Apricke, 15 Oberrödinghausen Railway Cut, 16 Hangenberg, 17 Dasberg, 18

Effenberg, 19 Müsselfeld, 20 Reigern Quarry near Hachen, 21 Borkewehr/Wocklum, 22 Stockum Trenches, 23 Weninghausen, 24 Brewer, 25 Kattensiepen, 26 Bilstein Cave, 27 Eulenspiegel, 28 Scharfenberg, 30 Grimmighausen. The Vingerhoets 93 Well (loc. 29) lies far outside the map in the subsurface of the eastern Münster Basin, ca. 40 km NNW of Brewer = Loc. 24 (for a detailed map see Clausen 2008)

Discussion: Dolomitisation and poor outcrop conditions prevent an easy recognition of the unconformity. However, there is locally no evidence for sediments of the Lower/Middle Crisis Interval. The Hangenberg Regression may have led to erosion and/or non-deposition. The presence of an unconformity was supported by the analysis and correlation of coral faunas (Weyer 2000). Mottequin and Poty (2014) mentioned from their adjacent Stolberg Section a 2 m thick sandstone-siltstone unit overlying Etroeungt (= Dolhain Fm.) dolomites. This unit, which is unknown at Binsfeldhammer, was interpreted by them as HSS equivalent.

Niederrhein subsurface, Süchteln-Sittard Well 1 (Fig. 6)

Location: Topographic sheet 4704 Viersen, r 2 526 830, h 5 682 220 (Fig. 9).

Literature: Bless et al. (1998), Ribbert (1998, 2008).

Summary of succession: Bless et al. (1998) described the DCB succession that was reached in a borehole in the Krefeld region (Niederhein) between ca. 224 and 265 m depth. It resembled both the Aachen and Velbert regions. It can be summarised as follows, re-assigning the strata to currently used lithostratigraphic units:

Pont d'Arcole Formation: 227.0–231.5 m, bluish-grey, calcareous and pyritic shales, intercalated by two levels of dolomitic limestone with foraminifers (e.g. *Chernyshinella glomiformis*), ostracods and rare trilobites, middle Tournaisian, Lower Alum Shale Event Interval.

Hastière Formation (“Lower Dolomite” = Steinkothen Member): 231.5–243.0 m, bluish-grey, partly dolomitised

and peloidal limestone, in the lower part with an interval of micaceous and calcareous sandstones, with crinoids, ostracods (*Pseudoleperditia*), and rare foraminifers (*Bisphaera*, *Earlandia*, *Diplosphaerina*, *Endothyra*), lower Tournaisian, Middle/Upper or post-Crisis Interval.

Hangenberg Shale equivalent: 243.0–244.5 m, bluish-grey, calcareous shale, Crisis Interval, undifferentiated.

Etroeungt Formation (= Dolhain Formation):

244.5–251.7 m, dark-grey shallow-water crinoidal limestone (grain- and rudstones) with rugose corals (*Campophyllum*, “*Palaeosmilia*”, *Syringaxon*, metriophyllids), syringoporids, a michelinid, stromatoporids, brachiopods, bryozoans, gastropods, ostracods, trilobites (*Omegops*), calcareous algae, miospores (*Retispora lepidophyta*), and foraminifers (*Quasiendothyra kobeitusana*), uppermost Famennian, pre-Crisis Interval.

251.7–258.7 m, dark-grey, silty, laminated shale, with an intercalated unit of crinoid limestone with brachiopods, syringoporids, rare stromatoporids, gastropods, ostracods, eridostracans (*Cryptophyllum*), calcareous algae, and foraminifers (*Q. aff. kobeitusana*), uppermost Famennian.

258.7–259.8 m, bluish-grey limestone and marl with corals (syringoporids, *Campophyllum*, heterocorals), stromatoporids (*Atelodictyon ratingense*, *Amphipora*), calcareous algae, ostracods, and foraminifers (*Q. aff. kobeitusana*), lower part of uppermost Famennian, transgressive on upper Famennian sandstones (= Evieux Formation).

Discussion: The separation of the Etroeungt and Hastière Formations by a shale unit is not known from the Aachen region and suggests an intermediate palaeogeographic position towards

the Velbert region, despite the assumed barrier of a Krefeld High. The latter had probably a different outline than shown in most reconstructions (see brief discussion in Becker et al. 2016b). It is possible that the sandstones intercalated within the “Lower Dolomite” correlate with the Hangenberg Sandstone (Middle Crisis Interval) but the available biostratigraphic data are too sparse for a reliable interpretation.

Velbert Anticline

DCB successions along the northern margin of the Velbert Anticline are characterised by a lateral facies transition (e.g. Franke et al. 1975; Herbig et al. 2001). The upper part of the thick Velbert Formation is characterised in the Ratingen area by the increasing intercalation of limestones with neritic fauna, such as rugose corals, brachiopods, phacopids, stromatoporids, ostracods, and foraminifers. Following Drevermann (1902), Bärtling and Paeckelmann (1928) and Paul (1939a), the term Etroeungt Member is revived for this succession (the former “Etroeungt-Schichten”). It is not wise to neglect this interval of reduced clastic input within an undivided Velbert Formation due to its importance for correlation towards the Ardennes. Because it is unsuitable as a mapping unit, it cannot be separated regionally as a full formation, unlike as in the Ardennes. Future facies and faunal studies may support a lithostratigraphic differentiation between the type Etroeungt Formation of the southern Dinant Syncline, the dolomitised neritic facies settings of the Vesdre-Aachen region (proposed Dolhain Formation), and the Velbert Anticline. There, the term “Angertal Schichten” was established as a lower subdivision of his Etroeungt by Paul (1939a) on faunal, not on lithological, grounds, but it is principally available as a member name if neritic workers agree on a lithostratigraphical definition and type section. As outlined by Amler and Herbig (2006), the uppermost Famennian limestones grade east of Heiligenhaus into a siliciclastic facies with an important influx of oolithic material, especially in the lower Tournaisian (Laupen Member). To the NNW of the Velbert Anticline, DCB beds were once also accessible at two small distinctive saddles of the Lintorf region (sheet 4607 Kettwig). For example, Paul (1938a) suggested the presence of *Postclymenia* in the Diepenbrock area.

Ratingen-Cromford (Fig. 6)

Location: Old, mostly water-filled quarry in the Angerbach Valley in a recreation area N of Ratingen (“Naturpark Blauer See”), NW end of exposed Velbert Anticline (Fig. 9), topographic sheet 4607 Heiligenhaus, r 2 560 000/h 5 686 160 (GPS N 51° 18' 25.44", E 6° 51' 35.4"). An adjacent railway cut is the type locality of the Steinkothen Member (Amler and Herbig 2006) and formed the base for the initial bed-by-bed investigations of Paul (1939a).

Literature: Drevermann (1902: type locality of *Phacops bergicus*, *Sphenotus? ratingensis*, *Prothyris bergica*, and *Euchondria vera*), Nekhoroshev (1932: type locality of the bryozoans *Orthopora bifurcata* and *Monotrypella (?) cromfordensis*), Gallwitz (1932), Liebus (1932: early foraminifer records), Paul (1937a: type locality of *Derbyia steinhagei*, *Clathrodictyon ratingense*, *Buxtonia paeckelmanni*, *Thomasina angusta*, and *Brachythyris ratingensis*; 1938b, 1939a), Conil et al. (1964), Strel (1966, 1969), Conil and Paproth (1968), Paproth and Strel (1970, 1982), Franke et al. (1975), Paproth et al. (1976), Price and Korn (1989), Brauckmann (1990), Amler et al. (1994), Herbig et al. (2001), Aretz et al. (2006), Winkler-Prins and Amler (2006), Ernst et al. (2015).

Summary of succession: The section is well known since the original description by Paul (1939a). Water filled the quarry after it was abandoned, which rendered large parts of the outcrop difficult to access. As noted by Conil and Paproth (1968), there is exposure along the path leading from the park entry to the open-air stage. Coral- and bryozoan-rich beds of the Velbert Formation (Etroeungt Member) are easily accessible along a small paved track along the railway. The DCB interval is as follows:

Pont d’Arcole Formation (“Zwischenschiefer”): Ca. 2.5 m dark, laminated shales, siltstone, and marls with *S. (S.) crenulata*, *S. (S.) quadruplicata*, and other conodonts (*S. (S.) crenulata* Zone), spiriferids, productids and other brachiopods, middle Tournaisian, Lower Alum Shale Event Interval.

Hastiére Formation, Steinkothen Member (type locality, “Ostracodenkalk”):

Beds 24–25, 14.85 m, dark-grey, micritic, argillaceous, partly dolomitic limestone with shale intercalations, crinoids, brachiopods (type level of *Cyrtina ratingensis* (Paul, 1937a), *Piloricilla paeckelmanni* (Paul, 1937a), and of the insufficiently known *Thomasina angusta* Paul, 1937a), abundant fenestellids, ostracods, and corals, at the top with *S. (S.) lobata* (*S. (S.) lobata* Subzone), still with *Quasiendothrya* (Conil et al. 1964, p. 62) and other foraminifers, Upper Crisis Interval to lower Tournaisian (post-Crisis Interval).

Hangenberg Shale/Sandstone:

Beds 23, 16 m grey-brown, sandy, micaceous shales and thin, platy, micaceous sandstones, Middle Crisis Interval.

Hangenberg Black Shale equivalent:

Bed 22, ca. 5m greenish-grey shales, occasionally with sandy lenses, bivalves (*Guerichia*), spiriferids (e.g. *Sphenospira julii*), productids (type level of *Whidbornella caperata paeckelmanni* (Paul, 1939a); *Tornquistia polita*), and *Post. cf. evoluta* (*evoluta* Zone, UD VI-E), Lower Crisis Interval in neritic, (sub)oxic, siliciclastic facies.

- 24 m gap (variably 12–28 m according to different authors) -

Velbert Formation, Etroeungt Member (“Angertal Schichten”):

Beds 20–21, 21.3 m dark-bluish-grey limestones and marls with diverse foraminifers (including *Quasiendothyra* and many others), ostracods (*Cryptophyllus*), trilobites (*Omegops*), bivalves, *Post. cf. evoluta* (“*Striatoclymenia euryomphala*” from Bed 21, Paul 1939a; UD VI-D), syringoporids, rugose corals (“*Palaeosmilia*” *aquisgranensis*), and calcimicrobes (*Girvanella*), pre-Crisis Interval and Crisis Prelude.

Beds 17–19, 13 m sandy and micaceous shale and thin sandstones, interrupted by ca. 1 m of dark-bluish-grey crinoidal limestone (Bed 18); with foraminifers, trilobites (*Omegops*), bivalves, gastropods (*Naticopsis*), brachiopods (productids, orthotetids: type level of *Derbyia steinhagei* Paul, 1937a, orthids, spiriferids, terebratulids), fenestellids, and spores (*Retispora lepidophyta* and many others, floral lists in Paproth and Streel 1970, p. 376, and Paproth and Streel 1982, p. 12; LL Zone).

Bed 16, 8.7 m light- to dark-grey, medium- to thick-bedded, solid crinoidal limestone with stromatoporids (type level of *Clathrodictyon ratingense* Paul, 1937a, pectinid bivalves, brachiopods, solitary rugose corals (“*Palaeosmilia*” *aquis-granensis*), syringoporids, foraminifers (*Quasiendothyra kobeitusana*), pre-Crisis Interval, uppermost Famennian.

Discussion: It is very unfortunate that the critic interval, from very fossiliferous limestones of the assumed Crisis Prelude to the shale with *Postclymenia* and basal Hastière Formation, is currently not accessible. The Cromford section provided unique opportunities for the correlation and intergradation of Rhenish pelagic and neritic successions and for the understanding of DCB extinction patterns in the two shelf realms. As evident from the comments by Winkler-Prins and Amler (2006), the Cromford brachiopods require revision, which is true for most other faunal elements from the locality.

Paul (1939a) mentioned shales with *Post. cf. evoluta* from numerous other adjacent localities on sheet Kettwig: valley below Sondert, debris of the Thalburg Mine, Ruthen, Giesenhaus area, road slope between Roßdelle and Müllerbaum, valley end at Scharpenhaus, Herberg, and Steinloch Mine. It is remarkable that the pure or calcareous *Postclymenia* shales, the supposed shallow-water Hangenberg Black Shale equivalents, yielded also a rich, oxic neritic fauna, consisting of diverse brachiopods (productids, orthids, spiriferids, terebratulids), bivalves (pectinids, nuculids, *Grammatodon*), fenestellid bryozoans, and gastropods. It is especially regrettable that a directly underlying, 10 cm thick bluish-grey, crystalline limestone with numerous *Postclymenia* from Scharpenhaus (Paul 1939a, p. 676, Bed 2) cannot be sampled any more for conodonts, microfacies, or geochemistry.

Klein-Steinkothen (Fig. 6)

Location: Two small old, partly overgrown quarries in the Angerbach Valley E of Eggerscheidt and W of Ratingen-Hösel, NW flank of the Velbert Anticline (Fig. 9), topographic sheet 4607 Heiligenhaus, r 2 563 250/h 5 687 560 (GPS N 51° 19.129', E 6° 54.425').

Literature: Nekhoroshev (1932), Gallwitz (1932: type locality of *Orthotetes wunstorfi*, *Chonetes ratingensis*, *Plicoconetes cromfordensis cromfordensis*, and *Pl. cromfordensis latus*), Paul (1939a), Böger (1962), Conil et al. (1964), Streel (1966), Conil and Paproth (1968), Paproth and Streel (1982), Richter (1992), Ammer et al. (1994), Ammer and Herbig (2006: introduction of the Steinkothen-Subformation = Member), Denayer et al. (2011), Herbig et al. (2019).

Succession: There are remnants of two old limestone quarries, which are separated by an outcrop gap (ridge covered by wood) that is difficult to bridge by trenching. Unfortunately, intense re-sampling did not produce any conodonts from the neritic, shallow-water, mixed limestone-siliciclastic facies. The DCB interval can be summarised as follows (based on Herbig et al. 2019):

Hastière Formation, Steinkothen Member (“Ostracodenkalk”):

Beds 28.1 to 28.16, 6.5 m (up to 8.3 m) medium- to thick-bedded, dark, bluish to black, macrofossil-poor limestones with crinoids, ostracods, foraminifers, calcimicrobes (*Issinella*), rare rugose corals (*Siphonophyllia* at the top, new *Campophyllum* record from Bed 28–3), large-sized *Quasiendothyra kobeitusana* at the base (Conil and Paproth 1968), and with the zonally non-diagnostic *Po. inornatus* s.l. at the top (record of Böger 1962), ?Upper Crisis Interval to lower Tournaisian.

- 10–12 m gap -

Velbert Formation, Etroeungt Member:

Beds 27A–27G, 2.3-m limestone with foraminifers, brachiopods, solitary rugose corals (“*Clisiophyllum*” *omaliusi*), abundant crinoid ossicles, and *Bi. jugosus* (Böger 1962), as an indicator of the pre-Crisis Interval.

Bed 26, 1.2 m silty, bluish-grey, micaceous shale.

Beds 22–25, 1.6 m silty limestones grading upwards into crystalline, crinoidal limestones with brachiopods, solitary rugose corals, and miospores (*Retispora lepidophyta*).

Beds 2–21, 9.15-m alternating calcareous siltstones and sandstones with some plant debris.

Beds 1A–1K, 5.6 m dark-bluish, sometimes nodular, crinoidal foraminifer grainstones (abundant *Quasiendothyra*, *Paracalligeloides*, *Bisphaera*, *Diplosphaerina*, *Eotuberitina* etc.) with calcimicrobes (*Girvanella*), stromatoporids, solitary rugose corals (*Campophyllum*, “*Palaeosmilia*” *aquis-granensis*), and brachiopods, uppermost Famennian.

Lateral section, beds below Bed 1 with a kosmoclymeniid (“*Oxyctylomenia*” of Paul 1939a).

Discussion: It is intriguing that stromatoporids locally do not range to the top of the Velbert Formation. The presence of “Strunian”-type fossils (corals, quasiendothyrids) in the lower part of the Hastière Formation resembles the Cromford succession. It questions the precise extinction level of shallow-water faunas in relation to the pelagic extinction at the base of the Hangenberg Black Shale. Therefore, Denayer et al. (2019) suggested that neritic extinctions occurred on the Ardenne Shelf during the maximum regression (“Hangenberg Sandstone Event”). However, since *Pr. kockeli* enters already in the basal marker limestone of the Hastière Formation (e.g. Bouckaert and Groessens 1976), the survival of various neritic taxa lasted obviously well into the transgressive Upper Crisis Interval. This explains why at Klein-Steinkothen no major regression can be recognised within the exposed Hastière Formation above the level of the last quasiendothyrids and “Strunian”-type corals. In the absence of age-diagnostic conodonts or brachiopods, the timing and patterns of neritic extinction are locally difficult to resolve.

Hefel

Location: Disused, partly pond-filled old quarry N of Velbert (Fig. 9), a natural reserve, at the small settlement Hefel, sheet 4608 Velbert, r 2 573 340, h 5 691 780.

Literature: Bärtling and Paeckelmann (1928), Gallwitz (1932), Paul (1937a), Franke et al. (1975), Paproth et al. (1976), Paproth and Strel (1982), Herbig et al. (2001), Amler and Herbig (2006).

Succession: The 58 m thick succession ranges from the Etroeungt Member to the Richrath Formation. The DCB part is strongly condensed and incomplete. Paproth et al. (1976) illustrated two specimens of *Post. cf. evoluta* (as *Cymaclymenia euryomphala*) from a calcareous silt/sandstone at the base (Bed 1), which may correlate with the “Drewer Sandstone” (Crisis Prelude). This tentative interpretation is based on the fact that the *Postclymenia* level was overlain by probable Hangenberg Shale equivalents (Beds 4–6), followed by thin oolites (Beds 4–6, Laupen Member of Hastière Formation). The section requires new investigations but it is doubtful that the *Postclymenia* level is still accessible. For example, Amler and Herbig (2006) observed that the oolithic basal Laupen Member eroded into the top limestone of the “Strunian”.

Velbert 4 Well (Fig. 6)

Location and literature: NE end of Velbert Anticline (Fig. 9; see map in Herbig et al. 2014).

Succession: The well was regionally unique since it provided an almost complete core through the uppermost Famennian to upper Viséan of the region. The DCB interval was as follows:

Pont d’Arcole Formation: 1.4 m dark-grey shale with two carbonate beds, a bioclastic dolomite and an oncolithic

brachiopod-bearing rudstone, middle Tournaisian, Lower Alum Shale Event Interval.

Hastière Formation, Laupen Member: 8 m oolithic and peloidal grainstone, lower Tournaisian.

- 0.5 m gap -

Hangenberg Sandstone: 10 m alternating grey shale and sandstone, Middle Crisis Interval II.

Hangenberg Shale: 3.5 m calcareous shale, Middle Crisis Interval I.

Hangenberg Black Shale: 1 m irregularly laminated grey shale, Lower Crisis Interval.

Velbert Formation, Etroeungt Member: 30.5 m bioclastic, tempestitic, marly limestone with crinoids, bryozoans, brachiopods, and ostracods, but lacking calcareous algae and age-diagnostic foraminifers

Discussion: The special importance lies in the local recognition of a HBS to HSS sequence, which provides a correlation with the Sauerland-type succession. Unfortunately, there is so far no record of biostratigraphical markers.

Motorway Junction Langenhorst (Fig. 6)

Location: Exposures created temporarily during the construction of the motorway A44 NW of Velbert (Fig. 9), topographic sheet 4608 Velbert, r 2 572 450, h 5 691 320.

Literature: Michels (1986), Haude and Thomas (1989), Amler et al. (1990), Amler (1993), Brauckmann et al. (1993).

Succession: The outcrop was completely covered or grown over after the end of the roadworks. The lower Tournaisian is locally strongly condensed and probably incomplete.

Pont d’Arcole Formation: (“Zwischenschiefere”):

Beds 81–85, ca. 3 m calcareous, argillaceous siltstone with plant remains and neritic fauna (e.g. with *Tylothyris* and *Brachymetopus germanicus*), middle Tournaisian, Lower Alum Shale Event Interval.

Hastière Formation, Laupen Member:

Beds 79–80, upper “oolite-siltstone unit”, ca. 3 m oolites without conodonts, Middle/Upper Crisis Interval to lower Tournaisian.

- ?unconformity (no Hangenberg Black Shale and Hangenberg Shale equivalents) –

Velbert Formation, Etroeungt Member:

Beds 75c–78, lower “oolite-siltstone unit”, first with ca. 2.2 m oolites alternating with micritic limestone and siltstone, then with ca. 1.5 m siltstone; with *Bi. ultimus ultimus* (Beds 75i, 77b, 78a: “*Bi. ziegleri*”), *Bi. costatus*, and *Bi. bispathodus* (*Bi. ultimus ultimus* Zone to *S. (E.) praesulcata* s.l. Zone); ?regressive Crisis Prelude.

Beds 65–75b, top part of “sandstone-siltstone unit”, ca. 9.5 m siltstones with a *Cyrtoclymenia* sp. (Bed 71), phacopids (*Omegops* sp., Beds 65–75b), *Pseudowaribile quae sita* (Beds 67, 71–75b), *Brachymetopus drevermanni* (Beds 71–75b, the oldest species of the genus), *Prospera struniana* (Bed 71), other neritic fauna, and a thin limestone near the top (Bed 74).

Beds 40–64, upper “sandstone-siltstone unit”, ca. 13.5 m alternating siltstones, thin sandstones, and calcareous sandstones to sandy limestones with neritic fauna including *Omegops* sp. (?lower part of uppermost Famennian).

Wuppertal area (western Remscheid-Altena Anticline)

B224 outcrops NE of Aprath (Fig. 6)

Location: Temporary outcrops were created during excavations and trenching for the B224 road, which crosses the western part of the narrow Herzkampe Syncline ESE of Wülfrath and NW of Wuppertal-Elberfeld (Fig. 9). A multidisciplinary approach led to a voluminous monograph on the Upper Devonian to Lower Carboniferous (Thomas 1992). The uppermost Devonian und lower Tournaisian were developed as calcareous and micaceous shales and siltstones, which differ from the typical sequence of the Velbert Anticline. The succession, which has no current outcrop, can be summarised as follows (see Korn and Thomas 1988; Thomas 1992; Korn 1992b):

Kahlenberg Formation: Dark-grey to black shale in the upper part of Bed 07, which yielded imprints of smooth-shelled goniatites with up to 15 cm diameter.

Hangenberg Formation equivalent (un-named new formation):

Bed 07, ca. 9 m calcareous siltstones, post-Crisis Interval.

Bed 06/3, 30 cm bioturbated, silty, unfossiliferous limestone.

Stockum Limestone equivalents:

Bed 06/2, 40 cm grey-brown siltstone with abundant *Macrobole dreverensis*, possibly Upper Crisis Interval III.

Bed 06/1, 20 cm silty shale with pyritised goniatites and micritic limestone concretions with goniatites, such as *Ac. (St.) subbilobatum* (auct.), *Ac. (St.) intermedium* (auct.), *Ac. (St.) kleinerae*, *Ac. (Str.) carinatum*, and *Ac. (Str.) caesari* (middle/higher parts of *Ac. (St.) prorsum* Zone, UD VI-F), probably Upper Crisis Interval II (unfortunately, without conodont record).

Hangenberg Shale:

Beds 05/31–60, 6.5 m grey, calcareous siltstones with partly abundant *Guerichia venusta* and *Pseudowaribole* sp., Middle Crisis Interval.

?Hangenberg Black Shale equivalent:

Bed 05/30, marl with large septaria, pyrite accumulations, and a goniatite identified as *Acutimitoceras* sp. (no conodonts), ?Lower Crisis Interval.

Velbert Formation (s.l.):

Beds 05/21–29, 3.5 m calcareous siltstones with rare oncoids.

Bed 05/20, 70 cm calcareous siltstones with oncoidal rudipackstones and neritic fauna (brachiopods, gastropods, small solitary Rugosa), ?Crisis Prelude.

Beds 05/2–19, 3.4 m grey, platy, unfossiliferous, calcareous siltstone.

Bed 05/1, 10–20 cm dark grey to black, lenticular, micritic limestone with *Pa. gracilis gonioclymeniae* (*Bi. ultimus ultimus* Zone), *Rabienops granulatus*, and *Rab. wedekindi*.

Discussion: The regional occurrence of Stockum Limestone was already known to Paeckelmann (1922a, p. 286), who described the DCB section exposed in the railway cut at Kirchenfeld, between Dornap and Aprath (sheet 4708 Elberfeld, ca. r 2 574 500, h 5 681 100). His Bed 9, a dark-grey shale with dark limestone nodules, yielded *Macrobole dreverensis* and “*Brancoceras ornatissimum*”. Beyond doubt, the latter refers to a species of *Ac. (Stockumites)* with strong growth ornament. Most interesting is the association with a neritic brachiopod fauna, including productids, spiriferids, chonetids, orthids, and others, which requires revision. A younger, lower Tournaisian gastropod-brachiopod fauna with *Syringothyris* came from Bed 6, from 4 m below the Lower Alum Shale Event level (Bed 4).

The most westernly occurrences of Stockum Limestone, interrupting a succession with few pelagic fossils, underline its transgressive nature. The lower level of large septaria and ammonoids at the B224 may express locally the transgressive Hangenberg Black Shale interval. It is unfortunate that there are no conodont and miospore data and that there are no available outcrops.

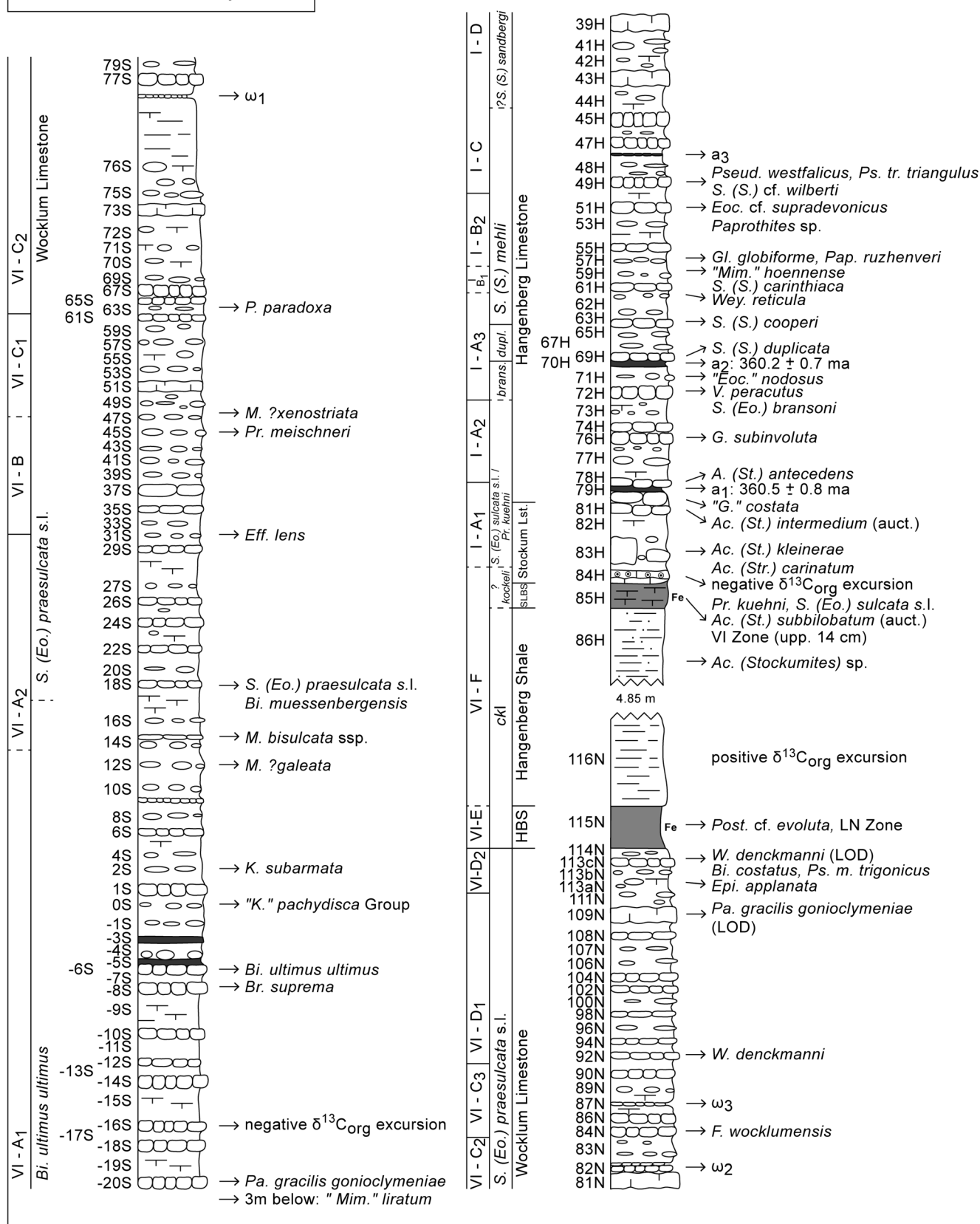
Am Haken Brickwork Quarry (Fig. 6)

Location: Former Brickwork Quarry “Am Haken”, second quarry N of the Üllendahl road in Wuppertal-Elberfeld, now completely filled and covered, sheet 4708 Wuppertal-Elberfeld, ca. r 2 580 550, h 5 683 100 (Fig. 9). A second, southern quarry was situated right at the road.

Literature: Paeckelmann (1913: type locality of *Platybole bergica*; 1922b, 1923, 1928), Schindewolf (1921, 1923b, 1926), Schmidt (1924a, b), Richter and Richter (1926), Paeckelmann (1928), Paul (1938b, 1939a), Basse and Lemke (2011), Zhang et al. (2019). It is the type section of *Aganides infracarbonicus* Paeckelmann, 1913, a poorly understood prionoceratid. Based on the examination of its types, it was synonymised by Schindewolf (1921) with “*Brancoceras Denckmanni* Wedekind, 1918” (see Paeckelmann 1922, p. 585, footnote 2), which, however, is another problematic species.

Summary of succession: Paeckelmann (1923, p. 283) gave a relatively detailed log for this unfortunately lost section, which was more fossiliferous and distinctive in terms of lithofacies in comparison to the adjacent Riescheid section. It filled a gap that enabled the westward correlation from the “standard succession” of the northern Sauerland to the Bergisches Land. However, the succession was disturbed by faulting. A modern lithostratigraphic

Hasselbachtal Auxiliary GSSP



◀ **Fig. 10** DCB succession at the (currently most covered) Hasselbachtal Auxiliary GSSP, showing occurrences of index conodonts and ammonoids, the position of marker bentonites (ω_{1-3} and a_{1-3}), and their geochronological ages, miospore zones, and changes of carbon isotopes (for references see text, for lithology legend, see Fig. 13)

terminology does not exist. The interpretation of Paeckelmann's data leads to the following summary:

Kahlenberg Formation (Lower Alum Shale):

Bed 7, ca. 2 m of alum shale, Lower Alum Shale Event Interval, middle Tournaisian.

Hangenberg Formation equivalent (un-named new formation):

Bed 8, ca. 4 m, dark-grey, Flinz-type limestones (dark turbiditic limestones), in the lower part alternating with shale, post-crisis lower Tournaisian, equivalent of upper part of Hangenberg Limestone.

Bed 9, 3.15 m grey, calcareous shales with thin beds or concretions of partly pyritic, Flinz-type limestone, ?equivalent of lower part of Hangenberg Limestone, post-Crisis Interval, lower Tournaisian.

Near top of Bed 10, black, deeply weathered shale with pyritic “*Aganides*” *infracarbonicus* Paeckelmann, 1913, probably a species of *Ac.* (*Stockumites*), and *Cymaclymenia* sp. (Schindewolf 1921, p. 146), Stockum Level Black Shale, ?Upper Crisis Interval.

Main Bed 10, 3.3 m platy, thin-bedded, bluish-grey shale, with *Postclymenia*, ?equivalent of Hangenberg Shale, Middle Crisis Interval.

Bed 11, 4.6 m alternating bluish-grey to greenish shales, dark-grey, hard, micaceous shale, and thin-bedded, micaceous fine sandstones and siltstones, with trace fossils (resembling “*Nemertites*”), *Postclymenia* and *C. striata* (Schindewolf 1926, p. 97), probably Lower/Middle Crisis Interval.

“Oberer Cypridinenschiefer” (proposed new Brahm Formation):

Bed 12, 20 cm red marl with squashed clymeniids, possibly Crisis Prelude II.

1 m grey shale with thin sandstones, probably Crisis Prelude I.

20 cm grey and reddish limestone with *Richterina* and *Drevermannia*, upper *hemisphaerica* Zone, pre-Crisis Interval.

4.4 m grey and greenish shale, micaceous shale, and thin sandstones with squashed clymeniids, *Guerichia*, and *Richterina*.

Discussion: Most important was a relatively diverse pre-Crisis (“Etroeungt”) fauna with various trilobites (e.g. *Rabienops circumpectans*), brachiopods, bivalves, crinoids, and bryozoans, which requires revision (outdated species list in Paeckelmann 1913, pp. 137–138), and the recognition of the *Postclymenia* levels. An adjacent section, again with *Postclymenia*, was exposed in a brook S of Mirker Hain (sheet 4708 Wuppertal Elberfeld, ca. r 2 579 930, h 5 682 950). Another diverse “Etroeungt” fauna (again with *Rabienops circumpectans*) was collected by H. Schmidt in the former Müller & Preuss Brickwork Quarry, E of the Am Haken Quarry (Paeckelmann 1913, p. 151; trilobites in Richter and Richter 1926). Recent excavations in the Üllendahl region did not reach the DCB (pers. comm. S. Helling).

circumpectans) was collected by H. Schmidt in the former Müller & Preuss Brickwork Quarry, E of the Am Haken Quarry (Paeckelmann 1913, p. 151; trilobites in Richter and Richter 1926). Recent excavations in the Üllendahl region did not reach the DCB (pers. comm. S. Helling).

Riescheid (Fig. 6)

Location: S-N running former railway cut (“Hatzfelder Straßenbahn”) just E of a garden colony in Wuppertal-Wichlinghausen, sheet 4709 Wuppertal-Barmen, sheet 4709 Barmen (Fig. 9), r 2 573 630, h 5 684 520 (GPS N 51° 17' 15.2", E7° 11' 32.4").

Literature: The long research history started with the work of W. Paeckelmann (1913, 1922a); it has been summarised by Hartenfels et al. (2016).

Summary of succession: For a detailed log see Hartenfels et al. (2016). In the near-absence of macrofauna and conodonts, the DCB stratigraphy is based on the miospore data of Higgs and Streel (1984) and Higgs (in Becker et al. 1993). New palynomorph investigations are under way by C. Hartkopf-Fröder (Krefeld).

Kahlenberg Formation: Ca. 1.2 m dark-grey shale (Beds 91a–91c, Unit 2 of Zimmerle et al. 1980) with very poor macrofauna and miospores of the HD Zone (Higgs and Streel 1984), Lower Alum Shale Event Interval, middle Tournaisian.

- unconformity (no record of the lower Tournaisian VI Zone or Hangenberg Limestone equivalents) -

(proposed) **Brahm Formation** (previously “Obere Cypridinenschiefer”), **Member 4** (Unit 1 of Zimmerle et al. 1980): Ca. 9 m alternating grey, silty shales, and fine- to middle-grained calciturbidites with poor macrofauna (Beds 49b–90):

Within last meter (Samples Rh 02 and Rh 04), “LE Zone”, Middle Crisis Interval.

7 to 1 m below top (Samples Rh 7 to Rh 01 with *Verrucosisporites nitidus*), LN Zone, Lower/Middle Crisis Interval.

10 m below the top (Sample Rh 10, ca. Bed 82a), LE Zone, pre-Crisis Interval.

15 to 12.5 m below the top (Samples Rh 15 to Rh 12–13, up to ca. Bed 72), LL Zone.

Discussion: Richter and Richter (1926) recorded *Weyerites wocklumeriae*, a typical uppermost Famennian phacopid, from a dark-grey limestone. Paeckelmann (1923, p. 284) as well as Fuchs and Paeckelmann (1928, p. 38) noted the presence of *Postclymenia* at Riescheid. This indicates that time equivalents of the Hangenberg Black Shale may be distinguishable in the lower LN Zone interval. The DCB unconformity disqualifies Riescheid as a possible GSSP

section but its importance lies in the miospore record, which provides marine-terrestrial correlations.

Northern Sauerland (eastern Remscheid-Altena Anticline)

In the northern Sauerland, between Hagen in the west and Warstein in the east, the “standard” DCB succession (see summary in Becker et al. 2016a) is developed. A major channel fill, the Seiler Conglomerate, forms a short W-E interruption in the Iserlohn area (e.g. Gallwitz 1928; Ziegler 1970; Paproth 1986). The widely used traditional lithological terms do not conform to modern lithostratigraphical standards. The Wocklum Beds or Wocklum Limestone have been based on its distinctive faunas (Wocklumian, UD VI; Schindewolf 1937), not on a sedimentary change that would enable a clear separation from the underlying Dasberg Beds (now Dasberg Formation). Attempts to identify a subordinate marker in the best and continuous sections (Oese, Oberrödinghausen, Effenberg), in order to justify at least a member status, failed so far. In the type section near Wocklum (see below), there is a reddish unit with large kalloclymeniids above a faulted zone. At Oese, a possibly correlative, peculiar interval of red shales and red nodules occurs above the oldest Wocklumian ammonoids. However, we did not trace it in the other sections. Consequently, we continue the use of the term Wocklum Limestone in a traditional, biostratigraphically defined form. The whole interval from the base of the Hangenberg Black Shale to the base of the Lower Alum Shale is assigned to the Hangenberg Formation, which is subdivided into informal members.

Hasselbachtal Auxiliary DCB Stratotype (Figs. 6, 10)

Location: Brook cut of the Hasselbach E in the forest of Hohenlimburg-Reh (Hagen), northern Sauerland, northern limb of Remscheid-Altena Anticline (Fig. 9), topographic sheet Hagen-Hohenlimburg at r 2 507 000/h 5 194 220.

Literature: Schmidt (1924a, b), Gallwitz (1932: brachiopod records), Paul (1937a: lingulids from the Lower Alum Shale), Groos-Uffenorde and Uffenorde (1974), Paproth and Strel (1982), Becker et al. (1984), Higgs and Strel (1984, 1994), Paproth et al. (1986b), Brauckmann and Hahn (1984), Bless and Groos-Uffenorde (1984), Byvsheva et al. (1984), Becker (1985, 1988, 1996, 2000), Hahn et al. (1990), Kramm et al. (1991), Claoué-Long et al. (1993), Brauckmann et al. (1993), Higgs et al. (1993), House (1993), Korn (1993), Kürschner et al. (1993), Winter (1993), Bless et al. (1993), Becker and Paproth (1993), Becker et al. (1993), Luppold et al. (1994), Higgs and Strel (1994), Sartenaer (1997: type locality of

Novaplatirostrum sauerlandense), Korn and Weyer (2003), Trapp et al. (2004), Kaiser (2005), Kaiser et al. (2006), Korn et al. (2010), Feist and Weyer (2018), Korn and Price (2019).

Summary of succession: There were two separate sections along the southern and northern slope of the brook. The southern section is still present and exposes the Wocklum Limestone. Despite protection as a geological heritage, the northern auxiliary stratotype section has been mostly covered by the property owner. Prior to this unfortunate development, the upper Wocklum Limestone was systematically re-sampled in order to improve the ammonoid record. This results in an update of taxon ranges for the northern Wocklum Limestone. The middle Tournaisian to lower Viséan succession was explored in a borehole (Higgs et al. 1993; Luppold et al. 1994) but apart from the miospores it was not studied in the same detail as the outcrop. The following summary combines published and new data. It has a focus on the FODs of stratigraphically relevant taxa.

Hangenberg Limestone: Strongly cyclic succession of grey micritic limestones, nodular and calcareous shales.

Beds 47H–45H with zonally non-diagnostic goniates, *S. (S.) carinithiaca*, *S. (S.) mehli*, *Ps. triangulus triangulus*, *Dinodus* sp., and other conodonts (upper *S. (S.) mehli* Zone).

Bed 48H top, metabentonite a3.

Bed 49H with *Pseud. westfalicus* (ca. base *Pseud. westfalicus* Zone, LC I-C), *S. (S.) obsoleta*, *S. (S.) duplicata* sensu Hass (= *S. (S.) cf. wilberti*), *Ps. triangulus triangulus*, *S. (S.) lobata* (?M2), and other conodonts (upper *S. (S.) mehli* Zone).

Bed 51H with *Eoc. cf. supradevonius*, *Paprothites* sp. (top *Parag. sphaerooides* Subzone, LC I-B₂), *S. (S.) carinithiaca*, *S. (S.) bransoni* (*S. (S.) mehli* Zone), and a probably diogenetically triggered negative C_{carb} carbon isotope excursion (Kaiser 2005).

Bed 57H with *Paragattendorfia* sp., *Gl. globiforme*, *H. gracilis*, *Wey. molaris*, and *Pap. ruzhencevi* (*Parag. sphaerooides* Subzone, LC I-B₂).

Bed 59H with *Ac. (St.) convexum*, “*Mim.*” *hoennense* (probably *Pap. dorsoplanus* Zone, LC I-B₁), *S. (S.) carinithiaca*, *S. (S.) duplicata*, *Ps. triangulus inaequalis*, and other conodonts (*S. (S.) mehli* Zone).

Bed 62H with *Wey. reticula*.

Bed 63H with *S. (S.) cooperi* (M2) (base *S. (S.) mehli* Zone).

Bed 69H with *S. (S.) duplicata*, *Ps. primus* ssp., *Ps. triangulus inaequalis* (base *S. (S.) duplicata* Zone), and *Liobolina* cf. *submonstrans*.

Bed 70H, thin metabentonite a2, dated by Trapp et al. (2004) as 360.2 ± 0.7 ma.

Bed 71H with “*Eoc.*” *nodosus* and *G. subinvoluta* (“*Eoc.*” *nodosus* Subzone, LC I-A₃).

Bed 72H with *V. peracutus* ("Eoc." *nodosus* Subzone, LC I-A₃) and *S. (Eo.) bransoni* (base *S. (Eo.) bransoni* Zone).

Bed 76H with *G. subinvoluta* and *Ac. (St.) subbilobatum* (auct.) (*G. subinvoluta* Zone/Subzone, LC I-A₂).

Bed 78H with *Ac. (St.) antecedens* (LC I-A₂) and *Ps. primus* ssp. (*S. (Eo.) sulcata* s.l./*Pr. kuehni* Zone).

Bed 79H, thin metabentonite a1, first dated by Kramm et al. (1991) and Claoué-Long et al. (1993), revised by Trapp et al. (2004) as 360.5 ± 0.8 ma.

Bed 80H with "G." *costata* and "Mim." cf. *simile* (Korn and Weyer 2003, base *G. subinvoluta* Zone, LC I-A₂); basal post-Crisis Interval.

Upper Stockum Limestone:

Bed 81H with *Ac. (St.) intermedium* (auct.) (top *Ac. (St.) prorsum* Zone, LC I-A₁), *Pr. kockeli*, *Po. purus purus*, *Po. purus subplanus*, ?*Texathyris tarpata*, and *Macrobole* cf. *drewerensis*.

Bed 83H with *Ac. (St.) kleinerae*, *Ac. (Str.) carinatum* (upper *Ac. (St.) prorsum* Zone, LC I-A₁), *Po. purus purus*, *Pr. kockeli*, *Pr. kuehni*, and *Belgibole abruptirhachis abruptirhachis*.

Bed 84H, bipartite, thin bed with an upper, oolithic, fossiliferous turbidite that eroded an underlying bioturbate, bioclastic wackestone without fauna; with *Pr. kockeli*, *Pr. kuehni*, *S. (Eo.) sulcata* s.l., and numerous reworked Famennian conodonts (base *S. (Eo.) sulcata* s.l./*Pr. kuehni* Zone), strong negative excursion of C_{org} carbon isotopes; base Upper Crisis Interval III.

Stockum Level Black Shale: Bed 85H, 65 cm, solid, dark-grey, calcareous, and pyritic shale with *Ac. (St.) subbilobatum* (auct.) and *Ac. (Stockumites)* sp. (including *Ac. (St.) cf. prorsum* of Becker 1988 and *Ac. (Ac) acutum* of Korn 1993; middle to top part, *Ac. (St.) prorsum* Zone, UD VI-F), no conodonts, LN/VI Zone boundary at 14 cm below top (Higgs and Strel 1984) corresponding closely to the Hasselbachatal borehole section (Higgs et al. 1993); Upper Crisis Interval I/II, Lower Stockum Limestone equivalent.

Hangenberg Shale: Bed 86H, ca. 4.85 m of greenish-grey, silty shale with *Guerichia* (several species), rare squashed *Ac. (Stockumites)* sp., and a strong positive excursion of C_{org} carbon isotopes (Kaiser 2005); Middle Crisis Interval.

Hangenberg Black Shale: Bed 115N, 20 cm, transgressive, laminated, and pyritic black shale, with *Guerichia* and rare *Post. cf. evoluta* (base *Post. evoluta* Zone, UD VI-E; base ckl); main Hangenberg Extinction at the sharp base, which was marked by a pyrite seam; base Lower Crisis Interval, base LN Zone (Higgs and Strel 1994).

Wocklum Limestone: Strongly cyclic alternation of greenish, calcareous shales, nodular shales, and grey

nodular limestones, intercalated by a few, distinctive metabentonites.

Bed 114N with the last *W. denckmanni*, *P. paradoxa*, *F. wocklumensis*, *Liss. wocklumeri*, *L. similis*, *C. cf. sudetica*, *Ebbighausenites seidlitzii* (new record), "Mim." *geminum* (top *Epi. applanata* Subzone, top UD VI-D₂), *S. (Eo.) prasesulcata* s.l., common *Pr. meischneri*, *Bi. costatus*, *Br. suprema*, *Ps. marburgensis trigonicus*, *Pa. gracilis gracilis*, and *Pa. gracilis sigmoidalis* (top *S. (Eo.) praesulcata* s.l. Zone), trilobites (*Chaunoproetus*, *Dianops*), and small orthids.

Beds 113a-bN with *Epi. applanata* and *Post. nephroides* (base *Epi. applanata* Subzone, base UD VI-D₂), base Crisis Prelude.

Bed 109N with the last *Pa. gracilis gonioclymeniae* (Stoppel in Becker et al. 1984; top of former Middle *costatus* Zone).

Bed 108N with *S. (Eo.) praesulcata* s.l., *Pr. meischneri*, *Ps. marburgensis trigonicus*, and other conodonts (upper *S. (Eo.) praesulcata* s.l. Zone), LE Zone (Higgs and Strel 1984).

Bed 107bN with *W. denckmanni*, *P. paradoxa*, *F. wocklumensis*, and *Ken. rostratum* (new records, *W. denckmanni* Subzone, UD VI-D₁).

Bed 101N with a member of the *Cyrt. procera* Group (new record).

Bed 92N with *W. denckmanni* (base *W. denckmanni* Zone, base UD VI-D₁), *Pr. meischneri*, *Bi. ultimus ultimus*, and other conodonts.

Bed 87N, metabentonite ω3.

Bed 84N with *F. wocklumensis* (base *May. nucleus* Subzone, UD VI-C₃).

Bed 82N, metabentonite ω2.

Bed 81N with *Ps. marburgensis trigonicus* (Kaiser 2005, much delayed FOD in the middle *S. (Eo.) praesulcata* s.l. Zone) and *Pr. meischneri*.

Bed 76S top: metabentonite ω1.

Bed 64S with *P. paradoxa* (base *P. paradoxa* Subzone, base UD VI-C₂).

Bed 46S with *M. ?xenostriata* (very evolute kosmoclymeniid with rursiradiate ornament, ca. *P. paprothae* Subzone, UD VI-C₁).

Bed 45S with the first *Pr. meischneri*, *Po. vogesi*, *S. (Eosiphonodella)* sp., *Bi. ultimus ultimus*, *Bi. muessenbergensis*, *Pa. gracilis gonioclymeniae*, and other conodonts (higher *S. (Eo.) praesulcata* s.l. Zone).

Bed 43S with the last *Eff. lens* and *M. ?galeata* (ca. top of *Eff. lens* Zone, top of UD VI-B).

Bed 32S with *Eff. lens* (base *Eff. lens* Zone, UD VI-B).

Bed 26S with *S. (Eo.) praesulcata* s.l. (*S. (Eo.) praesulcata* s.l. Zone).

Bed 23S with *Novaplatirostrum sauerlandense* (type level).

Bed 18S with *S. (Eo.) praesulcata* s.l. and *Bi. muessenbergensis* (Kürschner et al. 1993, base *S. (Eo.) praesulcata* s.l. Zone).

Bed 14S with *M. bisulcata* ssp. and *K. cf. undulata* (base *M. bisulcata* Zone, base UD VI-A₂).

Bed 12S with *M. ?galeata* (top *L. similis* Zone, top UD VI-A₁).

Bed 8S with *Br. suprema* (delayed FOD in the upper *Bi. ultimus ultimus* Zone).

Bed 4S with *K. cf. undulata*, *R. cf. quadripartitum*, and *Mim. cf. rotersi* (new records, *L. similis* Zone, UD VI-A₁).

Bed 2S with *K. subarmata*.

Bed 1S with “*Mim.*” *geminum*, *M. sublaevis*, *Cyrtoplacata*, and *Cyrt. lateseptata*.

Bed 0S with a member of the giant-sized “*K.*” *pachydisca* Group.

Bed -6S with the locally first *Bi. ultimus ultimus* (Kaiser 2005; *Bi. ultimus ultimus* Zone).

Bed -9S with “*Mim.*” cf. *liratum* (*L. similis* Zone, UD VI-A₁).

Bed -14S with *M. ?sublaevis* (*L. similis* Zone, UDS VI-A₁).

Bed -16S with “*Mim.*” *liratum* (new record, *L. similis* Zone), *Pa. gracilis gonioclymeniae* (*Bi. ultimus ultimus* Zone), and with a possibly diagenetically triggered negative excursion of C_{carbonate} carbon isotopes (Kaiser 2005).

Beds -20 to -18S with *Muessenbiaergia* sp. (new record), *Pa. gracilis gonioclymeniae*, *Bi. bispathodus*, and others (Kaiser 2005; *Bi. ultimus ultimus* Zone).

3 m below Bed 0S, “*Mim.*” *liratum* (*L. similis* Zone, basal UD VI-A₁).

Discussion: Since the northern and critical DCB part of the outcrop is currently covered, it cannot be considered in the new GSSP search. Attempts to trench a new exposure on lateral public ground was unsuccessful. In addition, Bed 85H, the basal part of the transgressive Crisis Interval III, was not calcareous enough to produce conodont faunas that could shed light on the *Pr. collinsoni*-*Pr. kockeli* transition. The thin metabentonites enable a high-precision correlation along the northern limb of the Remscheid-Altena Anticline (Hasselbachtal to Oese and Apricke, Korn and Weyer 2003). So far, only two of them have been dated geochronologically (Trapp et al. 2004: 360.5 ± 0.8 ma for Bed 79H, 360.2 ± 0.7 ma for Bed 70H).

Seiler Trenches N of Iserlohn (Fig. 6)

Location: In 1968, two trenches, Trenches 1 and 2, were dug in the Seiler area N of Iserlohn (sheet 4612 Iserlohn), northern Sauerland (Fig. 9), E of “In der Calle”. The precise location with geographical coordinates is shown in Koch et al. (1970), fig. 1. Subsequently, in 1969 and 1970, five additional trenches, Trenches 0 to III, and a “Paralleltrench”, were excavated in the a-b-parts of Trench 2, which positions are shown in Clausen et al. (1989a, fig. 15). All trenches were filled and

currently there are only minor exposures at “In der Calle”, which yield loose blocks of the famous Seiler Conglomerate.

Literature: Schmidt (1924a, b), Schindewolf (1926), Richter and Richter (1926), Gallwitz (1928, 1932), Matern (1929), Rabien (1954, 1960), Koch et al. (1970: type locality of *Pr. kuehni*, *Po. stadleri*, *Richterina (Fossilrichterina) intercostata serratocostata*, *Maternella (M.) circumcostatula*, *M. (M.) gruendeli*, and *M. (Zagoruendella) seilerensis*), Paproth and Streel (1982), Clausen et al. (1989a).

Summary of succession: The Seiler area exposed a unique, thick oolite-sandstone-shale succession in the DCB interval, the Seiler Channel (Paproth et al. 1986a, b). Partly, it corresponds to an incised valley fill formed after the main Hangenberg Regression (sequence boundary), which is the proximal equivalent of the Hangenberg Sandstone. However, conodonts proved that the overall succession is much more complex, with siliciclastic sedimentation starting much earlier in the uppermost Famennian. The source of the material must have been on a topographic high to the N (Koltonik et al. 2018), not on a Rhenish Island in the S, as proposed in former palaeogeographic reconstructions. The combined evidence from Gallwitz (1928), Koch et al. (1970), and Clausen et al. (1989a) leads to the following DCB summary:

Kahlenberg Formation (Lower Alum Shale): 25 m black shale, middle Tournaisian.

Hangenberg Limestone:

Trench 2, 25.0–33.9 m, olive-grey, partly micaceous shale, at the base with *Richterina (R.) latior*, *Maternella (M.) circumcostatula*, *M. (Zagoruendella) seilerensis*, and other ostracods (Samples 7a/7b), *R. (R.) latior* Zone, top lower Tournaisian.

Trench 2, Samples 10–8, Section III, Bed 9, Section II, Bed 17, Section I, Bed 14, and Section 0, Bed 11 with *S. (S.) lobata* M1, *S. (S.) obsoleta*, *S. (S.) sandbergi*, *S. (S.) quadruplicata*, and *Ps. triangulus triangulus* (*S. (S.) lobata* M1 Subzone).

Section III, Bed 8, Section II, Bed 16, and ?Section 0, Beds 9–10 with *S. (S.) quadruplicata*, *S. (Eo.) isosticha* (?cf.), and *S. (S.) obsoleta* (*S. (S.) sandbergi* Zone/Subzone).

Marker Bentonite 2.

Trench 2, Sample 12, Section II, Bed 15, Section I, Beds 11–13, Section 0, Beds 7–8 with *S. (S.) obsoleta*, *S. (S.) quadruplicata*, *S. (S.) mehli*, *S. (S.) cooperi*, and *Ps. triangulus triangulus* (upper part of *S. (S.) mehli* Zone).

Trench 2, Sample 13, Section III, Bed 7, Section II, Beds 13–14, Section I, Beds 9–10, and Section 0, Beds 4–6 with *S. (S.) mehli*, *S. (S.) carinithiaca*, *S. (S.) cooperi*, “*S. duplicata* sensu Hass” (= *S. (S.) cf. wilberti*), *S. (S.) quadruplicata* (?M2), and *Ps. triangulus triangulus* (lower *S. (S.) mehli* Zone).

Trench 2, Sample 14, Section III, Bed 6 with *Ps. triangulus triangulus*, first *S. (S.) quadruplicata* (?M2), and *S. (S.) duplicata* (top *S. (S.) duplicata* or basal *S. (S.) mehli* Zone).

Trench 2, Sample 15 (type level of *Pr. kuehni*), Section III, Beds 4–5, Section II, Beds 11–12, Section I, Bed 8, and Section 0, Bed 3 with *S. (S.) duplicata*, *S. (S.) bransoni*, and *Ps. triangulus inaequalis* (*S. (S.) duplicata* Zone).

Section II, Bed 10 with *S. (S.) bransoni* and *S. (Eo.) sulcata* s.l. (*S. (S.) bransoni* Zone).

Section I, Bed 7 and Section 0, Bed 2 with *S. (Eo.) sulcata* s.l., *Pr. kuehni*, *Pr. kockeli*, *Po. purus subplanus*, and *Ps. dentilineatus* (upper *S. (Eo.) sulcata* s.l./*Pr. kuehni* Zone), basal post-Crisis Interval.

Shale with Marker Bentonite 3 and a few conodont-poor limestone nodules below (Section II, Bed 9).

Stockum Limestone:

Trench 2, Sample 16, Trench 2b, Samples II 23–21, “Paralleltrench”, Beds 1–3, Section III, Bed 3, Section II, Beds 7–8, and Section I, Beds 5–6 with *Pr. kuehni*, *Pr. kockeli*, *Ps. dentilineatus*, rare *S. (Eo.) sulcata* s.l., *Po. purus purus*, and *Po. purus subplanus* (lower *S. (Eo.) sulcata* s.l./*Pr. kuehni* Zone), Upper Stockum Limestone, Upper Crisis Interval III.

Trench 2, Samples 18–17, Section III, Beds 1–2, Section II, Bed 6, Section I, Beds 3–4, Section 0, Bed 1 with *Pr. kockeli*, *Pr. collinsoni*, and *Pr. meischneri* (*Pr. kockeli* Zone), Lower Stockum Limestone, Upper Crisis Interval II.

Section II, Beds 1–5, Section I, Beds 1–2, and Section 0, Bed 0 with *Pr. collinsoni*, *Pr. meischneri*, *Neo. communis* ssp., and many reworked taxa (in Section I, upper *costatus-kockeli* Interregnum), Basal Stockum Limestone, Upper Crisis Interval I.

Seiler Formation, Upper Member (equivalents of Hangenberg Shale/Sandstone):

Trench 2, 37.4–54.6 m, olive-grey, silty shales alternating with thin, micaceous sandstones, top Middle Crisis Interval II.

Trench 2, 54.6–73.5 m, two packages of micaceous sandstone, in the lower part up to 15 cm thick beds, interrupted by a ca. 4 m thick silty shale interval.

Trench 2, 73.5–96.5 m, olive-grey silty shales and thin, micaceous sandstones.

Trench 2, 95.5–135.0 m, dark-grey to olive-grey, partly silty shales, with some calcareous concretions at 110.0–115.0 m and a 20 cm thick, micaceous and calcareous sandstone at ca. 128 m.

Trench 2, 135.0–152.2 m, dark-grey, solid, fine to coarse, micaceous sandstones, and conglomerates with quartz pebbles up to 3 cm in diameter.

Trench 2, 152.2–172 m, banded, olive-grey to dark-grey, partly silty and micaceous shale.

Trench 2, 172.0–203.8 m, predominant dark-grey, micaceous, fine- to middle-grained, partly conglomeratic sandstones and some intercalated, olive-grey, silty shales.

Trench 2, 203.8–225.0 m, fine to conglomeratic sandstones, partly with abundant ooids, and some packages

of olive-grey, silty, micaceous shale, base Middle Crisis Interval II.

Trench 2, 225.0–227.0 m, greenish-grey, silty, micaceous shale.

Trench 2, 227.0–228.0 m, oolite with some reworked pebbles of black limestone, base Middle Crisis Interval I; this is probably the level of *Postclymenia* found by Gallwitz (1928, p. 498) in oolite and in association with spiriferids, productids (productines and chonetines), and pectinids.

Hangenberg Black Shale equivalent:

Trench 2, 228.0–228.3 m, black, detrital limestone with bivalves, unfortunately, not sampled for conodonts, Lower Crisis Interval, upper part.

Trench 2, 228.3–229.5 m, dark-grey, micaceous shale, Lower Crisis Interval, lower part.

Seiler Formation, Middle Member (Wocklum Limestone time equivalents):

Trench 2, 229.5–230.0 m, light-grey, thin-bedded, micritic limestone with *Pa. gracilis gracilis*, *Bi. aculeatus aculeatus*, and *Bi. spinulicostatus* (Sample 51, probably top *S. (Eo.) praesulcata* s.l. Zone), Crisis Prelude.

- ca. 7.5 m gap -

Trench 2, 237.5–240.0 m, dark-grey, platy marl and dark-to olive-grey, slightly micaceous shale with *Maternella (M.) hemisphaerica*, *M. (M.) dichotoma*, *M. (M.) gruendeli*, and *R. (Fossirichterina) intercostata serratocostata* (Samples 53/52, *M. (M.) hemisphaerica*-*M. (M.) dichotoma* Zone), pre-Crisis Interval.

Trench 2, 240.0–241.5 m, bluish-grey, thin-bedded, detrital limestone with fragmented brachiopods and bivalves, *Pa. gracilis gracilis*, *Pa. gracilis sigmoidalis*, reworked *Pa. perlobata* ssp., *Ps. marburgensis trigonicus*, *Bi. costatus*, and other conodonts (Sample 54, *Bi. ultimus ultimus* Zone).

Trench 2, 241.5–251.5 m, grey, fine- to middle-grained, calcareous and micaceous sandstones, partly conglomeratic and olive-grey, silty shales in the upper part.

Trench 2, 251.8–252.6 m, sandy limestone conglomerate, clasts up to 3 cm, with *Pa. gracilis gonioclymeniae*, *Ps. marburgensis trigonicus*, and reworked middle Famennian palmatolepids (Sample 56, *Bi. ultimus ultimus* Zone).

Trench 2, 252.6–266.0 m, grey, fine- to middle-grained, micaceous sandstones and shale interbeds.

Trench 2, 266.0–266.4 m, coarse, light-grey limestone conglomerate with calcareous matrix, *Pa. gracilis gonioclymeniae*, *Bi. costatus costatus*, and many reworked lower/middle Famennian conodonts (Sample 57, basal *Bi. ultimus ultimus* Zone).

Discussion: Conodont faunas from the post-Crisis Hangenberg Limestone of the Seiler are most important to understand the Rhenish lower Tournaisian siphonodellid succession. Therefore, it is very unfortunate that no re-sampling is currently possible. Another interesting feature is the brief report of a detrital black limestone at the base of the Crisis Interval, which, unfortunately, was not studied in detail. It may

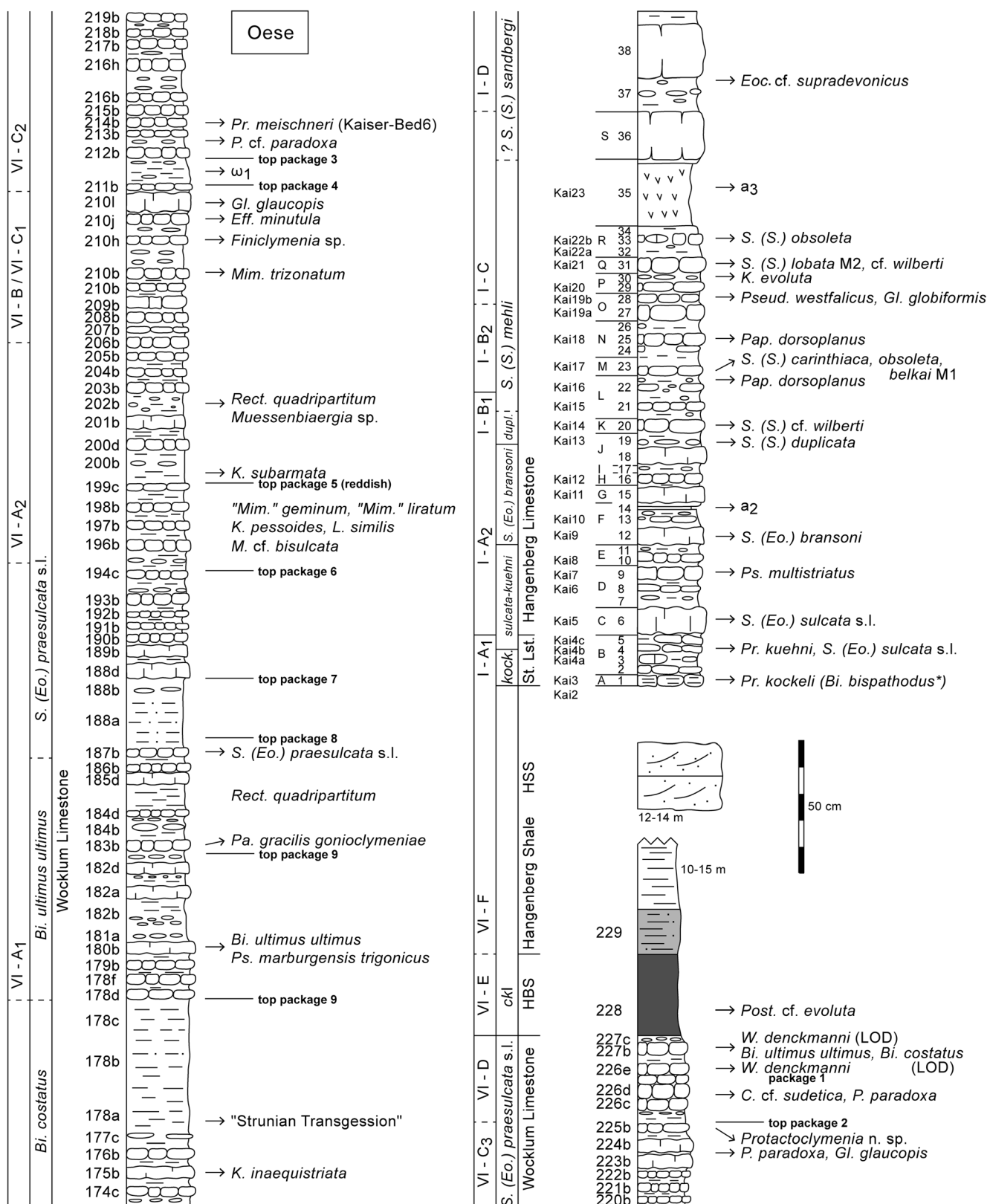


Fig. 11 Summary section log for the DCB succession at Oese (B7 roadcut), showing selected occurrences of index ammonoids, conodonts, and marker bentonites in relation to the numbers of Ziegler (1971: Hangenberg Limestone, A-S numbers), Becker et al. (1993: packages of Wocklum Limestone), Korn and Weyer (2003:

Hangenberg Limestone, nos. 1–38), Nowak (2008: Wocklum Limestone to Hangenberg Shale, nos. 174c–229), and Kaiser et al. (2017: Hangenberg Limestone, Kai numbers). For abbreviations and lithological units, see Fig. 1; for references to the numerous records, see text,* = reworked; for lithology legend, see Fig. 13

represent one of the globally rare limestones deposited during the main anoxic pulse.

In Trench 1 the pre-Crisis uppermost Famennian lacked the sandstones and conglomerates of Trench 2 and was rich in dark-grey platy limestones with conodonts. The Seiler Channel was characterised by a small-scale palaeotopography and fast lateral facies changes. Gallwitz (1928, p. 497) listed a Wocklumian ammonoid fauna with *K. subarmata*, *Mimimitoceras* (= “*Aganides? quadripartitus*”) and *Linguaclymenia/Muessenbiaergia* (“*Oxyclymenia bisulcata*”).

Oese (Figs. 6, 11)

Location: Northern slope of road cut of the B7 near Hemer-Oese, northern Sauerland (Fig. 9), topographic sheets 4612 Iserlohn to 4512 Menden, central point at r 3 415 640/h 5 696 900.

Literature: Schmidt (1924a, b), Ziegler (1962, 1971), Conil and Paproth (1968), Streel (1969), Paproth and Streel (1970, 1982), Henningsen (1972), Groos-Uffenorde and Uffenorde (1974), Stoppel 1977, Korn (1981a), Higgs and Streel (1984), Keupp and Kompa (1984), Paproth et al. (1986b), Struve (1989: type locality of *Rabienops evae*), Kürschner et al. (1993), Becker et al. (1993), Luppold et al. (1994), Becker (1996, 2000), Korn and Weyer (2003), Kaiser (2005), Bomfleur (2005), Nowak (2008), Hartenfels (2011), Kaiser et al. (2017), Korn and Price (2019).

Summary of succession: Although the section has been studied by numerous authors, there is no published bed-bed-bed fossil account for the complete Wocklum Limestone. Uppermost Famennian ammonoids have not been collected with the same precision as at adjacent sections (e.g. Becker et al. 1993). The uppermost Famennian summary is based on Luppold et al. (1994), Korn (2002), and Nowak (2008), with still preliminary conodont data. For the lower Tournaisian, there are several logs (e.g. Ziegler 1971; Luppold et al. 1994; Korn 2002; Kaiser 2005), partly with different bed numbers, which are synthesised here:

Kahlenberg Formation (Lower Alum Shale): Laminated, unfossiliferous black alum shale with a lenticular, laminated, siliceous, massive limestone (no conodonts) in the lower part (first depicted by Paproth and Streel 1982).

Hangenberg Limestone: Ca. 1.5 m of cyclic, bioturbated, grey, solid cephalopod limestone (bioclastic wackestone), nodular limestone, nodular shale, and calcareous shale; macrofauna in specific beds (Kullmann in Paproth and Streel 1982, Kullmann in Becker et al. 1993; Korn and Weyer 2003):

Korn-Bed 37(c), nodule layer with *Eoc. cf. supradevonicus* (higher part of *Parag. patens* Zone, LC I-D).

Korn-Bed 36 (Bed S), massive limestone, radiolarian wackestone, with *Eoc. supradevonicus* (ca. base *Parag. patens* Zone, LC I-D).

Korn-Bed 35 (Kaiser-Bed 23), 30 cm tuffitic clay bed, probably metabentonite a3 (high in the *S. (S.) mehli* and *Pseud. westfalicus* Zones at Hasselbachthal).

Korn-Bed 33 (Bed R, Kaiser-Bed 22b), nodule layer with *Nic. cf. trochiforme* and *S. (S.) obsoleta* (upper part of *S. (S.) mehli* Zone).

Korn-Bed 31 (Bed Q, Kaiser-Bed 21), solid limestone with *S. (S.) cf. wilberti*, *S. (S.) carinithiaca* (Fig. 2o), and *S. (S.) lobata* M1 (*S. (S.) mehli* Zone).

Korn-Bed 30 (upper part of Kaiser-Bed 20), nodule layer with *Kaz. evoluta*, *Pseudaritetes* sp., and *Wey. molaris* (upper part of *Pseud. westfalicus* Zone).

Korn-Bed 28 (lower part of Kaiser-Bed 20), nodule layer with *Pseud. westfalicus*, *Pseud. cf. subtilis*, *Gl. globiforme*, *Paragattendorfia* n. sp. I, *Wey. molaris*, and “*Wey.*” *concava* (base *Pseud. westfalicus* Zone, LC I-C).

Korn-Bed 25 (Bed N, Kaiser-Bed 18), nodular limestone with *Pap. dorsoplanus* and other goniatites (upper *Pap. dorsoplanus* Zone, LC I-B₂).

Korn-Bed 23 (Bed M, Kaiser-Bed 17), nodular limestone with *S. (S.) obsoleta*, *S. (S.) carinithiaca*, *S. (S.) belkai* M1 (*S. (S.) mehli* Zone), and other conodonts; base of the “*triangulus triangulus* Zone” after Ziegler (1971).

Korn-Bed 22, upper part (Kaiser-Bed 16), nodular limestone with *Pap. dorsoplanus*, *Paragattendorfia* n. sp. I and II (*Parag. sphaerooides* Subzone, LC I-B₂).

Korn-Bed 20 (Bed K, Kaiser-Bed 14) with *S. (S.) duplicata*, *S. (S.) duplicata* sensu Hass (= *S. (S.) cf. wilberti*), an intermediate between *S. (S.) duplicata* and *S. (S.) cooperi*, *S. (Eo.) sulcata* s.l., *Ps. triangulus inaequalis*, and other conodonts, including many problematical juvenile siphonodellids (?basal *S. (S.) mehli* Zone).

Korn-Bed 19 (Bed J, Kaiser-Bed 13), solid limestone with *S. (S.) duplicata*, *Ps. triangulus inaequalis*, and an atypical *S. (S.) cooperi* (*S. (S.) duplicata* Zone).

Korn-Bed 15 (Bed G, Kaiser-Bed 11) with “*Mim.*” *varicosum*.

Korn-Bed 14, upper part, thin metabentonite a2 (upper part of *S. (Eo.) bransoni* Zone at Hasselbachthal).

Korn-Bed 13 (lower part of Kaiser-Bed 10), nodule layer with abundant *Pr. kockeli* and *S. (Eo.) sulcata* s.l., base of the “*triangulus inaequalis* Zone” according to Ziegler (1971).

Korn-Bed 12 (Bed F, Kaiser-Bed 9), solid limestone with *S. (Eo.) bransoni* (base *S. (Eo.) bransoni* Zone).

Korn-Bed 9 (Bed D, Kaiser-Bed 7), nodular limestone with *Ps. multistriatus*.

Korn-Bed 6 (Bed C, Kaiser-Bed 5), solid limestone with *S. (Eo.) sulcata* s.l., *S. (Eo.) praesulcata* s.l., *Ps. primus* ssp., and *Po. purus subplanus* (*S. (Eo.) sulcata* s.l./*Pr. kuehni* Zone); basal post-Crisis Interval.

Stockum Limestone equivalents:

Korn-Bed 4 (lower part of B, Kaiser-Bed 4b), nodular limestone with *Pr. kuehni* (Fig. 2i), *Pr. kockeli*, *S. (Eo.) sulcata* s.l.,

Po. purus purus, and *Clydagnathus plumulus* (base S. (*Eo.*) *sulcata* s.l./*Pr. kuehni* Zone), Upper Stockum Limestone; Upper Crisis Interval III.

Korn-Beds 2–3 (Kaiser-Bed 4a), nodular limestone and subsequent nodule layer with *Pr. meischneri*, Lower Stockum Limestone; Upper Crisis Interval II.

Korn-Bed 1 (Bed A, Kaiser-Bed 3), laminated, graded, micaceous, silty, turbiditic limestone with *Pr. kockeli* (Kürschner et al. 1993; Luppold et al. 1994), and reworked *Bi. bispodus* and *Pa. gracilis gracilis* (*Pr. kockeli* Zone); Upper Crisis Interval II.

Hangenberg Sandstone: 12–14 m micaceous, siliceous and calcareous, fine sandstone in partly massive beds with ripple cross-bedding, flaser bedding, mudclasts at the base, channels, and plant debris (for sedimentology see Keupp and Kompa 1984), LN Zone in the upper part; Middle Crisis Interval II. The base is currently not exposed. The provenance of the sand is from the north (Koltonik et al. 2018), not from a shoal in the southerly core of the Remscheid-Altena Anticline (Paproth et al. 1986a).

Hangenberg Shale: 10–15 m thin-bedded, silty, greenish-grey, calcareous shale, which is rich in miospores (Higgs and Strel 1984); Middle Crisis Interval I.

Hangenberg Black Shale: Ca. 15 cm laminated, black shale with common *Post. cf. evoluta* (Fig. 3k; *Post. evoluta* Zone, UD VI-E, 15 cm), with sharp base, and grading upwards into ca. 15 cm silty, dark-grey shale; main Hangenberg Extinction at the base, Lower Crisis Interval.

Wocklum Limestone: Strongly cyclic, fossiliferous alternation of solid nodular limestone, nodular shale, and mostly greenish (exceptionally reddish), silty, calcareous shale. The logs in Luppold et al. (1994, with numbers) and Korn (2002, without numbers, = Korn and Weyer 2003) do not match well.

Upper 35 cm (Korn-Beds 1–2, Becker-package 1, Nowak-Beds 226a–227c) with *W. denckmanni* (Nowak-Beds 226e, 227b, 227c), *P. paradoxa* (Nowak-Beds 226b, 226d, 226e), *F. wocklumensis* (cf. Nowak-Bed 226d), *Liss. wocklumeri* (Nowak-Beds 226d, 227b), *C. striata* (Nowak-Bed 226d), *C. ?involvens* (Nowak-Bed 227b), *C. cf. sudetica* (Nowak-Bed 226d), *Cyrtoclymenia* n. sp. (Nowak-Bed 227a), “Mim.” *geminum* (Becker-package 1), “Mim.” cf. *liratum*, *Sp. orbiculare* spp., *Ken. rostratum*, *May. nucleus* (Nowak-Bed 227b) (*W. denckmanni* Zone, UD VI-D), *Bi. ultimus ultimus* (reported as *Bi. ziegleri ziegleri* in Luppold et al. 1994), *Bi. costatus*, *Ps. marburgensis trigonicus*, *Pa. gracilis* (three subspecies), *Br. suprema*, and *Po. obtectus* (top of *S. (Eo.) praesulcata* s.l. Zone), pre-Crisis Intervall and Crisis Prelude.

Ca. 80 cm nodular limestone and shale (Becker-package 2, Korn-Beds 3–6, Nowak-Beds 213b–225b) with two more solid limestones (Nowak-Beds 233b, 224b), *P. paradoxa* (Nowak-Beds cf. 213a, cf. 217b, 224b), *L. wocklumeri* (Nowak-Beds 218b, 224b, 225b), *Gl. glaucopis* (Nowak-

Bed 224b), *Finicylymenia* sp. (Nowak-Bed 225b), *C. striata* (Nowak-Beds 218b, cf. 225b), *Protactoclymenia* n. sp. (Nowak-Bed 225b), *Sp. muensteri orbiculare* (ca. Nowak-Bed 223b), *May. sinuconstrictum* (loose specimen, Figs. 3g–h), *R. lineare* (Nowak-Bed 225b), and *R. quadripartitum* (Nowak-Bed 225b) (*P. paradoxa* to *May. nucleus* Subzones, UD VI-C_{2/3}), with the first *Pr. meischneri* in Bed 6 and the last *Pa. gracilis gonioclymeniae* in Bed 5 of Kaiser (2005).

12 cm calcareous shale (Becker-package 3, between Korn-Beds 6 and 7, Nowak-Beds 212a–213a), with bentonite ω1 (within *P. paradoxa* Subzone, UD VI-C₂, at Hasselbachthal).

78 cm nodular limestone and shale (upper part of Becker-package 4, Korn-Beds 7 to > 10, Nowak-Beds 202b–211b) with *Eff. minutula* (e.g. Nowak-Bed 210j), *Mim. trizonatum* (Nowak-Bed 210b), *Gl. glaucopis* (Nowak-Bed 210l), *C. striata* (e.g. Nowak-Bed 205a), *C. costellata* (*Eff. lens* Zone to *P. paprothae* Subzone, UD VI-B to VI-C₁), and *S. (Eo.) praesulcata* s.l. (Kaiser 2005; *S. (Eo.) praesulcata* s.l. Zone).

Ca. 40 cm shale (lower third of Becker-package 4, Nowak-Beds 199c–202a) with three nodular limestone beds (Nowak-Beds 199c, 200d, 201b) and two nodule layers, *Muesseniaergia* sp. (Nowak-Bed 202a) and *K. subarmata* (Nowak-Bed 200a) (*M. bisulcata* Zone, UD VI-A₂).

Ca. 40 cm reddish marker interval (Becker-package 5, Nowak-Beds 195a–199c) with *M. cf. bisulcata*, *K. pessoides*, *K. subarmata*, *L. similis*, *C. involvens*, *C. costellata*, “Mim.” *geminum*, “Mim.” *liratum*”, *R. quadripartitum*, and other goniatites (*M. bisulcata* Zone, UD VI-A₂).

Ca. 45 cm nodular limestone and shale (Becker-package 6, Nowak-Beds 188d–194c).

Ca. 30 cm greenish-grey, silty shale (Becker-package 7, Nowak-Beds 188a–c) with rare limestone nodules (Nowak-Bed 188b).

46 cm nodular shale and three beds of nodular limestones in the upper part (Becker-package 8, Nowak-Beds 183b–187b) with *R. quadripartitum* (probably *L. similis* Zone, UD VI-A₁), the oldest *S. (Eo.) praesulcata* s.l. in the upper part (Nowak 2008, Bed 187b, base *S. (Eo.) praesulcata* s.l. Zone) and *Pa. gracilis gonioclymeniae* at the base (upper *Bi. ultimus ultimus* Zone).

55–60 cm reddish nodular limestone, nodular shale, and shale (Becker-package 9, Nowak-Beds 178d–183a) with *Ps. marburgensis trigonicus* and *Bi. ultimus ultimus* (Nowak-Bed 180b, lower *Bi. ultimus ultimus* Zone), basal Wocklum Limestone.

50 cm greenish-grey, silty shale (Nowak-Beds 178a–c), “Strunian Transgression”.

Discussion: The thin beds of the *kockeli* Zone are, unfortunately, locally rather poor in conodonts and devoid of ammonoids. This diminishes the DCB potential of the section. The shale package

at the base could be used for a lithostratigraphic distinction of the overlying Wocklum Limestone but has not yet been correlated with the Oberrödinghausen section. The lower reddish interval (Nowak-Beds 178d–183a) may correlate with a distinctive reddish unit at Wocklum that yielded large-sized *Kalloclymenia*.

Apricke (Fig. 6)

Location: Small gully ca. 1 km N of Apricke, topographic sheet Iserlohn, near eastern end of Remscheid-Altena Anticline (Fig. 9), r 17 690/h 96 250.

Literature: Schmidt (1924a, b), Richter and Richter (1926: type locality of *Cyrtosymbole nepia* and *Phacops wedekindi*), Matern (1929), Paul (1939b), Korn (1981a), Paproth and Streel (1982), Higgs and Streel (1984), Paproth et al. (1986b), Korn and Price (1987), Luppold et al. (1994), Feist et al. (2000: type locality of *Haasia aprickensis*, *Anglibole archinalae*, and *Struveproetus ocellatus*), Becker (2000), Korn and Weyer (2003), Korn and Price (2019).

Summary of succession: The section logs and description in Luppold et al. (1994) and Korn and Weyer (2003), unfortunately, have a different bed numbering and differ, especially for the Wocklum Limestone nodule layers. For the Stockum/Hangenberg Limestones, we give preference to the more detailed 2003 numbering, but adding an H (1994 numbers in brackets), in order to enable a clear distinction from the partly identical Wocklum Limestone numbers.

Kahlenberg Formation (Lower Alum Shale): ca. 1.5 m black shale.

Hangenberg Limestone: 2 m cyclic alternation of solid or nodular, poorly fossiliferous limestone and calcareous shale, followed by a 1.7 m thick grey shale unit (Beds 11–15).

Bed 34H (16) with *S. (S.) lobata* (M2?), *S. (S.) obsoleta*, *Ps. pinnatus*, and *Ps. triangulus triangulus* (upper part of *S. (S.) sandbergi* Zone).

Bed 29H (upper part of 22), thin metabentonite a3 (upper part of *S. (S.) mehli* Zone).

Bed 25H (25) with *S. (S.) lobata* (M2?) and “*S. duplicata*” s.l. (*S. (S.) mehli* Zone).

Bed 15H (within 32), thin metabentonite a2 (upper part of *S. (Eo.) bransoni* Zone).

Beds 13H/14H (33) with “*S. duplicata*” s.l. (*S. (Eo.) bransoni* Zone).

Bed 8H (between 36 and 35), thin metabentonite a1 (see position above the first gattendorfiid at Hasselbachtal).

Stockum Limestone equivalents:

Bed 6H (36) with *S. (Eo.) sulcata* s.l., *Pr. kockeli*, and *Po. purus purus* (*S. (Eo.) sulcata* s.l./*Pr. kuehni* Zone); Upper Stockum Limestone, Upper Crisis Interval III.

Bed 5H (37), thin turbiditic limestone with *Pr. kockeli* and the normally rare *Po. biconstrictus*; possibly Upper Crisis Interval III.

Bed 4H, very thin turbiditic limestone, onset of a minor DCB regression.

Bed 2H, nodular limestone with *Ac. (Str.) cf. carinatum*, *Ac. (Stockumites) sp.* (upper *Ac. (St.) prorsum* Zone), and *Pr. kockeli* (Lower Stockum Limestone).

Bed 1H, thin, solid, laminated, turbiditic limestone with numerous small-sized goniatites, *Po. purus purus* and *Ps. primus* ssp. (*Pr. kockeli* Zone), Upper Crisis Interval II.

Hangenberg Shale: Bed 41, ca. 4.8 m greenish-grey shale, more silty towards the top, middle ckl, upper part with LN Zone; Middle Crisis Interval.

Hangenberg Black Shale: Bed 42, 15–20 cm black shale with *Post. cf. evoluta* (*C. euryomphala* in Paproth and Streel 1982), lower ckl, Lower Crisis Interval; main Hangenberg Extinction at the base.

Wocklum Limestone: Cyclic alternation of fossiliferous, solid cephalopod limestone, nodular limestone, nodular shale, and calcareous shale.

Bed 1, five layers of limestone nodules with *Wocklumeria* and other ammonoids (*W. denckmanni* Zone, UD VI-D), and the last *Bi. ultimus ultimus* (recorded as *Bi. ziegleri ziegleri*), *Bi. muessenbergensis*, *Br. suprema*, *Pa. gracilis gracilis*, *Pa. gracilis sigmoidalis*, and *Ps. marburgensis trigonicus* (top *S. (Eo.) praesulcata* s.l. Zone), type level of *Haasia aprickensis*, *Anglibole archinalae*, and *Struveproetus ocellatus*, Crisis Prelude.

Bed 3, five layers of limestone nodules with *Wocklumeria* (*W. denckmanni* Zone, UD VI-D), pre-Crisis Interval.

Bed 4, bipartite solid flaser limestone (?top *P. paradoxa* Zone (UD VI-C), with *Bi. ultimus ultimus* and *Pa. gracilis gonioclymeniae* (*S. (Eo.) praesulcata* s.l. Zone by ammonoid correlation).

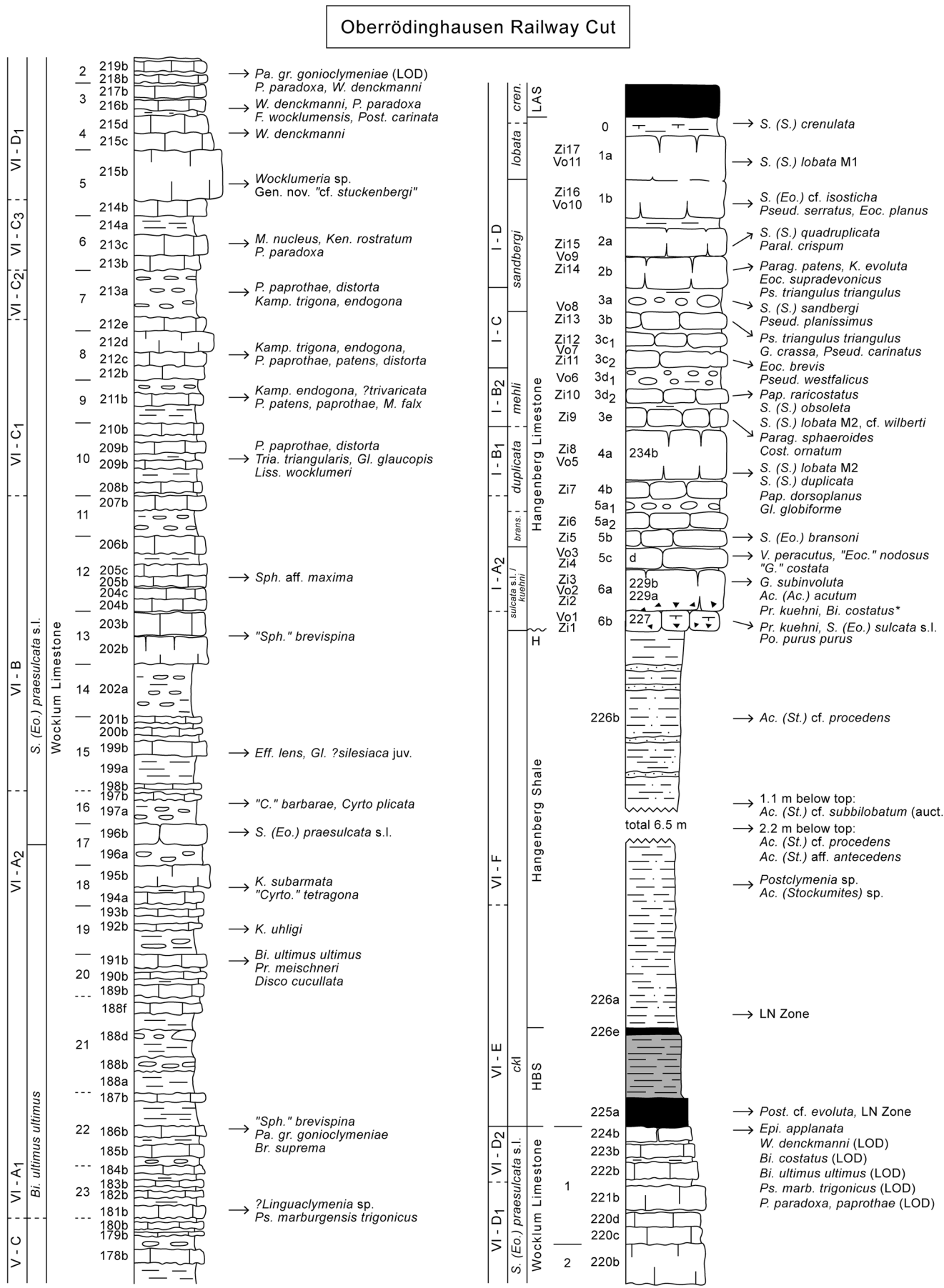
Bed 7, lower part, metabentonite ω3 (within *May. nucleus* Subzone, UD VI-C₃, see position of ω3 at Hasselbachtal).

Bed 8 with the *P. paradoxa* Zone (UD VI-C).

Discussion: Beds 1H–6H (39–36) should be re-sampled for conodonts in order to find a *Protognathodus* succession. Korn and Weyer (2003) proposed to correlate the turbiditic Bed 1H with the turbiditic Bed 84H at Hasselbachtal. If this is correct, Beds 2H–6H at Apricke correlate with the Upper Stockum Limestone interval (Beds 83H–81H) at Hasselbachtal, which is supported by the overlying thin metabentonite a1 in both sections. However, it is also possible that the thin Hasselbachtal turbidite (Bed 84H) correlates with the upper thin turbidites at Apricke (Beds 4H/5H).

Oberrödinghausen Railway Cut (Figs. 7, 12)

Location: This is the original DCB stratotype section selected in 1935. It lies at the eastern slope of railway cut near



◀ Fig. 12 Summary section log for the DCB succession in the Oberrödinghausen Railway Cut (Hönne Valley), showing selected occurrences of index ammonoids, conodonts, and marker bentonites. Bed numberings after Schindewolf (1937: Wocklum Limestone, nos 23–1), Voges (1959, 1960: Hangenberg Limestone samples, Vo numbers), Vöhringer (1960: Hangenberg Limestone, nos. 6–1), Ziegler (1971: Hangenberg Limestone, Zi numbers), Korn and Weyer (2003: Hangenberg Limestone, some subdivision of Vöhringer numbers), and Sacher (2016: Wocklum Limestone to basal Hangenberg Limestone, nos. 178b–234b). For abbreviated zones and lithological units, see Fig. 1; for references to the numerous records, see text, * = reworked; for lithology legends, see Fig. 13

Oberrödinghausen, eastern end of Remscheid-Altena Anticline (Fig. 9), topographic sheet 4613 Balve, r 3 419 400/h 5 696 100. An adjacent section (type locality of *K. (K.) schindewolfi* Korn and Price, 1987) was formerly exposed on the eastern slope of the road cut in Oberrödinghausen (see section logs in Ziegler 1962 and Luppold et al. 1994, p. 22). In addition, the DCB was encountered in the Oberrödinghausen 1 borehole (e.g. Higgs and Strel 1984; Van Steenwinkel 1984).

Literature: Schmidt (1924a, b), Paeckelmann (1924), Richter and Richter (1926: type locality of *Perliproetus gradatus* and *Weyrites wocklumeriae*; 1951), Matern (1929), Schindewolf (1926): type locality of *Eoc. supradevonius*, *Eoc. spiratissimus*, and “*Eoc.*” *planus*; 1937: type locality of *W. plana*, *W. aperta*, *Postglatziella carinata*, *Kamp. endogona*, *Kamp. trigona*, and *Triacylmenia triangularis*), Paeckelmann and Schindewolf (1937), Paul (1937b, 1939b), Paeckelmann and Kühne (1938), Rabien (1954), Bischoff (1957), Voges (1959, 1960), Vöhringer (1960: type locality of *N. trochiforme*, *N. subacre*, *N. acre*, “*Mim.*” *exile*, “*Mim.*” *simile*, *Ac. (St.) depressum*, *Ac. (St.) undulatum*, *Ac. (St.) convexum*, *Ac. (St.) antecedens*, *Ac. (Str.) heterolobatum*, *H. multislucata*, *H. gracilis*, *H. sphaeroidalis*, *Gl. globiforme*, *Parag. patens*, *Cost. ornatum*, “*Gatt.*” *costata*, “*Gatt.*” *reticulum*, *Wey. concava*, “*Wey.*” *molaris*, *Kazakhstania evoluta*, *Pap. raricostatus*, *Pseud. subtilis*, *Pseud. planissimus*, *Pseud. serratus*, *V. peracutus*, *Eoc. brevis*, and “*Eoc.*” *tener*), Ziegler (1962: type locality of *Spathognathodus supremus*, *Spath. wernerii*, *Ps. trigonica*, *Ps. brevipennata*, *Po. vogesi*, *Po. obliquicostata*, and *Pa. deflectens sigmoidalis*; 1971), Strel (1969), Paproth and Strel (1970), Eickhoff (1973), Stoppel 1977, Korn (1981a, 1992a, 2006), Paproth and Strel (1982), Brauckmann and Hahn (1984), Ziegler and Sandberg (1984b), Higgs and Strel (1984, 1994), Van Steenwinkel (1984), Korn and Price (1987), Korn and Luppold (1987), Price and Korn (1989), Kürschner et al. (1993), Brauckmann et al. (1993), House (1993), Luppold et al. (1994), Becker (1996, 1997, 2000, 2002), Cröner and Feist (2000), Korn and Weyer (2003), Korn and Vöhringer (2004), Kaiser (2005), Ebbighausen and Korn (2007), Clausen and Korn (2008), Becker et al. (2016a), Korn et al. (2016), Sacher et al. (2016), Sacher et al. (2016), Kaiser et al. (2017), Feist and Weyer (2018), Mottequin et al. (2019), Korn and Price (2019).

Summary of succession: The section is extremely useful for ammonoid-conodont correlation but the conodont record for the uppermost Famennian is still incomplete (Sacher 2016; Sacher et al. 2016). The Famennian part has been logged at much higher resolution than before by M. Sacher and S. Hartenfels (Sacher-beds). In the lower Tournaisian, the detailed conodont data of Ziegler (1971) have never been published. Therefore, the combined data of Voges (1959) and Kaiser et al. (2017) form the main account for the Carboniferous conodonts. The ammonoid record is mostly from Schindewolf (1937) and Vöhringer (1960), but with various subsequent updates (e.g. Luppold et al. 1994; Becker 2000; Korn 2006; Becker et al. 2016a). The summary focuses on the FODs and LODs of taxa:

Kahlenberg Formation (Lower Alum Shale): More than 15 m black shale with miospores of the HD Zone at the base (Higgs and Strel 1984), in the middle with phosphorite nodules, and then gradually siliceous (Becker et al. 1993).

Hangenberg Limestone: 1.5 m alternating, fossiliferous flaserlimestone, nodular limestone, nodular shale, and grey shale.

Bed 1a (Ziegler-Bed 17, Voges-Sample 11), ca. 12 cm limestone with *S. (S.) lobata* M1, *Po. radinus*, and *Dinodus leptus* (upper part of *S. (S.) sandbergi* Zone = *S. (S.) lobata* M1 Subzone).

Bed 1b (Ziegler-Bed 16, Voges-Sample 10), ca. 12 cm solid limestone with *Pseud. serratus*, *Eoc. planus* (upper *Parag. patens* Zone, LC I-D), *S. (Eo.) cf. isosticha*, and *S. (S.) quadruplicata* (Fig. 2t) (higher *S. (S.) sandbergi* Subzone).

Beds 2a–2b (Ziegler-Beds 14–15, Voges-Sample 9), 18 cm solid limestone with *Parag. patens*, “*G.*” *costata* (Figs. 5p–q, type level), *Kaz. evoluta*, *Eoc. supradevonius*, *Paralytoceras crispum* (lower part of *Parag. patens* Zone, LD I-D), *S. (S.) sandbergi*, *S. (S.) quadruplicata*, *S. (S.) belkai* M1 (Figs. 2q–r), *Ps. triangulus triangulus* (Bed 2u), and *Elictognathus bialatus* (lower *S. (S.) sandbergi* Zone and Subzone).

Bed 3a, 10 cm nodular shale with abundant *Pseud. westfalicus* and *Pseud. planissimus* (top *Pseud. westfalicus* Zone, top LC I-C), *S. (S.) sandbergi* (record of Korn and Weyer 2003), *S. (S.) cf. lobata* (= M2), and *S. (S.) belkai* M1 (basal *S. (S.) sandbergi* Zone and Subzone).

Bed 3b (Ziegler-Bed 13, Voges-Sample 8), 8–9 cm nodular limestone with *G. crassa*, *Pseud. carinatus*, *Ac. (St.) depressum*, “*Mim.*” *simile*, *N. acre* (upper part of *Pseud. westfalicus* Zone, LC I-C), *Ps. triangulus triangulus*, *S. (S.) cf. wilberti*, and *Pinacognathus profunda* (top part of *S. (S.) mehli* Zone).

Beds 3c₁–c₂ (Ziegler-Beds 11–12, Voges-Sample 7), ca. 12 cm nodular limestone with *Pseud. westfalicus*, *Pseud. subtilis*, *Eoc. brevis*, *Eoc. tener*, *Eoc. spiratissimus* (*Pseud. westfalicus*

Zone, LC I-C), S. (*S.*) *belkai* M1 (Fig. 2p), and S. (*S.*) *lobata* M2 (Fig. 2s) (*S. (S.) mehli* Zone).

Bed 3d (Ziegler-Bed-10, Voges-Sample 6), 9 cm limestone with *Pap. raricostatus*, *H. gracilis* (higher part of *Parag. sphaeroides* Subzone, LC I-B₂), *S. (S.) obsoleta*, *S. (S.) belkai* M2, *S. (S.) lobata* M2, and *S. (S.) cf. wilberti* (higher part of *S. (S.) mehli* Zone).

Bed 3e (Ziegler-Bed 9), 4 cm limestone with *Parag. sphaeroides* (compare cf. specimen of Figs. 5n–o), *Cost. ornatum*, and *Wey. molaris* (*Parag. sphaeroides* Subzone, LC I-B₂), not sampled for conodonts (possibly lower part of *S. (S.) mehli* Zone).

Beds 4a–b (Ziegler-Beds 7–8, Voges-Sample 5), 18 cm solid limestone with *Pap. dorsoplanus*, *Gl. globiforme*, *H. multisulcata*, “*Mim.*” *exile* (*Pap. dorsoplanus* Zone/Subzone, LC I-B₁), *S. (S.) duplicata* (Fig. 2m, Bed 4b, Fig. 2n, Bed 4a), *S. (S.) lobata* M2, *Ps. marginata*, *Ps. triangulus inaequalis*, protognathodids with atypical ornamentation (Fig. 2e–g) (*S. (S.) duplicata* Zone), and *Liobilina nebulosa*.

Bed 5b (Ziegler-Bed 5), 6 cm limestone with *S. (Eo.) bransoni* (Fig. 2l, *S. (Eo.) bransoni* Zone).

Bed 5c-d (Ziegler-Bed 4, Voges-Sample 3), 7 cm limestone with “*Eoc.*” *nodosus*, *V. peracutus*, *G. subinvoluta* (Figs. 5l–m), *G. involuta* (= *tenuis*), “*G.*” *costata*, “*Wey.*” *concava*, “*Mim.*” *varicosum*, “*Mim.*” *hoennense*, *Ac. (Str.) heterolobatum*, *N. trochiforme*, and *N. subacre* (“*Eoc.*” *nodosus* Subzone, LC I-A₃).

Bed 6a (Kaiser 2005; Ziegler-Beds 2/3, Voges-Sample 2, Sacher-Beds 228b–230b, Luppold et al. 1994; Beds 6B–D), 20 cm solid limestone with *G. subinvoluta*, *G. involuta* (new record), *Wey. reticula*, *H. sphaeroidalis*, *Ac. (Ac.) acutum*, *Ac. (St.) antecedens*, *Ac. (St.) undulatum*, *Ac. (St.) convexum* (*G. subinvoluta* Zone/Subzone, LC I-A₂), *S. (Eo.) sulcata* s.l., *Pr. kockeli*, “*Po. spicatus*”, *Po. purus purus*, *Po. purus subplanus*, *Ps. primus*, *Ps. multistriatus* (*S. (Eo.) sulcata* s.l./*Pr. kuehni* Zone); basal post-Crisis Interval.

Upper Stockum Limestone:

Bed 6b (Kaiser 2005; Sacher-Bed 227, Luppold et al. 1994, Bed 6A), ca. 5 cm nodular shale with carbonate sand clasts (Van Steenwinkel 1984) with *S. (Eo.) sulcata* s.l., *Pr. kuehni*, *Pr. “praedelicatus-cordiforme”*, *Pr. kockeli* (partly transitional towards *Pr. kuehni*, Fig. 2h), *Po. purus purus*, *Po. purus subplanus*, reworked *Pa. glabra pectinata* and *Bi. ultimus ultimus* (Luppold et al. 1994), and other conodonts (basal *S. (Eo.) sulcata* s.l./*Pr. kuehni* Zone), *Belgibole abruptirhachis*, and *Macrobole drewerensis* Group; Upper Crisis Interval III. - unconformity (basal VI Zone and Lower Stockum Limestone/*kockeli* Zone = Upper Crisis Interval I-II missing) -

Hangenberg Shale: Sacher-Beds 226a–b, ca. 6.5 m of greenish silty shale and thin siltstones with *Postclymenia* sp., *Ac. (St.) cf. procedens*, *Ac. (St.) aff. antecedens*, and *Ac. (St.) cf. subbilobatum* (auct.) (lower *Ac. (St.) prorsum* Zone, UD VI-F); Middle Crisis Interval I/II, LN Zone (Higgs in Becker et al. 1993).

Hangenberg Black Shale: Ca. 28 cm laminated shale with a sharp lower base, a main lower black shale (Sacher-Bed 225a, 8 cm), a middle dark-grey package (Sacher-Beds 225b–d, 17.5 cm), a thin upper black shale (Sacher-Bed 225e, 2 cm); with *Post. cf. evoluta* (*Post. evoluta* Zone, UD VI-E), basal LN Zone (Higgs and Strel 1994); transgressive Lower Crisis Interval.

Wocklum Limestone: Ca. 3.7 m, cyclic alternation of variably fossiliferous, nodular limestone, nodular and greenish-grey, calcareous shale. Bed numbers are those of Schindewolf (1937), with numbers in brackets from Sacher (2016). FODs and LODs of stratigraphically significant taxa are preferentially listed.

Bed 1 (220c–224b) with *Epi. applanata*, the last *W. denckmanni* (type level of the synonymous *W. aperta* Schindewolf, 1937, and *W. plana* Schindewolf, 1937; e.g. Beds 222b, 223b, 224b), *P. paradoxa* (e.g. Beds 220c, 220d), *P. paprothae*, *F. wocklumensis* (e.g. Bed 224b), *Liss. wocklumeri*, *Cyrt. angustiseptata*, *Cyrt. plicata*, “*Cyrt.* hexagona”, N. Gen. “cf. stuckenbergi”, *Sp. muensteri orbiculare*, *Ebbighausenites seidlitzii*, *May. nucleus*, *Ken. rostratum* (= *biforme*), *Balvia globularis*, “*Mim.*” *liratum* (e.g. Bed 223b), “*Mim.*” *lentum* (e.g. Bed 220d) (*Epi. applanata* Subzone, UD VI-D₂), the last *Bi. costatus*, *Bi. ultimus ultimus*, *Bi. bispathodus*, *Bi. spinulicostatus*, *Br. suprema*, *Pa. gracilis gracilis*, *Pa. gracilis sigmoidalis*, and *Ps. marburgensis trigonicus* (top *S. (Eo.) praesulcata* s.l. Zone), *Po. obtectus*, *Elictognathus tylus*, *Dinodus cf. wilsoni*, the last *Rabienops granulatus*, *Rab. wedekindi wedekindi*, *Weyerites wocklumeriae*, *Dianops anophthalmus*, *Chaunoproetus (Ch.) palensis*, *Heliproetus subcariantiacus*, and *Semiproetus (Anglibole) anglicus*.

Bed 2 (218b–220b) with *W. denckmanni*, *P. paradoxa*, *P. paprothae*, *R. lineare* (Bed 218b), and the LOD of *Pa. gracilis gonioclymeniae* (top former Middle *costatus* Zone).

Bed 3 (ca. 216b–217b) with *W. denckmanni*, *P. paradoxa*, *F. wocklumensis*, “*C.*” *barbarae*, *Postglatzia carinata*, *Discoclymenia cucullata*, *Ken. rostratum*, and *May. nucleus* (UD VI-D₁).

Bed 4 (ca. 215c–d) with *W. denckmanni*, *P. paradoxa*, *P. paprothae*, and *F. wocklumensis* (UD VI-D₁).

Bed 5 (214b–215b) with *Wocklumeria* sp., *P. paradoxa*, *P. paprothae*, *Postglatzia* sp. juv., and Gen. nov. “cf. stuckenbergi” (a new cyrtoclymeniid genus with strongly flattened flanks and venter; base *W. denckmanni* Zone, UD VI-D₁).

Bed 6 (ca. 213b–214a) with *May. nucleus*, *Ken. rostratum*, *P. paradoxa*, *P. paprothae*, and *Gl. glaucopis* (*P. paradoxa* to *May. nucleus* Subzones, UD VI-C_{2–3}).

Bed 7 (ca. 212e–213a) with *P. paprothae*, *P. distorta*, *P. patens*, *Kamp. trigona*, *Kamp. endogona*, *Tria. triangularis*, and *Gl. glaucopis* (*P. paprothae* Subzone, UD VI-C₁).

Bed 8 (ca. 212b–212d) with *P. paprothae*, *P. distorta*, *P. patens*, *Kamp. trigona*, *Tria. triangularis*, and *Gl. glaucopis* (*P. paprothae* Subzone, UD VI-C₁).

Bed 9 (ca. 211a–212a) with *P. paprothae*, *P. distorta*, *P. patens*, *Kamp. endogona*, *Kamp. trivaricata*, *Tria. triangularis*, and *M. falc* (= *Prionoceras nucleus* n. mut. in Schindewolf 1937) (*P. paprothae* Subzone, UD VI-C₁).

Bed 10 (ca. 208a–210b) with *P. cf. paprothae*, *P. distorta*, *Tria. triangularis*, *Liss. wocklumeri*, *Gl. glaucopis*, *Gl. minervae*, and the locally youngest *Selwoodites* n. sp. aff. *cornwallensis* (base *P. paprothae* Subzone, UD VI-C₁).

Bed 11 (207a–b) with “*Sph.*” *brevispina*, and *Eff. lens* (top UD VI-B).

Bed 12 (204b–206b) with “*Sph.*” *brevispina*, *Sph. aff. maxima*, *C. semistriata* (e.g. Bed 204c), and *Eff. lens* (UD VI-B).

Bed 13 (202b–203b) with “*Sph.*” *brevispina*, *Sp. muensteri orbiculare*, *R. cf. quadripartitum*, and *Eff. lens* (UD VI-B).

Bed 14 (202a), nodular shale with *C. striata* and questionable *Effenbergia* (UD VI-B).

Bed 15 (198b–201b) with *Effenbergia lens* (*Prionoceras* n. sp. IV in Schindewolf 1937, see comment by D. Weyer in Mottequin et al. 2019, p. 6), *Glatziella*, and *K. pessoides* (base *Eff. lens* Zone, UD VI-B).

Bed 16 (ca. 197a–198a) with *K. cf. subarmata*, “*C.*” *barbarae*, *Ebbighausenites seidlitzii*, and rectimitoceratids (UD VI-A₂).

Bed 17 (196a–196b) with *K. cf. subarmata*, “*Sphenoclymenia*” (UD VI-A_{1/2}), and *S. (Eo.) praesulcata* (Kürschner et al. 1993), *S. (Eo.) praesulcata* s.l. Zone).

Bed 18 (ca. 194a–195b) with *K. subarmata*, *Sp. muensteri orbiculare*, and “*Cyrt.*” *tetragona* (UD VI-A_{1/2}).

Bed 19 (ca. 192a–193b) with *K. uhligi* and *Ebbighausenites seidlitzii* (UD VI-A₁).

Bed 20 (ca. 188a–191b) with *Discoclymenia cucullata*, *R. lineare*, *Bi. ultimus ultimus* (Bed 191b, Sacher 2016), and *Pr. meischneri* (Kürschner et al. 1993).

Bed 22 (ca. 185a–187b) with “*Sph.*” cf. *brevispina* and the oldest *Selwoodites* n. sp. aff. *cornwallensis*, *Pa. gracilis gonioclymeniae*, and *Br. suprema*.

Bed 23 (ca. 181b–184b) with probable *Linguaclymenia* (recorded as *Oxyclymenia bisulcata* in Schindewolf 1937; perhaps base of *L. similis* Zone, UD VI-A₁) and *Ps. marburgensis trigonicus* (Bed 181b, Sacher 2016; base *Bi. ultimus ultimus* Zone).

A corresponding, adjacent section that is now overgrown was exposed for a long time along the main road through the

Hönne Valley (Luppold et al. 1994; Korn and Weyer 2003; both with section logs). The top Wocklum Limestone was very fossiliferous (with abundant *W. denckmanni*, *F. wocklumensis*, *Cyrtoclymenia*, *Gl. glaucopis*, and other ammonoids, RTB collection). Korn and Weyer (2003) mention an unpublished collection of ca. 3.000 ammonoid specimens from the Wocklum Limestone by a Tübingen Ph.D. student, and of further 500 specimens collected by D. Korn. This material includes probably further interesting records. Despite the only 200 m distance to the railway cut, the Hangenberg Shale is thicker and contains massive Hangenberg Sandstone beds. Two research boreholes, Oberrödinghausen 1 and 2, were drilled in 1979 and studied for conodonts (zonal identifications by W. Ziegler) and palynology (Higgs and Streel in Becker et al. 1993).

Discussion: The local DCB unconformity excludes the section from a re-consideration as a GSSP candidate, despite its enormous significance for ammonoid-conodont stratigraphy/correlation at levels below and above the Hangenberg Crisis Interval. This situation could have changed if the Hangenberg Extinction had been re-considered as the future DCB level, as proposed first by Paul (1937b, footnote on p. 748), and then by Walliser (1984). However, the majority of the DCB Task Group voted against this option in 2016.

The re-sampling of the basal Hangenberg Limestone by Sacher (2016: Bed 227) yielded an Upper *Protognathodus* Fauna with *Pr. kockeli*, *Pr. kuehni*, *Po. purus purus*, *Po. purus subplanus*, *Neo. communis communis*, *Neo. communis namdipensis*, *Neo. talassicus*, and other conodonts (several *Bispathodus*, including reworked *Bi. costatus* M2, and *Mehlina*) but not with a single siphonodellid. This fully supported the stratigraphic results of Kaiser (2005). It shows that there is a thin layer of Upper Stockum Limestone preserved and that the hiatus at the base of the limestone successions corresponds to the DCB regression known from Hasselbachthal. Luppold et al. (1994) reported a different fauna with *Pr. kockeli*, *S. (Eo.) sulcata* s.l. and different reworked Famennian conodonts from their corresponding Bed 6A. This faunal difference points to a complex mixture of reworking and condensation. It needs to be stressed that there is no record of any species of the *Gattendorfia* Fauna in Beds 6b = 6A = 227.

Hangenberg (Fig. 7)

Location: Trenches from 1973 at the Hangenberg near Deinstrop, northern Sauerland (Fig. 9), topographic sheet 4613 Balve, r 3 423 900/h 5 695 750.

Literature: Schmidt (1924a, b), Paeckelmann (1924), Paeckelmann and Kühne (1938), Stoppel 1977, Luppold et al. (1994).

Succession: Although this was the original type area for the Hangenberg Beds (now Hangenberg Formation) of Schmidt (1924a, b), there is hardly any outcrop. A trench dug in 1973 had to be filled quickly; it was measured by Leuteritz and

Schäfer and described by Stoppel 1977. Luppold et al. (1994) provided details for natural outcrops in the vicinity. Both sources together give the following succession:

Kahlenberg Formation (Lower Alum Shale): Unfossiliferous black shale, Lower Alum Shale Event Interval, middle Tournaisian.

Hangenberg Limestone:

1.3 m grey limestone, compact in the lower part, more nodular in the upper part, rich in conodonts in the first thick bed (Samples III–X) but still without zonation for the main and upper parts; with protognathodids (Fig. 2a–d).

A few cm of solid limestone (Sample II) with *S. (Eo.) sulcata* s.l. (*S. (Eo.) sulcata* s.l./*Pr. kuehni* Zone), probably basal post-Crisis Interval.

Lower Stockum Limestone: Thin, silty limestone layer at the base of the Hangenberg Limestone (Sample I) with *Pr. kockeli*, *Protognathodus* sp. 1 and sp. 2 (unusually ornamented morphs), *Po. purus subplanus*, *Ps. vogesi*, and probably reworked *Bi. ultimus ultimus* (recorded as *Bi. ziegleri ziegleri*) and *Pa. gracilis gracilis* (*Pr. kockeli* Zone), Upper Crisis Interval II.

Hangenberg Sandstone: Ca. 22 m alternating olive-grey or dark-grey shales, silty shales, siltstones, and micaceous, calcareous sandstones, Middle Crisis Interval II.

Hangenberg Shale:

Bed of bluish-grey, argillaceous limestone without any fauna; local Middle Crisis Interval Ib.

Ca. 6.5 m platy, olive-grey to dark-grey shale, local Middle Crisis Interval Ia.

Bed of reddish, strongly micaceous sandstone (Stoppel 1977), base ckl.

- unconformity (no Hangenberg Black Shale; eroded?) –

Wocklum Limestone:

Fossiliferous bluish-grey limestone with *Wocklumeria* (*W. denckmanni* Zone, UD VI-D), *Bi. costatus*, *Bi. ultimus ultimus* (recorded as *Bi. ziegleri ziegleri*), *B. muessenbergensis*, *Pa. gracilis* ssp. (three subspecies), *Br. suprema*, and *Ps. marburgensis trigonicus* (top *S. (Eo.) praesulcata* s.l. Zone) at the top (Bed 1, Crisis Prelude).

Discussion: The presence of a limestone unit at the boundary between Hangenberg Shale and Hangenberg Sandstone in the section of Leuteritz and Schäfer was regionally unique. Unfortunately, it was unfossiliferous.

Dasberg (Fig. 7)

Location: Although the Dasberg ca. 1 km WNW of Hövel (northern Sauerland, Fig. 9, sheet 4613 Balve, ca. r 3 424 100, h 5 693 400) provided the name for the Dasberg Formation and Dasberg-Stufe (Dasbergian), there are only very small natural outcrops. The knowledge of precise conodont and ammonoid stratigraphy, therefore, is based on temporary trenches (e.g.

Schindewolf 1937; Schäfer 1976). Only the trenches of D. Korn dug in the late eighties made the uppermost Famennian available (Clausen and Korn 2008).

Literature: Denckmann and Lotz (1900), Denckmann (1902), Wedekind (1914: type locality of *Costaclymenia kiliani*), Schmidt (1924a, b: type locality of *Oxyclymenia undulata* var. *coronata*, *C. striata* var. *serpentina*, and *Sellacymenia spinosa*), Paeckelmann (1924), Richter and Richter (1926), Lange (1929: type locality of *Oxy. bisulcata* var. *colubrina*), Paeckelmann and Kühne (1938), Paul (1939b), Schäfer (1976), Korn (1981a, 2017), Korn and Luppold (1987), Korn and Price (1987), Price and Korn (1989: type locality of *Sph. erinacea*), Clausen and Korn (2008), Korn et al. (2018), Korn and Price (2018, 2019: type locality of *Finiclymenia langei*).

Summary of succession: The following account of the Wocklum Limestone, with a focus on levels with FODs, is based on Clausen and Korn (2008).

Bed A, 11 cm, three layers of nodular limestone with *Kamp. endogona*, *Kamp. trigona*, *P. distorta*, *Mim. fuerstenbergi*, and *Liss. wocklumeri*.

Bed B, 21 cm, three layers of partly solid nodular limestone and overlying shale with *P. paprothae*, *P. patens*, *Eff. falk*, and *Ken. rostratum* (base *P. paprothae* Subzone, UD VI-C₁).

Bed D, 13 cm, three layers of nodular limestone with *Kos. schindewolfi*, *Eff. minutula*, *Soliclymenia solariooides*, *M. ademmeri*, and *Gl. glaucopis* (top of *Eff. lens* Zone, top UD VI-B).

Bed E, 19 cm, three layers of nodular limestone and intervening shale with *Mim. trizonatum*.

Bed F, 22 cm, seven layers of nodular limestone with *Eff. lens* (base *Eff. lens* Zone, UD VI-B).

Bed I, 22 cm, six levels of limestone nodules and nodular limestone with *M. bisulcata* and *M. parundulata* (base *M. bisulcata* Zone, UD VI-A₂).

Bed K, 21 cm, five levels of limestone nodules, nodular limestone and intervening shale with *M. galeata*, *Kos. undulata*, and “*Mim.*” *geminum* (upper part of *L. similis* Zone, upper UD I-A₁).

Bed L, 24 cm, four levels of nodular limestone followed by shale with *L. similis*, *M. sublaevis*, *Kalloclymenia* sp., *Cyrt. angustiseptata*, *Sph. erinacea* (type level, formerly Bed 0), and *Mim. alternatum* (lower *L. similis* Zone, lower UD VI-A₁).

Discussion: The rich ammonoid fauna of Korn’s trenches is very important since it considerably supplements the Oberrödinghausen, Müssenberg, Hasselbachtal, and Effenberg records, proving several range additions.

Effenberg (Fig. 7)

Location: Active quarry E of the road from Enkhausen to Herdringen, northern Sauerland (Fig. 9), topographic sheet 4613 Balve, r 2 527 700/h 5 695 950.

Literature: Paeckelmann (1924), Schmidt (1924a, b: type locality of *Chaenocardiola elongata*), Richter and Richter (1926), Paeckelmann and Kühne (1938), Paul (1939b), Korn (1981a, 1992a, 2004, 2017: type locality of *Gonioclymenia wunderlichii*), Paproth et al. (1986b), Korn and Luppold (1987), Korn and Price (1987: type localities of *K.* (*K.*) *undulata effenbergensis* from UD V-C and *K.* (*M.*) *parundulata* from UD VI-B), Price and Korn (1989), Korn in Becker et al. (1993), Luppold et al. (1994), Greifelt (2008), Hartenfels and Becker (2009), Hartenfels (2011), and Hartenfels and Becker (2016).

Summary of succession: The section in the NW corner of the quarry, where mining activities near the property margin stopped many years ago, exposes the top Hemberg Formation and Dasberg Formation, including the Wocklum Limestone, which are partly very fossiliferous and marked by the global *Annulata* Events and the Dasberg Crisis (e.g. Korn and Luppold 1987; Hartenfels and Becker 2009; Hartenfels 2011). A new bed-by-bed survey of the Dasbergian/Wocklumian transition and Wocklum Limestone started in autumn 2017 but there are still only preliminary ammonoid data; a first set of conodont samples has been processed but not yet been analysed. The DCB succession is currently exposed between several tracks within the SE part of the quarry but this outcrop has not yet been investigated in detail; probably, it will not persist in the future. DCB knowledge summarised here is based on data and bed numbers in Korn and Luppold (1987) and Luppold et al. (1994). **Kahlenberg Formation (Lower Alum Shale):** 2 m bleached black shale, Lower Alum Shale Event Interval, middle Tournaisian.

- ?unconformity (no upper part of Hangenberg Limestone) -

Hangenberg Limestone:

Beds 18 m–o, condensed nodular limestone with “*S. (S.) duplicata*” (*S. (S.) bransoni* to *S. (S.) duplicata* Zones).

Bed 18f–l, condensed nodular limestone with *Pr. kuehni* and *S. (Eo.) sulcata* s.l. (lower *S. (Eo.) sulcata* s.l./*Pr. kuehni*-Zone), post-Crisis Interval, lower Tournaisian.

Stockum Limestone:

Beds 18c–e, condensed nodular limestone with acutimitoceratids, transitional forms between *Pr. kockeli* and *Pr. kuehni* (top *Pr. kockeli* to *Pr. kuehni* Zones) and *Po. purus subplanus*, Lower/Upper Stockum Limestone, Upper Crisis Interval II/III.

Beds 18a–b, condensed nodular limestone with acutimitoceratids, *Pr. kockeli* (*Pr. kockeli* Zone), Lower Stockum Limestone, Upper Crisis Interval II,

Ca. 3 cm shale.

Ca. 3 cm calcareous shale with *Guerichia* mass occurrence, *Pr. collinsoni* and *Pr. kockeli* (*Pr. kockeli* Zone), Upper Crisis Interval II.

Hangenberg Sandstone: Ca. 20 cm siltstone.

Hangenberg Shale: 6 cm shale, slightly darker than the succession above.

- minor unconformity (no Hangenberg Black Shale) -

Wocklum Limestone: The lower part has the richest ammonoid faunas of the outcrop, partly forming kosmoclymeniid coquinas (Hartenfels et al. 2016, fig. 13). This level also yielded *C. semistriata* (Figs. 5i–j), abundant “*Mimimitoceras*”, *K. subarmata*, and giant-sized members of the “*K.*” *pachydisca* Group (Hartenfels et al. 2016, fig. 12).

Top ca. 10 cm with *Ps. marburgensis trigonicus*, *Bi. muessenbergensis*, *Bi. ultimus ultimus* (reported as *Bi. ziegleri ziegleri*), *Br. suprema*, and three subspecies of *Pa. gracilis* (top *S. (S.) praesulcata* s.l. Zone), pre-Crisis Interval/Crisis Prelude.

Cliff of solid nodular limestone above Bed 29 with *P. paradoxa* (*P. paradoxa* Subzone, UD VI-C₂).

Bed 23a, level of thick nodules with *K. subarmata* (?upper part of *L. similis* Zone, UD VI-A) and only long-ranging conodonts. The relationships with “Bed 93d”, the type level of *M. parundulata* Korn and Price, 1987, an alternative index species for the *M. bisulcata* Zone (UD VI-A₂), have not been published.

Bed 19, nodule level with “*Sph.*” *brevispina* (*L. similis* Zone, UD VI-A₁) and *Pa. gracilis gonioclymeniae* (*Bi. ultimus ultimus* Zone).

Bed 17a, nodule level with “*Sph.*” *brevispina* (*L. similis* Zone, UD VI-A₁), basal uppermost Famennian.

Discussion: The strong condensation of DCB beds and the ongoing quarrying disqualify the section for the GSSP search.

Müssenberg (Fig. 7)

Location: Trenches of D. Korn at the Müssenberg N of Hachen and S of Neheim-Hüsten, northern Sauerland (Fig. 9), topographic sheet 4613 Balve, r 3 429 280, h 5 695 320.

Literature: Denckmann and Lotz (1900), Richter and Richter (1926: record of *Phacops granulatus*), Korn (1981a, 1981b, 1989, 1992a, 1993), Paproth and Strel (1982), Luppold et al. (1984, 1994), Brauckmann and Hahn (1984), Korn and Price (1987), Korn and Luppold (1987), Clausen et al. (1989b), Hahn et al. (1990: type locality of *Belgibole abruptirhachis korni*), Becker and Weyer (2004), Clausen and Korn (2008), Klein and Korn (2016), Korn (2017: type locality of *Gonioclymenia pricei* from UD V-C), Korn et al. (2016), Korn and Price (2018, 2019: type locality of *F. czarnockii*), Feist and Weyer (2018).

Summary of succession: Müssenberg-1 section.

Hangenberg Limestone: Condensed, partly crinoidal cephalopod limestone.

Bed 0 with *S. (S.) carinthiaca*, “*S. duplicata*” s.l., and *Ps. triangulus triangulus* (*S. (S.) mehli* Zone).

Bed 1 with “*S. duplicata*” s.l., *Ps. triangulus triangulus* (?basal *S. (S.) mehli* Zone), “*V. peracutus*” (re-identified as an early karagandoceratid by Korn and Weyer 2003 and

Becker and Weyer 2004), *G. cf. involuta* (= cf. *tenuis*) ("Eoc". *nodosus* Subzone, LC I-A₃), and *Diacoryphe strenuispina*.

Bed 2 with *Ps. triangulus inaequalis* (*S. (S.) duplicata* Zone) and *Cyrtoproetus cf. blax*.

Bed 3C with *S. (Eo.) sulcata* s.l., "S. *duplicata*" s.l. (probably *S. (Eo.) bransoni* Zone), reworked *Pa. gracilis gracilis* and *Bi. costatus*, and *G. subinvoluta* (*G. subinvoluta* Subzone, LC I-A₂).

Upper Stockum Limestone: Grey cephalopod limestone.

Bed 3B with *Ac. (St.) intermedium* (auct.) and *C. striata*, the youngest known clymeniid (top LC I-A₁).

Bed 3A with *Ac. (St.) stockumense*, *Ac. (St.) procedens*, and other acutimitoceratids (middle LC I-A₁).

Bed 3a with *Pr. kuehni*, *Pr. kockeli*, *S. (Eo.) sulcata* s.l. (section Müssenberg-4), *Po. purus purus* (basal *S. (Eo.) sulcata* s.l./*Pr. kuehni* Zone), *Ac. (St.) intermedium*, (auct.) *Ac. (St.) kleinerae*, *Ac. (Str.) carinatum* (upper *Ac. (St.) prorsum* Zone, lower LC I-A₁), *Macrobole cf. funirepa* (also reported as *Phillibole drewerensis*), *Waribole superna*, and *Belgibole abruptirhachis korni* (type level); transgressive Upper Crisis Interval III.

- minor unconformity (no Hangenberg Sandstone and Lower Stockum Limestone) -

Hangenberg Shale: 1 cm greenish, silty shale with weathered pyrite, Middle Crisis Interval.

Base Bed 3: Main Hangenberg Extinction, base ckl.

- minor unconformity (no Hangenberg Black Shale) -

Wocklum Limestone: Cyclic alternation of bioturbated, micritic cephalopod limestones, partly with *Stromatactis* structures, nodular shales and calcareous shales. Ammonoid ranges mostly from Korn (1993) and Klein and Korn (2016).

Bed 4 with the last *P. paradoxa* (top *W. denckmanni* Zone, UD VI-D), *Bi. costatus*, *Bi. ultimus ultimus*, *Br. suprema*, *Pa. gracilis* ssp. (three subspecies), *Ps. marburgensis trigonicus* (top *S. (Eo.) praesulcata* Zone), *Haasia antedistans*, and *Silesiops cf. schindewolfi*; Crisis Prelude.

Bed 5 with mass occurrences of *Wocklumeria* and *Lissoclymenia* as indicator of increased condensation, with *Waribole warsteinensis* and *Chaunoproetus*; basal Crisis Prelude.

Bed 13 with *W. denckmanni* and *C. involvens* (base *W. denckmanni* Zone, UD VI-D) and trilobites.

Bed 14 with a rich trilobite fauna (*Rabienops wedekindi*, *Weyerites cf. wocklumeriae*, *Chaunoproetus*, *Skemmatopyge*, *Haasia*, *Typhloproetus*, *Silesiops*, *Waribole*: nine species in total).

Beds 19–17 with *May. nucleus*, *Ken. rostratum* (= *biforme*), *F. wocklumensis*, and *Postglatziella carinata* (base *May. nucleus* Subzone, UD VI-C₃).

Bed 25 with *P. paradoxa*, *Mim. trizonatum*, "Mim." *lentum*, and *B. globularis* (base *P. paradoxa* Subzone, UD VI-C₂).

Bed 29 with *Liss. wocklumeri* and *Mim. fuerstenbergi* (higher *P. paprothae* Subzone, upper UD VI-C₁).

Bed 34 with *P. paprothae*, *Kamp. endogona*, *Kamp. endogona*, *Gl. glaucopis*, *K. schindewolfi*, *L. clauseni*, *Mim. trizonatum*, *Eff. falk*, and *B. globularis* (base *P. paprothae* Subzone, UD VI-C₁).

Bed 38 with *Eff. lens* (base *Eff. lens* Zone, UD VI-B).

Bed 54 with "Mim." *geminum* (higher *M. bisulcata* Zone, UD VI-A₂).

Bed 55 with *S. (Eo.) praesulcata* s.l. (base *S. (Eo.) praesulcata* Zone).

Bed 67 with *M. bisulcata* and *M. parundulata* (base *M. bisulcata* Zone, UD VI-A₂).

Bed 78 with *K. subarmata* (higher *L. similis* Zone, UD VI-A₁).

Bed 80 with *Bi. ultimus ultimus* (recorded in Luppold et al. 1994 as *Bi. ziegleri ziegleri*) and *Pa. gracilis gonioclymeniae*.

Bed 83 with *Br. suprema* and *Kos. undulata* (*L. similis* Zone, UD VI-A₁).

Bed 85 with *Ps. marburgensis trigonicus* (base *Bi. ultimus ultimus* Zone) and "Sph." *brevispina* (ca. base of former "Sph." *brevispina* Zone).

Bed 90 with *L. similis*, *M. sublaevis*, *K. undulata*, *Postwarsteiniensis*, *Cyrto. plicata*, *Rodachia dorsocostata*, and "Mim." *liratum* (base *L. similis* Zone, UD VI-A₁).

Discussion: The Müssenberg trenches provided the best current record for the definition of the Rhenish Wocklum-Stufe (Wocklumian) and for its ammonoid zonation, especially in its lower part (interval of the former *K. subarmata* Zone sensu Schindewolf 1937). The DCB unconformities exclude it from any GSSP discussions.

Reigern Quarry, Hachen

Location: Mostly filled and overgrown old quarry in the forest ca. 500 m N of Hachen, northern Sauerland (Fig. 9), topographic sheet 4613 Balve, r 3 429 770/h 5 695 230 (GPS 51° 23' 15.77", N 7° 59' 25.20").

Literature: See compilation in the recent review by Söte et al. (2017). Subsequently, a *Sphenoclymenia brevispina* from Reigern was figured by Korn and Price (2019).

Succession: The Reigern Quarry is a very important locality for ammonoids from the lower part of the Wocklum Limestone (Korn 1981a, 1988b; Price 1982; Korn and Price 1987; Price and Korn 1989). The recent conodont study by Söte et al. (2017) proved the presence of the *Bi. ultimus ultimus* (Beds 1–23) and *S. (Eo.) praesulcata* s.l. Zones (Beds 24–39). The DCB is marked by a long-lasting major unconformity, with non-deposition starting before the base of the *P. paprothae* Subzone (UD VI-C₁) and lasting until the Viséan.

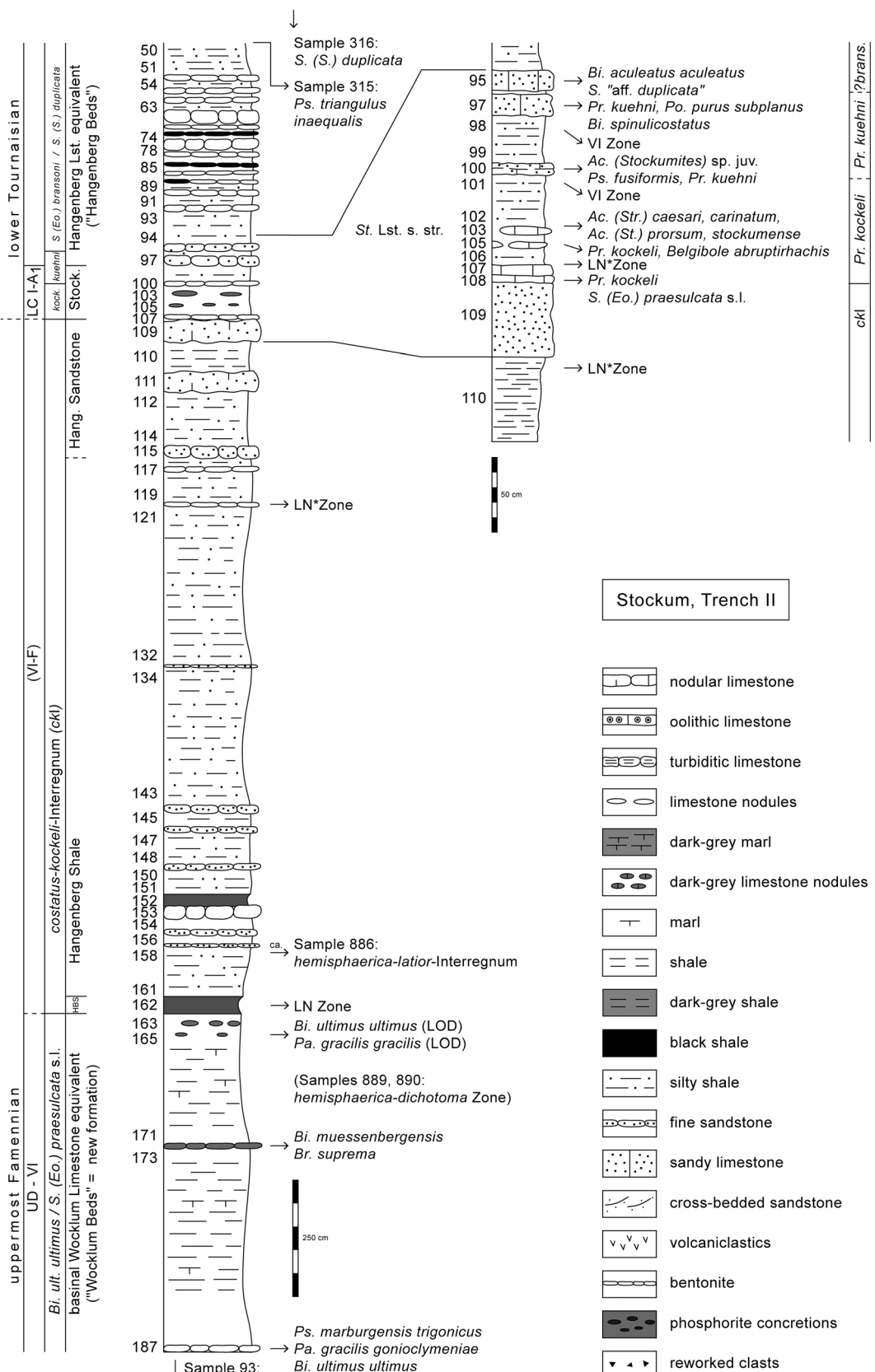


Fig. 13 Summary section log for the DCB transition at Stockum (re-drawn from the section log of Clausen et al. 1994, fig. 6) showing the occurrences of marker conodonts, ammonoids and miospore zones. For

abbreviated zones and lithological units see Fig. 1; for references to the numerous records see text; for lithology types see legends of Figs. 6, 7

Burgberg near Wocklum (“Borkewehr”)

Location: Forest track and old quarry at the SW slope of the Burgberg near Wocklum-Mellen, northern Sauerland (Fig. 9), topographic sheet 4613 Balve, r 3 422 050, h 5 688 650 (see quarry sketch in Schmidt and Pleßmann 1961, fig. 4).

Literature: Denckmann (1901), Wedekind (1918: type locality of *Epi. appланata* and *W. denckmanni*), Paeckelmann (1924), Schmidt (1924a, 1924b: first section measurements), Richter and Richter (1926), Schindewolf (1926), Lange (1929: type locality of *C. involvens* and *F. wocklumensis*), Matern (1929), Rabien (1954), Bischoff (1957: type locality of *Bi. ultimus ultimus*, *Pr. kockeli*, and *Tripodellus robustus*), Voges (1959, 1960), Schmidt and Pleßmann (1961), Strel (1969: failed attempt to find DCB spores), Eickhoff (1970; type locality of *Hyperammina aperta* and *?Moravammina constricta*), Ziegler (1971), Price and Korn (1989), Luppold et al. (1994), Becker (1996, 2000), Becker et al. (2016a), Becker and Hartenfels (2017), Hartenfels et al. (2017a, b), Hartenfels and Becker (2018, 2019), Korn and Price (2019: revision of *F. wocklumensis*), Herbig et al. (2019).

Discussion: The Burgberg or Borkewehr section is an important DCB GSSP candidate since it records the sharp Hangenberg Extinction of ammonoids and conodonts, the subsequent Hangenberg Black Shale, equivalents of the Hangenberg Shale and Sandstone, and, notably, the early protognathid evolution after the Hangenberg Regression. For a refined section log see Becker et al. (2016a). A new bed-by-bed study of ammonoids, conodonts, corals, microfacies, and geochemistry has been completed and will be presented in 2021 in a separate contribution to this journal.

Stockum Trenches (Figs. 7, 13)

Location: Forest track slope and various adjacent trenches on the southern slope of the Spitze Kahlenberg, 900 m ESE of Stockum, sheet 4713 Plettenberg, ca. r 3 430 190, h 5 684 600 (Fig. 9).

Literature: Henke (1924), Schmidt (1924a), Schmidt (1924b: type locality of *Aganides carinatus*, *Pleurotomaria (Mourlonia) Henkei*, and *Spiriferina tarpata*; 1925: type locality of *Aganides prorsus*), Gallwitz (1928), Richter and Richter (1951), Weyer (1965a, 1977), Ziegler (1969: type locality of *Pr. meischneri* and *Pr. collinsoni*, 1970), Alberti et al. (1974), Paproth and Strel (1982), Brauckmann and Hahn (1984), Keupp and Kompa (1984), Kasig et al. (1984), Bless and Groos-Uffenorde (1984), Korn (1984, 1994), Hahn et al. (1990), Higgs et al. (1993), House (1993), Clausen et al. (1989b, 1994: detailed locality maps and revision), Higgs and Strel (1994), Strel and Korn et al. (2016), Mottequin et al. (2019).

Summary of succession: Results from the different trenches can be combined to a synthetic DCB section, giving both the

units of Alberti et al. (1974: Alb-letters) and the more detailed bed numbering of Clausen et al. (1994):

Kahlenberg Formation (Lower Alum Shale):

Unit Alb-E, 5 m black shale, in the upper part with cherts, with *S. (S.) crenulata*, *S. (S.) quadruplicata*, and *Ps. pinnatus* (Samples 351–350, Trench III; *S. (S.) crenulata* Zone), Lower Alum Shale Event Interval, middle Tournaisian.

Basinal Shale equivalents of Hangenberg Limestone (no valid member name, included as an upwards extension in the “Hangenberg Shale” in Korn 2010, or included in undivided “Hangenberg Schichten” in Herbig et al. 2018):

Unit Alb-D, 36 m greenish-grey, silty shales with some micaceous and calcareous silt and sandstones and limestone concretions, among ostracods first with *Richterina (R.) latior* (Sample 891), higher with abundant *Maternella cf. arcuata* and *M. schindewolfi*; type level of *Ungerella postmulticostata* and *U. stockumensis*. Conodont succession of Groos-Uffenorde and Uffenorde (1974):

Sample 353 (Trench III): first *S. (S.) lobata* (*S. (S.) lobata* M1 Subzone).

Sample 919 (Trench III): local first *S. (S.) obsoleta*.

Sample 921 (Trench III): first *S. (S.) sandbergi* and *Ps. triangulus triangulus* (*S. (S.) sandbergi* Zone and Subzone).

Samples 321–322 (Trench I) and Sample 325 (Trench III): *S. (S.) quadruplicata* (*S. (S.) mehli* Zone).

Sample 918 (Trench III): first *S. (S.) cooperi* (*S. (S.) mehli* Zone).

Sample 316 (Trench I): first *S. (S.) “duplicata s.str.”* (*S. (S.) duplicata* Zone).

Sample 315 (Trench I, ca. 5.2 m above Stockum Limestone s.str.): first *Ps. triangulus inaequalis* (*S. (S.) bransoni* to *S. (S.) duplicata* Zone).

Bed 95 (upper part of Unit Alb-C-e), 15–25 cm calcareous sandstone with *S. (S.) aff. duplicata* (*S. (S.) bransoni* to *S. (S.) duplicata* Zones), post-Crisis Interval.

Bed 97 (lower part of Unit Alb-C-e), 15–25 cm pyritic, calcareous sandstone with *Pr. kuehni*, *Bi. spinulicostatus*, *Po. purus subplanus* (Samples 331, 305), and others (*S. (Eo.) sulcata* s.l./*Pr. kuehni* Zone), miospores of the VI Zone, probably basal post-Crisis Interval.

Stockum Limestone:

Beds 98–99 (Unit Alb-C-d), 20–30 cm silty and micaceous shale with miospores of the VI Zone, ca. top Crisis Interval.

Bed 100 (Unit Alb-C-c), up to 8 cm-thick, dark-grey, sandy limestone (lower micrite cut off by a higher tempestite layer), rich in juvenile goniatites (acutimitoceratids) and conodonts, with *Pr. kuehni* (Sample 330 of Alberti et al. 1974), *Pr. kockeli*, *Ps. fusiformis*, and other conodonts (basal *S. (Eo.) sulcata* s.l./*Pr. kuehni* Zone), and trilobites (*Belgibole abruptirhachis abruptirhachis*, *Macrobole funirepa*; Sample 200), Upper Stockum Limestone, Upper Crisis Interval III.

Beds 101–102 (upper Unit Alb-C-b), ca. 35 cm silty shales with *Belgibole abruptirhachis abruptirhachis*, *Macrobole*

funirepa (Sample 923), and miospores of the basal VI Zone, basal Upper Crisis Interval III.

Bed 103 (middle Unit Alb-C-b), Stockum Limestone lenses s.str., very fossiliferous, dark-grey limestone lenses (biopelmicrite to cephalopod rudstone with recognisable sublayers), up to 8 cm thick, with abundant goniatiates (type level of *Ac. (St.) prorsum*, *Ac. (St.) stockumense*, *Ac. (Str.) carinatum*, and *Ac. (Str.) caesari*; upper part of *Ac. (St.) prorsum* Zone, LC I-A₁), *Pr. kockeli*, *Pr. collinsoni*, *Ps. nodomarginatus*, and other conodonts (upper *Pr. kockeli* Zone), *?Texathyris tarpata* (type level), *Belgibole abruptirhachis abruptirhachis*, top Lower Stockum Limestone, top Upper Crisis Interval II.

Beds 104–106 (lower Unit Alb-C-b), 40 cm silty shale to micaceous siltstone, including a level of very solid, dark-grey, laminated, pyritic limestone concretions (Bed 105) up to 30 cm in diameter, with *Pr. kockeli*, *Pr. meischneri*, *Pr. collinsoni*, *Neo. communis dentatus*, and other conodonts (*Pr. kockeli* Zone), and with *Belgibole abruptirhachis abruptirhachis*, *Macrobole ogivalis*, *Macrobole duodecimae*, and other trilobites (Samples 102, 923), ostracods (*Maternella* species), *Guerichia*, and miospores of the upper, atypical LN Zone, middle Lower Stockum Limestone, middle Upper Crisis Interval II.

Beds 107–108 (top Unit Alb-C-a), two thin limestone beds with *Pr. kockeli*, *Pr. meischneri*, *Neo. communis communis*, and *S. (Eo.) praesulcata*.l. (Sample 303, basal *Pr. kockeli* Zone), basal Lower Stockum Limestone, basal Upper Crisis Interval II.

Hangenberg Shale/Sandstone:

Bed 109 (Unit Alb-C-a), 50 cm calcareous and micaceous sandstone, Middle Crisis Interval.

Beds 110–119 (upper Unit Alb-C), ca. 3.3 m alternating greenish-grey, silty, micaceous shales, upwards increasingly with sandstones, with miospores of the upper, atypical LN Zone, Middle Crisis Interval II.

Beds 120–157 (lower/middle part of Unit Alb-C), ca. 9.5 m greenish-grey, silty, micaceous shale alternating with thin, partly laminated or calcareous, micaceous silt and sandstones, with a solid sideritic level (Bed 153) and a weathered, dark-grey, argillaceous, unfossiliferous limestone (Bed 152) in the lower part, and with miospores of the LN Zone, Middle Crisis Interval I; Sample 886 from the ca. lower meter with *Richterina (Richt.) costata* and *Richt. (Richt.) striatula (hemisphaerica-latior)* Interregnum).

Beds 158–161 (ca. top Unit Alb-B), ca. 50 cm greenish-grey silty shale, Middle Crisis Interval I.

Hangenberg Black Shale:

Bed 162 (within higher Unit Alb-B), ca. 35 cm black shale, base of LN zone (Higgs and Strel 1994), Lower Crisis Interval.

Basinal Shale equivalents of Wocklum Limestone (no modern formation name):

Beds 163–187 (lower/middle Unit Alb-B), 7.2 m greenish-grey to brownish, silty shales with thin, dark-grey limestones in the middle (Bed 172) and upper parts (Beds 163–165), with *Bi. ultimus ultimus* (including *Bi. ziegleri*, Bed 187 and Sample 933, ca. 8 m below), *Bi. costatus* (Bed 187), *Bi. muessenbergensis* (Bed 172), *Br. suprema* (Bed 172), *Ps. marburgensis trigonicus* (Bed 187), *Pa. gracilis gonioclymeniae* (Bed 187 and Sample 933, see Groos-Uffenorde and Uffenorde 1974), *Pa. gracilis gracilis*, and *Pa. gracilis sigmoidalis* (*Bi. ultimus ultimus* to *S. (Eo.) praesulcata* s.l. Zones); ostracods of the *Maternella* (*Mat.*) *hemisphaeria*-*Mat.* (*Mat.*) *dichotoma* Zones (Samples 889 and 890, 15–17.5 m below the Stockum Limestone s.str.) and trilobites (*Dianops*, *Weyerites*, *Typhloproetus*, *Chaunoproetus*, *Drevermannia*; Samples 202, 203); uppermost Famennian, pre-Crisis Interval to Crisis Prelude.

Discussion: The initial major significance of the Stockum Limestone lenses was the discovery of a distinctive conodont and ammonoid fauna that differs strictly from the pre-Crisis (typical topmost Devonian) *Wocklumeria* and post-Crisis (typical basal Carboniferous) *Gattendorfia* faunas. Since a similar fauna was lacking at Oberrödinghausen, it became clear that the stratotype includes a significant gap right at the boundary, which disqualified it and led to the search for a new DCB GSSP. Subsequently, a succession of *Protognathodus* faunas (*meischneri/collinsoni-kockeli-kuehni*) was established, which shows that the larger Stockum Limestone interval comprises in various localities up to three different levels (here: Upper Crisis Interval I–III). At Stockum, “older” (without *Pr. kuehni*) and “younger” (with *Pr. kuehni*) *Protognathodus* faunas were distinguished since Alberti et al. (1974); they characterise the Lower and Upper Stockum Limestone sensu Becker et al. (2016a). The resampling by Clausen et al. (1994) of the main goniatlite limestone of Schmidt (1924a, b), Bed 103, did not reproduce the Alberti et al. (1974) and Groos-Uffenorde and Uffenorde (1974) records of *Pr. kuehni*. This led to the assumption that the *kuehni* level was the slightly younger, thin Bed 100 of Clausen et al. (1994), which is also rich in goniatlites, but mostly only in juveniles. The presence of *Po. marginvolutus* and of pseudopolygnathids in Bed 103 (Luppold and Stoppel in Clausen et al. 1994, Strel and Korn 2016) is not typical for conodont faunas of the *kockeli* Zone of other Rhenish localities.

E of Weninghausen (Fig. 7)

Location: Former slopes along a track branching off to the N from the road from Linnepe to Wenighausen, sheet 4614 Arnsberg, ca. r 3 435 120 /h5 687 125 (Fig. 9).

Literature: Gallwitz (1928), Kühne (1938).

Succession: The shelf basin facies between the Stockum area and the seamount settings of the drowned Warstein, Belecke, and Brilon reefs towards the E/NE is mostly poor in

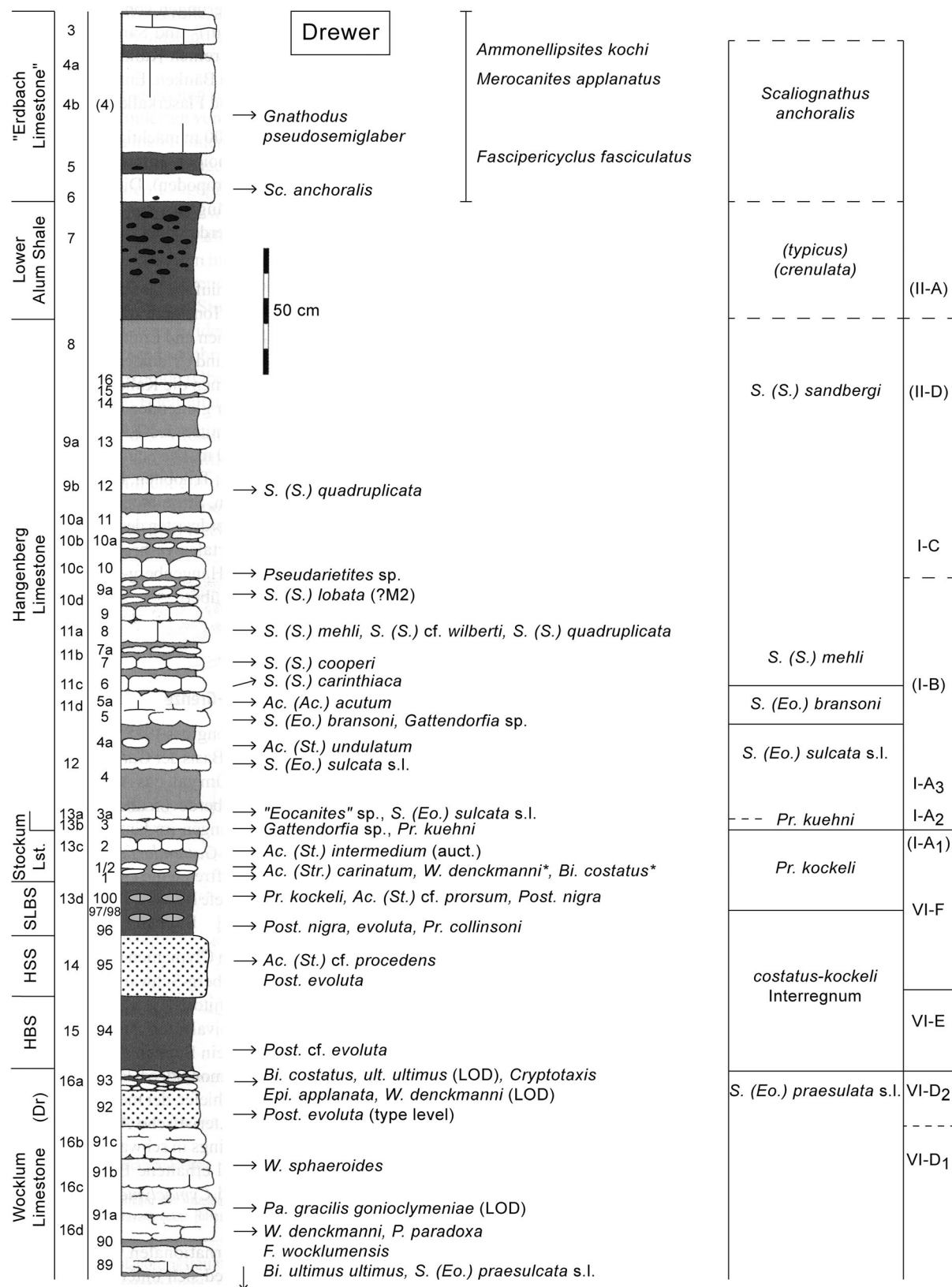


Fig. 14 Synthetic DCB succession of the Provincial Quarry Brewer near Belecke, showing occurrences of index ammonoids and conodonts, originally re-drawn from Clausen and Korn (2008), here updated from

Becker et al. (2016b). For abbreviated zones and lithological units see Fig. 1; for references to the numerous records see text, * = reworked; for lithology legend see Fig. 13

macrofauna. The recognition of the Crisis Interval in the undivided, more monotonous, shaly Hangenberg Formation is difficult and hampered by the lack of outcrops. As an exception, Gallwitz (1928) described a succession from the E of Weninghausen:

Kahleberg Formation: 20 m Lower Alum Shale with a sharp base, Lower Alum Shale Event Interval, middle Tournaisian.

Hangenberg Limestone equivalents: 34 m solid, dark-greenish to bluish-grey shales with large, bluish, quartzitic concretions and intercalated, up to 40 cm thick beds of sandy, very hard, reddish to violet limestone, post-Crisis Interval.

Stockum Limestone equivalent: 1.2 m dark marls and greenish, partly micaceous shale with *Ac. (St.) prorsum* (re-assigned to *Ac. (St.) substriatum* in Kühne 1938), *Ac. (St.) infracarbonicum*, ?*Texathyris tarpata*, and bivalves, Upper Crisis Interval.

Hangenberg Shale/Sandstone: Ca. 6 m greenish-grey shales with thin-bedded, calcareous, and micaceous sandstones, Middle Crisis Interval.

Wocklum Limestone equivalents:

Dark, calcareous shales with *Semiproetus (Anglibole) cf. anglica*, *Drevermannia schmidti*, *Weyerites*, and *Dianops*, ?Crisis Prelude.

15 cm argillaceous, brownish weathering limestone, ?regressive Crisis Prelude.

Ca. 8 m greenish-grey, calcareous shales with some argillaceous, reddish-grey limestone beds with *Dianops anophthalmus*, pre-Crisis Interval.

Eastern Sauerland (Belecke to Brilon regions)

Drewer (Figs. 7, 14)

Location: Abandoned and partly filled quarry (“Provinzialsteinbruch”) 1 km SW of Drewer and 2 km N of Belecke, NE Sauerland (Fig. 9), topographic sheet 4526 Belecke, at r 5 555 000, h 6 710 000. The section is situated in the core of the 2nd order Belecke Anticline.

Literature: A complete compilation was given by Becker et al. (2016b). Especially important are the papers by Schmidt (1922, 1924a, b), Schindewolf (1923b, 1926), Clausen and Leuteritz (1979b), Clausen et al. (1987, 1989a), Hahn et al. (1990), Korn (1991), Becker (1993, 1999), Korn et al. (1994b), Leuschner (1994), Clausen and Korn (2008), and Kumpan et al. (2015). New Drewer ammonoid specimens were included in Korn et al. (2016), Herbig (2016), Korn (2017), Korn and Price (2019), and Herbig et al. (2019).

Summary of succession: Sixteen lateral sections have been measured and sampled along the western and northern quarry walls (Korn 1991). Their correlation led to a synthetic succession with conodont and ammonoid ranges (Korn 2002; Clausen and Korn 2008; Becker et al. 2016b). It is not possible to plot unequivocally the samples and conodont faunas of the

strongly condensed sections at the NE Wall of Clausen et al. (1987, 1989a). The updated synthetic succession is as follows:

Belecke Member of Eichenberg Formation (Lower Alum Shale):

Ca. 1 m of black, pyritic and anoxic/euxinic (high U/Th ratios), unfossiliferous, laminated alum shales (middle Tournaisian).

Transgressive and anoxic/euxinic Lower Alum Shale Event at the sharp base.

Hangenberg Limestone: Strongly cyclic alternation of light-to middle-grey nodular limestone and calcareous shale, poor in macrofauna.

Bed 13 (= 9a) with *S. (Eo.) isosticha* and *S. (S.) quadruplicata* (top *S. (S.) lobata* M1 Subzone).

Bed 12 (= 9b) with *S. (S.) lobata* and *S. (S.) quadruplicata* (*S. (S.) lobata* M1 Subzone).

Bed 10 (= ca. 10a) with *Pseudarietites* sp. (*Pseud. westfalicus* Zone, LC I-C).

Bed 9a (= 10d) with *S. (S.) obsoleta* and *Ps. triangulus inaequalis* (top *S. (S.) mehli* Zone to basal *S. (S.) sandbergi* Zone).

Beds 8/9 (= 11a) with *S. (S.) mehli*, *S. (S.) quadruplicata* (morphotype unknown), and *S. (S.) cf. wilberti* (upper part of *S. (S.) mehli* Zone).

Beds 6/7 (= 11b/c) with *S. (S.) cooperi* M2, *S. (S.) carinthiaca*, *S. (S.) duplicata* (M2), and *Ps. triangulus triangulus* (lower part of *S. (S.) mehli* Zone).

Bed 5 (= 11d) with *S. (Eo.) bransoni* (*S. (Eo.) bransoni* Zone).

Bed 4 (= 12) with *S. (Eo.) sulcata* s.l. (Fig. 2j, k) (*S. (Eo.) sulcata* s.l./*Pr. kuehni* Zone).

Bed 3a (= 13a) with “*Eocanites*” sp. (“*Eoc.*” *nodosus* Subzone, LC I-A₃) and *S. (Eo.) sulcata* s.l. (*S. (Eo.) sulcata* s.l./*Pr. kuehni* Zone); a local new record of *Ac. (Str.) heterolobatum* (Figs. 5r–q) comes from a loose block with *Po. purus purus*, *Neopolygnathus*, and siphonodelloids.

Bed 3 (= 13b) with *Gattendorfia* sp. and *Ac. (St.) kleinerae* (*G. subinvoluta* Subzone, LC I-A₂), *Pr. kuehni* (Bed 13b, Clausen et al. 1989a), *S. (Eo.) sulcata* s.l. (section NF), *Ps. primus primus* (= *dentilineatus*), *Po. purus purus* (basal *S. (Eo.) sulcata* s.l./*Pr. kuehni* Zone), and *Liobolina submonstrans*; basal Post-Crisis Interval.

Stockum Limestone: Middle- to dark-grey nodular limestones and marls with conodonts of the *Protognathodus* Biofacies.

?Upper Stockum Limestone, Bed 2 (= 13c) with *Ac. (St.) intermedium* (auct.) (top *Ac. (St.) prorsum* Zone), transitional forms between *Pr. kockeli* and *Pr. kuehni* (?*S. (Eo.) sulcata* s.l./*Pr. kuehni* Zone), reworked *Bi. costatus* and *Pa. gracilis gracilis*, and *Liobolina* sp. 1; ?Upper Crisis Interval III.

Lower Stockum Limestone, Bed 1 and 1/2 (= 13d) with *Ac. (Str.) carinatum* (upper *Ac. (St.) prorsum* Zone), *Pr. kockeli*, *Po. purus subplanus*, *Polygnathus* ?n. sp., and *Cryptotaxis*

culminidirectus (upper part of *Pr. kockeli* Zone), *Belgibile abruptirhachis abruptirhachis*, *Macrobole*, reworked *Liss. wocklumeri* and (perhaps) *Post. evoluta*, ?minor transgression, local Upper Crisis Interval IIc.

Base of Bed 1, laterally discontinuous reworking level with re-sedimented *Wocklumeria*, *Pa. gracilis* ssp., *Ps. marburgensis trigonicus*, *Bi. costatus*, *Bi. ultimus ultimus*, ostracods and trilobites, ?regressive phase, local Upper Crisis Interval IIb.

Stockum Level Black Shale: Beds 96–100, local lenticular unit of black shale with black limestone nodules and conodonts of the *Protognathodus* Biofacies.

Beds 99–100 with *Post. evoluta*, *Post. nigra*, and *Ac. (St.) cf. prorsum* (upper *Ac. (St.) prorsum* Zone), with *Pr. kockeli* (lower part of *Pr. kockeli* Zone), local Upper Crisis Interval IIa.

Beds 96–98 with *Post. evoluta* and *Post. nigra* (middle *Ac. (St.) prorsum* Zone) and impoverished *Pr. meischneri*-*Pr. collinsoni* Fauna (upper ckI), initial post-glacial transgression, Upper Crisis Interval I.

Hangenberg Sandstone:

Bed 95, thin- to slightly cross-bedded, fossiliferous, pyritic, micaceous, lenticular siltstone with *Ac. (St.) cf. procedens* and *Ac. (St.) cf. prorsum* (lower *Ac. (St.) prorsum* Zone, UD VI-F), no conodonts (middle ckI), important regression (high Zr/Al ratio), with sequence boundary at the sharp, discontinuous base, Middle Crisis Interval II.

Hangenberg Black Shale:

Bed 94, 40 cm organic-rich, black, fissile alum shale, poor in macrofauna but with rare *Post. cf. evoluta*, base of *Post. evoluta* Zone (UD VI-E) and lower ckI (no conodonts so far), maximum flooding (low Zr/Al ratio), anoxic (high U/Th ratios), Lower Crisis Interval II.

Main Hangenberg Extinction of ammonoids and conodonts at the somewhat gradual base, Lower Crisis Interval I.

Wocklum Limestone: Strongly cyclic alternation of grey, nodular mudstones/wackestones and calcareous shales:

Bed 93, last three nodules layers (7–10 cm), dark-grey, pyritic, with *Epi. appplanata*, the last *W. denckmanni* (Figs. 5a–b), *P. paradoxa*, *F. wocklumensis*, *Cyrtoclymenia*, *May. nucleus*, and *Ebbighausenites* (*Epi. appplanata* Subzone, UD VI-D₂), the last *Bi. costatus*, *Bi. ultimus ultimus*, *Ps. marburgensis trigonicus*, and *Pa. gracilis* ssp., *Rabienops horni*, ?*Cryphops wocklumeriae*, and *Chaunoproetus stockumensis*; minor deepening, Crisis Prelude II.

Bed 92, local, 30–40-cm thick, lenticular “**Drewer Sandstone**”, a pyritic, calcareous and micaceous, laminated siltstone, type level of *Post. evoluta*, regressive phase, Crisis Prelude I.

Bed 91 with *W. denckmanni* and *W. sphaeroides* (*W. denckmanni* Zone, UD VI-D₁).

Samples 3–5 (Korn et al. 1994) with *P. paradoxa* and *Glatziella glaukopis* (*P. paradoxa* Subzone, UD VI-C₂).

Sample 1 (Korn et al. 1994) with *Gl. cf. minervae* and *Gl. glaukopis* (*M. galeata* to *P. paprothae* Zones, UD VI-A₂ to C₁).

In the 1978 section of Clausen et al. (1989a), the top of the Wocklum Limestone is followed by a bed (Sample 7) with mixed, dominant pre-crisis conodonts and a single *Pr. kockeli*. The next bed (Sample 6) had already *S. (S.) bransoni*. Therefore, the critical DCB interval was missing by extreme condensation. The situation was not much better in their section sampled in 1979.

Discussion: Brewer is the only Rhenish section, where the shallowing upwards in the upper Wocklum Limestone led to a siltstone intercalation, the “Drewer Sandstone”, which is a good marker for the base of the Crisis Prelude. The Middle Crisis Interval is locally very condensed, possibly due to an unconformity at the base of the silty equivalent of the Hangenberg Sandstone. Therefore, there is locally no Hangenberg Shale. The lateral disappearance of several units, for example of the Hangenberg Black Shale, Brewer, and Hangenberg Sandstones, reflects a steep palaeoslope. Due to increasing turbulence upslope, siliciclastics did not settle towards the top of the seamount. The reworking in the Upper Crisis Interval, within the *Pr. kockeli* Zone, either reflects a minor regression or was the result of local synsedimentary tectonics, which triggered slumping. Glide folds are well-developed higher in the Carboniferous (Kronberg et al. 1960).

GSSP Prospects: Brewer would be a prime GSSP candidate if the DCB was defined by the Hangenberg Black Shale. For a higher boundary, its advantages are a thick and complex Upper Crisis Interval. Its main disadvantages are the lateral pinching out of beds, the inaccessibility of the Stockum Level Black Shale and its important limestone nodules in the vertical quarry wall, and the scarcity of conodonts in the critical units. Above the Wocklum Limestone, many conodont taxa tend to be represented in normal-sized samples by single specimens only (see tables in Clausen et al. 1989a). Therefore, it is hardly possible to study morphological changes within protognathids above the Hangenberg Sandstone. Apart from the top Wocklum Limestone, ammonoids are also rare.

Kattensiepen (Fig. 7)

Location: Variably active quarry at the road from Rüthen to Suttrop, topographic sheet 4516 Rüthen, r 3 457 980/h 5 703 750, northern limb of Warstein Anticline (Fig. 9; asymmetric Kattensiepen Anticline).

Literature: Staschen (1968), Struckmeier (1974), Stoppel 1977, Heuser et al. (1977), Clausen and Leuteritz (1979b), Clausen et al. 1984b, Luppold et al. (1994), Korn (2002, 2017), Koch et al. (2003: type locality of the arthropod *Sutropcaris bottkei*), Slotta et al. (2011).

Summary of succession: The Famennian to basal Carboniferous consist of ca. 60 m, very strongly cyclic,

well-bedded nodular limestone. Only the *Annulata* Event beds are rich in macrofauna, especially in ammonoids. Based on logging by H. Uffenorde, the DCB succession includes:

Belecke Member of Eichenberg Formation: 2.5 m dark-grey shale with phosphatic nodules, especially at the base and above a short outcrop gap.

Hangenberg Limestone: 70 cm middle-grey, nodular, argillaceous limestone with *S. (Eo.) sulcata* s.l./*Pr. kuehni*, *Ps. triangulus inaequalis*, and *Ps. triangulus triangulus* Zones in succession, post-Crisis Interval.

?Stockum Limestone: 40 cm silty limestone.

Hangenberg Sandstone: 58 cm grey, calcareous, micaceous siltstone, Middle Crisis Interval II.

Hangenberg Shale: 17 cm silty shale, Middle Crisis Interval I.

- short outcrop gap –

Wocklum Limestone: Nodular and flaserlimestone.

Discussion: Luppold et al. (1994) note that the strongly condensed DCB interval is represented by siliciclastics without macrofauna and relevant conodonts. Unconformities (gaps) are likely and the tectonic deformation is strong. This excludes the quarry from further DCB discussions.

Bilstein Cave

Location: Old shooting exercise ground 400 m SE of the entrance to the Bilstein Cave, ca. 3 km SW of Warstein, topographic sheet 4516 Warstein, r 3 453 210/h 5 698 930 (Fig. 9).

Literature: Sandberger (1853), Schmidt (1922, 1924a, b), Paul (1939b; type-region of *Pterochaenia schmidtii*), Richter and Richter (1949), Clausen et al. (1979), Korn (1981a), Clausen et al. (1984b), Luppold et al. (1994), Korn et al. (2016).

Succession: This DCB succession is strongly tectonised, silicified, and incomplete. It yielded important upper/uppermost Famennian ammonoids (type locality of *C. warsteinensis* Korn in Clausen et al. 1979, and *C. nephroides* Korn, 1981a). Since there is a significant unconformity above the Wocklum Limestone, the section is irrelevant for the current DCB discussion.

Eulenspiegel (Fig. 7)

Location: Middle to uppermost Famennian nodular limestones of a special saddle (Eulenspiegel Anticline), reaching ca. until UD VI-B/C, were exposed in an old quarry at the old road from Kallenhardt-Heide to Rüthen (topographic sheet 4516 Warstein, r 3 461 370, h 5 704 120; Fig. 9). The DCB became episodically accessible ca. 150 m to E, along the western slope, when a new road from Rüthen to Nuttlar was built. This outcrop is now grown over.

Literature: Schmidt (1922, 1924a, b), Richter and Richter (1926; type locality of *Waribole eulenspiegelia*), Paul (1939b), Clausen and Leuteritz (1979a, b), Clausen et al.

(1984a, b), Clausen et al. (1987, 1989a), Luppold et al. (1994), Sartenaer (1997).

Succession (based on Clausen et al. 1989a and Luppold et al. 1994):

Kahlenberg Formation: Ca. 1.3 m Lower Alum Shale, in the upper part with phosphorite concretions, Lower Alum Shale Event Interval, middle Tournaisian.

Hangenberg Limestone: Strongly condensed flaserlimestones.

- ?minor unconformity (upper Hangenberg Limestone, *S. (S.) sandbergi* Zone) -

Bed 24, ca. 25 cm flaserlimestone with *S. (S.) mehli*, *S. (S.) duplicata*, *S. (S.) bransoni*, *S. (S.) cf. wilberti* (“*duplicata* sensu Hass”), *S. (S.) carinithiaca*, and *Ps. triangulus inaequalis* (*S. (S.) mehli* Zone) -

Bed 23, ca. 30 cm, thick-bedded flaserlimestone with *S. (S.) bransoni*, *S. (Eo.) sulcata* s.l., and others (*S. (S.) bransoni* Zone).

Bed 22, ca. 15 cm flaserlimestone with *Pr. kuehni*, *Pr. kockeli*, *Pr. collinsoni*, *Pr. meischneri*, *S. (Eo.) sulcata* s.l., *Ps. dentilineatus* (= *Ps. primus primus*), *Po. purus purus*, and others (*S. (Eo.) sulcata* s.l./*Pr. kuehni* Zone), post-Crisis Interval.

- ?minor unconformity (Upper Crisis Interval III) -

Stockum Limestone:

Bed 21, 10 cm flaserlimestone with *Pr. kockeli*, *S. (Eo.) praesulcata* s.l., *Po. purus subplanus*, *Po. inornatus*, bispathodids, and *Neo. communis communis* (*Pr. kockeli* Zone), Lower Stockum Limestone, Upper Crisis Interval II.

Bed 20, ca. 12 cm shale.

Beds 18/19, two layers of limestone nodules, not sampled for conodonts, possibly Basal Stockum Limestone, Upper Crisis Interval I.

Hangenberg Shale/Sandstone: Bed 17, ca. 60 cm silicified, hard, calcareous shales and siltstones, Middle Crisis Interval.

Hangenberg Black Shale: Bed 16, ca. 25 cm black shale with small *Guerichia*, Lower Crisis Interval.

Wocklum Limestone:

Ca. 1.1 m well-bedded, dark-grey flaserlimestone with very thin shale interbeds, poor in macrofauna.

Bed 15 with *Wocklumeria* sp. (*W. denckmanni* Zone, UD VI-D) and the last *Bi. ultimus ultimus* (including *Bi. ziegleri*), *Ps. marburgensis trigonicus*, *Pa. gracilis* (three subspecies), and with *Pr. meischneri* (top *S. (Eo.) praesulcata* s.l. Zone), ?Crisis Prelude.

Beds 12–14 with *Ps. marburgensis trigonicus* and rare *Bi. ultimus ultimus*, without siphonodellids (higher *Si. (Eo.) praesulcata* s.l. Zone), pre-Crisis Interval.

Bed 11 with *Po. inornatus* and *S. (Eo.) prasesulcata* s.l. (*Si. (Eo.) praesulcata* s.l. Zone).

Beds 5–10 with *Bi. ultimus ultimus*, *Pa. gracilis gonioclymeniae*, and *Ps. marburgensis trigonicus* (*Bi. ultimus ultimus* Zone), uppermost Famennian.

Discussion: The section was of special importance since it showed the joint entry of *Pr. kuehni* and *S. (Eo.) sulcata* s.l. in Bed 22. However, the dominance of siphonodellids in that

bed clearly place it in the basal Hangenberg Limestone, whilst there is no protognathodid succession within the locally condensed Stockum Limestone.

Scharfenberg (Fig. 7)

Location: Former small quarry and slope on the eastern side of the road from Scharfenberg to Brilon, NE Sauerland (Fig. 9), topographic sheet 4517 Alme, r 3 467 670/h 5 698 630.

Literature: Matern (1929), Paechelmann and Kühne (1936), Stoppel (1977), Clausen et al. (1989a), Luppold et al. (1994).

Succession: The following summary is mostly based on Clausen et al. (1989a):

Kahlenberg Formation (Lower Alum Shale): Black shale, Lower Alum Shale Event Interval, middle Tournaisian.

Hangenberg Limestone: Ca. 1.5 m alternation of 11 grey to light-grey, partly argillaceous, nodular limestone beds and layers of limestone nodules with grey to dark-grey silty shales, poor in macrofauna.

Beds 12–14 with *S. (S.) obsoleta*, *S. (S.) lobata*, *S. (S.) quadruplicata*, and *S. (S.) cooperi* (probably *S. (S.) lobata* M1 Subzone).

Beds 10–11 with *S. (S.) mehli*, *S. (S.) carinithiaca*, *Ps. triangulus inaequalis*, and other conodonts (main *S. (S.) mehli* Zone).

Beds 8–9 with “*S. duplicata* sensu Hass” (= *S. (S.) cf. wilberti*) (lower *S. (S.) mehli* Zone).

Bed 7 with *S. (S.) duplicata*, *S. (S.) bransoni*, and other conodonts (*S. (S.) duplicata* Zone).

Bed 6 with *S. (S.) bransoni* and *S. (Eo.) sulcata* s.l. (*S. (S.) bransoni* Zone).

Beds 4–5 with *Pr. kuehni*, *Pr. kockeli*, abundant *Ps. dentilineatus* (= *Ps. primus primus*), and *S. (Eo.) sulcata* s.l. (*S. (Eo.) sulcata* s.l./*Pr. kuehni* Zone), post-Crisis Interval.

Stockum Limestone:

Beds 1–3, ca. 50 cm alternation of four grey to dark-grey limestone beds and grey or greenish-grey silty shales, with *Pr. kockeli*, *Pr. collinsoni*, *Pr. meischneri*, *Po. inornatus*, and *Po. purus subplanus* (in Bed 3), *Pr. kockeli* Zone with high *Protognathodus* frequency, Upper Crisis Interval II.

Hangenberg Shale: Ca. 150 cm olive-grey to greenish-grey, silty shales, Middle Crisis Interval.

Hangenberg Black Shale: Ca. 10 cm black shale, Lower Crisis Interval.

Wocklum Limestone equivalents (no modern formation name): Olive to greenish-grey shales without macrofauna, pre-Crisis Interval to Crisis Prelude.

Eastern Münsterland subsurface

Vingerhoets 93 Well near Oelde (Fig. 7)

Location: Topographic sheet 4115 Rheda-Wiedenbrück, r 3 442 850, h 5 644 880, 40 km NNW of Dreher, ca. 1 km NNE

of Oelde. The location has been assigned to the surfacing NE end of the Bochum Syncline.

Literature: Bless et al. (1976), Clausen (2008: map with precise position).

Succession: The DCB succession drilled in the Vingerhoets 93 Well has only very briefly been published but it is remarkable because the Hangenberg Black Shale with *Post. evoluta* has been penetrated:

“Upper Hangenberg Formation s.l.” (Stockum to Hangenberg limestone equivalents):

Above 1680.6 m, dark-grey shales with a few beds of silty limestone.

1680.6–1691 m, dark shales with thin beds of silty limestone with *Ac. (St.) intermedium* (auct.), Upper to post-Crisis Interval.

Hangenberg Shale/Sandstone:

1691–1700 m, dark shale, cherts, and siltstones; upper part of Middle to Upper Crisis Interval.

1700–1716 m, dark shales, siltstones, and partly calcareous sandstones with chonetids and tabulate corals, neritic Middle Crisis Interval.

Hangenberg Black Shale:

1716–1720 m, black, cherty shale with *Post cf. evoluta* (reported as *C. euryomphala*), UD VI-E, transgressive Lower Crisis Interval.

Un-named Formation (proposed name: Vingerhoets Formation):

1720–1734.6 m, quartzitic, partly calcareous sandstone, pre-Crisis interval to Crisis Prelude.

Discussion: Further to the S, DCB beds were also reached by the Anröchte Well (4415/1001, Dölling and Piecha 2010, sheet 4415 Anröchte, r 3 449 455, h 5 712 859). Equivalents of the Wocklum Limestone could be proven by a conodont sample with *Pa. gracilis gonioclymeniae*. However, there was no evidence for the Hangenberg Black Shale above, and all of the Crisis Interval and lower Tournaisian (Hangenberg Formation) are represented by unfossiliferous grey shale and siltstone. The Lower Alum Shale Event could be recognised by a change to dark-grey to black shales.

Attendorn-Elspe Syncline (central Sauerland)

The section at Trockenbrück described by Kronberg et al. (1960) is tectonically too complex and too incomplete to be re-considered here.

Grimminghausen

Location: Track slopes N of the village zur Sange, Grimminghausen region, Elspe Syncline, central Sauerland (Fig. 9), sheet 4713 Eslohe, r 3,444 920, h 5 676 520. Luppold et al. (1994) mentioned a new adjacent outcrop

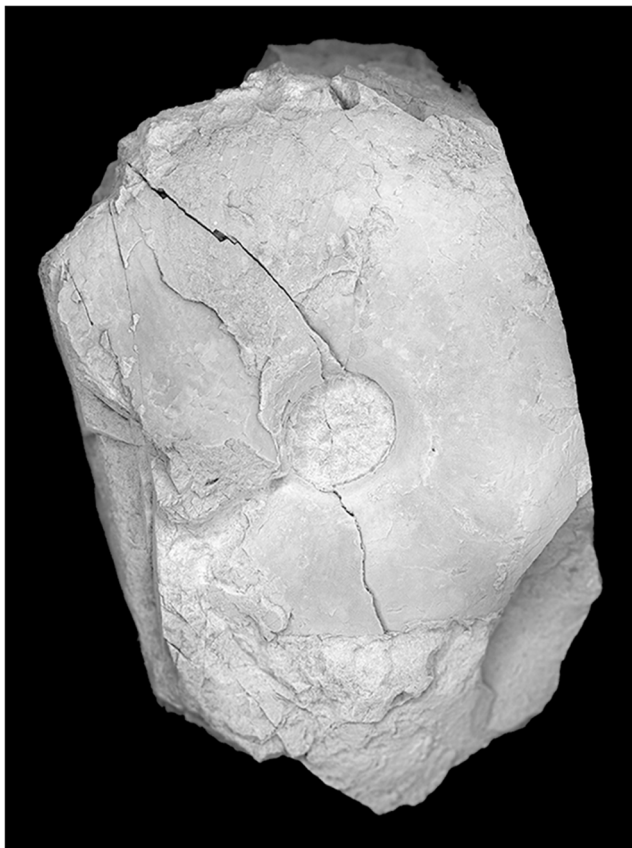


Fig. 15 *Gattendorfia involuta*, new typical, convolute specimen from the base of Bed 6a (*G. subinvoluta* Subzone, LC I-A₂, base of true Hangenberg Limestone) of the Oberrödinghausen Railway Cut, lateral view (incomplete preservation prevents a meaningful ventral view), B6C.54.11, × 1

created during excavations for a garage but details of their complete logging of the Hangenberg Limestone were not published subsequently.

Literature: Weber (1934), Rabien (1954, 1960: type locality of *Richterina (Richt.) robusta*), Streel (1969: failed attempt to retrieve useful miospore assemblages), Ebert and Müller (1973), Clausen et al. (1994).

Succession: The combined evidence from the literature is as follows:

Kahlenberg Formation (Lower Alum Shale): 25–30 m dark-grey to black, thin-bedded shale/alum shale, in the upper part cherty, Lower Alum Shale Event Interval, middle Tournaisian.

Hangenberg Limestone: 4.8 m, 30 individual beds of hard, grey, poorly fossiliferous, often lenticular/nodular limestone, at the top with *G. crassa*, *Ac. (St.) cf. intermedium* (auct.) (“*G. crassa* Zone”, LC I-C/D), and *Richterina (R.) robusta* (type level), post-Crisis interval.

Hangenberg Shale s.l.: Grey shales with abundant ostracods (*Richt. (Richt.) striatula*) and guerichiids, allegedly also with a last phacopid; undifferentiated Crisis Interval.

Wocklum Limestone equivalents:

15 m grey shale and few, thin limestone beds with abundant ostracods (*Richt. (Richt.) striatula*, *Maternella (Mat.) hemisphaerica*, and others, *M. (Mat.) hemisphaerica-M. (Mat.) dichotoma* Zone) and trilobites (*Silesiops schindewolfi*, *Weyrites wocklumeriae*, *Dianops*, *Chaunoproetus palensis*), upper pre-Crisis Interval to Crisis Prelude.

15 m grey shales and nodular limestone with *Wocklumeria* sp., *May. nucleus*, prionoceratids (*W. denckmanni* Zone, UD VI-D), *Drevermannia schmidti*, *Maternella (Mat.) hemisphaerica*, and other ostracods, pre-Crisis Interval.

Taxonomic notes (RTB)

Siphonodella (Siphonodella) lobata (Branson and Mehl, 1934) Morph 2

1959 *Siphonodella lobata*—Voges: pl. 35, fig. 39 (only).

1966 *Siphonodella lobata*—Klapper: pl. 2, figs. 2–3 (only).

1985 *Siphonodella (Siphonodella) lobata*—Ji: pl. 3, figs. 11–12 (only).

1985 *Siphonodella lobata*—Ji et al.: pl. 20, figs. 9, 10–11, 14, pl. 21, figs. 13–20 (only).

1989 *Siphonodella (Siphonodella) lobata*—Ji: pl. 14, figs. 3a–b, 4a–b.

2017 *Siphonodella lobata*—Kaiser et al.: figs. 10.6 and 10.13 (only).

Definition: Morphotype of *S. (S.) lobata* with an only incipient side lobe of the platform, which lacks a secondary carina at maturity on the oral surface.

Stratigraphic range: Lower Tournaisian, *S. (S.) mehli* to *S. (S.) sandbergi* Zones.

Gattendorfia involuta Schindewolf, 1924 (emend.)

*1924 *Gattendorfia involuta* nov. sp.—Schindewolf, p. 105

1924 *Gattendorfia* n. sp.—Schmidt, p. 151

1926 *Gattendorfia involuta*—Schindewolf, p. 94

*cf. 1952 *Gattendorfia tenuis* n. sp.—Schindewolf, pp. 297–298, text-fig. 18, pl. 3, figs 1a–1b (holotype)

1960 *Gattendorfia tenuis*—Vöhringer, p. 153, text-figs 28–29, pl. 5, figs 6a–6b (neotype of *G. involuta*)

cf. 1965a *Gattendorfia tenuis*—Weyer, pp. 447–448, pl. 6, figs 1a–1b (further synonymy)

1972 *Gattendorfia tenuis*—Weyer, p. 342

cf.1977 *Gattendorfia tenuis*—Weyer, p. 173, pl. 1 figs 2–3
 cf.1986 *Gattendorfia tenuis*—Bartzsch and Weyer, pl. 2, fig.2
 1994 *Gattendorfia involuta*—Korn, p. 71
 1994 *Gattendorfia tenuis*—Korn, p. 75, figs 65B, 66E–H,
 67D, 68B

Type: The original of *G. tenuis* in Vöhringer (1960: pl. 5, figs 6a–6b), Tübingen Collection, no. 1130/91, is here selected as the neotype. Its suture has been illustrated by Vöhringer (1960: fig. 38) and Korn (1994: fig. 67D).

Discussion: Attached to a discussion of his new genus *Paragattendorfia*, Schindewolf (1924) briefly introduced two new species of *Gattendorfia*. His *Gattendorfia involuta* was explained to differ from the type species of the genus (*G. subinvoluta*) by its more compressed and more narrowly umbilicated conch shape with higher whorls. This brief characterisation was sufficient at the time (before 1931) for a valid species definition (see Article 12 of the Code for Zoological Nomenclature). Statements in Weyer (1965a, 1972) and Korn (1994) that *G. involuta* is a nomen nudum are unjustified. Possibly influenced by Richter (1948; see discussion in Weyer 1972, p. 340), who wrongly advocated that an illustration was mandatory for a valid species definition, Schindewolf (1952, p. 298) assumed himself that his “third *Gattendorfia* species” from 1924 did not yet have a valid name. Therefore, he re-described it as *G. tenuis*, not mentioning at all his given name from 1924. He further stated that his previously available well-preserved specimens from Oberrödinghausen and Silesia, the *involuta* syntypes, had been lost. Therefore, he selected a specimen collected by Schwan from Gleitsch, Thuringia, as the holotype of *G. tenuis* (Tübingen collection Ce 1012/37). The neotype of *G. involuta* selected here is a well-preserved specimen from one of the two type localities (Oberrödinghausen). Vöhringer (1960) and Korn (1994) illustrated several cross-sections of *G. involuta* topotypes (as *G. tenuis*), which enable a morphometric characterisation. *Gattendorfia tenuis* is a subjective junior synonym since it is based on a form from Thuringia, not from the Rhenish Massif. Its previously assumed identity with *G. involuta* has to be tested by investigations of ontogenetic morphometry. Two early whorl cross-sections of *G. tenuis*, illustrated by Weyer (1977) from the Schleiz region of Thuringia, suggest a gradual change from broadly depressed to higher whorls during the fifth whorl, possibly earlier than in typical *G. involuta* (during the 7th whorl in the *involuta* topotype Ce 1130/176, illustrated by Vöhringer 1960 and Korn 1994). This may reflect intraspecific variability but more morphometric data are required to solve the question.

The new specimen illustrated in Fig. 15 is the so far oldest representative of the species from the basal *G. subinvoluta* Subzone (base of Bed 6a at Oberrödinghausen, *G. subinvoluta* Subzone, LC I-A₂). It suggests that *G. involuta* belonged to the root stock of the Gattendorfiinae.

A currently incomplete knowledge of morphology and distribution patterns is not only true for the pair *G. involuta*–*G. tenuis*. It also applies to *G. subinvoluta*, which holotype and a topotype from Gattendorf, Franconia (see Frech 1902; Schindewolf 1923a; Korn 1994), lack the constrictions that are well developed in Rhenish representatives figured by Vöhringer (1960), Korn (1994, 2006), Korn and Weyer (2003), and here (Fig. 31, m). However, Vöhringer (1960, p. 151) noted that constrictions are absent in some specimens from Oberrödinghausen and R. Richter collected in 1925 an adult from there (housed in the Senckenberg collection, Frankfurt a.M.) that has no constriction in the last ca. 250° of the last whorl at 72 mm diameter. This suggests ontogenetic changes, with increasing spacing of constrictions towards maturity. Thuringian *G. subinvoluta* illustrated by Bartzsch and Weyer (1982) also lack prominent constrictions, which supports a possible difference between Rhenohercynian and Saxothuringian populations. These were biogeographically separated in the basal Carboniferous by a narrow oceanic system.

Conclusions

1. The Rhenish Massif is one of the most important classical regions for DCB research, which successions set the standards for conodont, ammonoid, and event stratigraphy. A large part of the data was published only in regional journals or in German. Therefore, the initiative of this special issue to summarise internationally the DCB knowledge is a good opportunity to make this information better available.
2. The uppermost Famennian to basal middle Tournaisian interval can be subdivided into ten conodont zones, which are mostly defined by the FADs of species. As an exception, one zone, the *costatus-kockeli* Interregnum, is defined by the global extinction (LADs) of important taxa, such as *Bi. costatus* and *Bi. ultimus* (all subspecies), *Ps. marburgensis trigonicus*, and the last palmatolepids (all subspecies of *Pa. gracilis*, assuming a reworked nature of rare post-Hangenberg Extinction records).
3. The poor definition and ongoing revision of the oldest siphonodellids require to add currently the phrase s.l. (sensu lato) to identifications as *S. (Eo.) praesulcata* and *S. (Eo.) sulcata*. The type of *S. (Eo.) praesulcata* originated from a level above the main Hangenberg Extinction. It is likely that the most common and stratigraphically most useful pre-extinction siphonodellid will receive in future a different species name, with implications for zonal nomenclature. It is also possible that the use of the name *S. (Eo.) sulcata* eventually will be restricted to forms close to its lost holotype.

4. Due to large taxonomic uncertainties concerning *S. (S.) jii*, it is better to return to the original definition of the Upper *duplicata* Zone in the lower Tournaisian, resulting in a re-naming as *S. (S.) mehli* Zone. It replaces the *S. (S.) jii* Zone of Becker et al. (2016). *Siphonodella (S.) carinthiaca* and *S. (S.) cooperi* (M2 or s. str.) are important additional marker taxa entering in the same zone. Lower Tournaisian forms from the Rhenish Massif that were previously identified as *S. duplicata* sensu Hass are preliminarily assigned to *S. (S.) cf. wilberti*, until the variability of the middle Tournaisian species *S. (S.) wilberti* is fully established.
5. The *S. (S.) sandbergi* Zone is subdivided into successive *S. (S.) sandbergi* and *S. (S.) lobata* M1 subzones. The new, morphologically less advanced *S. (S.) lobata* M2 enters significantly earlier. The Rhenish siphonodellid record questions a subdivision of the *S. (S.) sandbergi* Zone based on the FAD of *S. (S.) quadruplicata*, at least unless ranges of early (M2) and typical forms (M1) of the latter are fully established.
6. More data are required to correlate the FADs of *Ps. triangulus inaequalis* and *Ps. triangulus triangulus* precisely with the siphonodellid succession.
7. The uppermost Famennian to top lower Tournaisian of the Rhenish Massif can be subdivided into a dozen ammonoid zones, with four additional subzones. New are the *May. nucleus* Subzone (UD VI-C₃), an upper subdivision of the former *P. paradoxa* Subzone/Zone, the “*Eoc.*” *nodosus* Subzone (LC I-A₃), an upper subdivision of the *G. subinvoluta* Zone, and the *Parag. sphaeroides* Subzone (LC I-B₂), an upper subdivision of the *Pap. dorsoplanus* Zone.
8. Based on litho- and conodont stratigraphy, a succession of *Ac. (Stockumites)* faunas can be recognised within the *Ac. (St.) prorsum* Zone, which straddles the DCB. However, the evidence, often from different outcrops, is still insufficient to enable a subzone subdivision.
9. The extended Hangenberg Crisis is formally subdivided into a regressive Crisis Prelude (top *S. (Eo.) praesulcata* s.l. Zone, UD VI-D₂, “Drewer Sandstone” and top Wocklum Limestone, HST), transgressive Lower Crisis Interval (lower *costatus-kockeli* Interregnum, UD VI-E, HBS, TST, with the main pelagic extinction at the base, regressive Middle Crisis Interval (upper *costatus-kockeli* Interregnum, main UD VI-F, with a sequence boundary between the HS, a FSST, and the HSS, a LST), transgressive Upper Crisis Interval (*Pr. kockeli* Zone to lower part of *S. (Eo.) sulcata* s.l./*Pr. kuehni* Zone, top UD V-F/ LC I-A₁, Stockum Limestone and lateral black shales/ marls, TST with parasequences), and subsequent basal Carboniferous post-Crisis Interval (Hangenberg Limestone, HST). Terrestrial extinctions (top of LN Zone) and obviously also the extinction of various neric fossil groups occurred high within the Upper Crisis Interval. The bases of the Pont d’Arcole Formation (in neritic western settings) and Lower Alum Shale (in the deeper, eastern Kulm facies) mark a sudden flooding (TST base) that defined the classical middle Tournaisian (Tn 2).
10. The west-east transition from neritic to pelagic facies and faunas enables the correlation of shallow and deep shelf environments. The selection of the best/most significant sections led to a review of 30 successions, from the Aachen region in the west, through sections along the Velbert and Remscheid-Altena Anticline (Bergisches Land to northern Sauerland), to the eastern Sauerland (Warstein region), the subsurface to the north, and the Attendorn-Elspe Syncline in the central Sauerland. Unfortunately, more than half of the sections were temporary (bore holes, roadwork exposures, trenches) or have been destroyed subsequently and are not available any more for research. Further ten sections include outcrops gaps or unconformities near the DCB, which excludes them for the current search for a new DCB GSSP.
11. The Apricke section has only insufficiently been studied so far and requires moderate excavations for further investigations. The important Oese and Drewer sections are poor in conodonts in the Upper Crisis Interval but represent important auxiliary sections, wherever the future GSSP will be placed. The currently best Rhenish section at the Borkewehr or Burgberg near Wocklum is regarded as a GSSP candidate. Many new data will be presented in a forthcoming separate manuscript that will be submitted soon to this journal.
12. The complete set of reviewed sections and different facies developments recommends the Rhenish Massif as a package of auxiliary sections, in which a future GSSP would be embedded.

Acknowledgements Traudel Fährenkemper (WWU Münster) produced the majority of the illustrations. Lukas Afhüppé and Davina Mathijssen (both WWU) processed and picked conodont samples from various sections. We dedicate this review to the enormous research investigations of previous “Rhenish” DCB workers, especially to (in alphabetical order) M.R.W. Amher, G. Bischoff, C.-D. Clausen, D. Stoppel, H.-G. Herbig, D. Korn, K. Leuteritz, F.-W. Luppold, E. Paproth, M. Streel, A. Voges, and W. Ziegler. We like to thank B. Mottequin (Brussels) and C. Spalletta (Bologna) for their helpful reviews.

Funding Open Access funding enabled and organized by Projekt DEAL.

Compliance with ethical standards

Conflict of interest The authors declare that they have no conflict of interest.

Open Access This article is licensed under a Creative Commons Attribution 4.0 International License, which permits use, sharing, adaptation, distribution and reproduction in any medium or format, as long as you give appropriate credit to the original author(s) and the source,

provide a link to the Creative Commons licence, and indicate if changes were made. The images or other third party material in this article are included in the article's Creative Commons licence, unless indicated otherwise in a credit line to the material. If material is not included in the article's Creative Commons licence and your intended use is not permitted by statutory regulation or exceeds the permitted use, you will need to obtain permission directly from the copyright holder. To view a copy of this licence, visit <http://creativecommons.org/licenses/by/4.0/>.

References

- Alberti, H., Groos-Uffenorde, H., Strel, M., Uffenorde, H., & Walliser, O. H. (1974). The stratigraphical significance of the *Protognathodus* fauna from Stockum (Devonian/Carboniferous Boundary, Rheinisches Schiefergebirge). *Newsletters on Stratigraphy*, 3(4), 263–276.
- Amler, M. R. W. (1993). Shallow marine bivalves at the Devonian/Carboniferous Boundary from the Velbert Anticline (Rheinisches Schiefergebirge). *Annales de la Société géologique de Belgique*, 115(2), 405–423.
- Amler, M. R. W., & Herbig, H.-G. (2006). Ostrand der Kohlenkalk-Plattform und Übergang in das Kulm-Becken im westlichen Deutschland zwischen Aachen und Wuppertal. *Schriftenreihe der Deutschen Gesellschaft für Geowissenschaften*, 41, 441–477.
- Amler, M. R. W., Thomas, E., Weber, K. M., & Wehking, S. (1990). Bivalven des höchsten Oberdevons im Bergischen Land (Strunium; nördliches Rhein. Schiefergebirge). *Geologica et Palaeontologica*, 24, 41–63.
- Amler, M. R. W., Rathmann, S., & Richter, E. (1994). Henry Paul's "Etroeungt-Schichten" des Bergischen Landes – Biostratigraphie und Biofazies am Nordrand des Velberter Sattels. *Archäologie im Ruhrgebiet*, 1994, 73–98.
- Aretz, M., Poty, E., Herbig, H.-G., Delculée, S., & Hecker, P. (2006). *From Palaeocarst to Calciturbidites – a carbonate platform-slope-transect from the Mississippian limestone in eastern Belgium to the Kulm Basin in western Germany*. Unpublished Field Guide, Carboniferous Conference Cologne, "From Platform to Basin", September 4–10, 2006. *Kölner Forum für Geologie und Paläontologie*, 16, 1–41.
- Bardashev, N. P., Bardashev, I., Weddige, K., & Ziegler, W. (2004). Stratigraphy and conodonts of the Lower Carboniferous of the Shishkat section (southern Tien-Shan, Tajikistan). *Senckenbergiana lethaea*, 84(1/2), 225–301.
- Bärtling, R., & Paeckelmann, W. (1928). *Blatt Velbert, Nr. 2650. Erläuterungen zur Geologischen Karte von Preußen*, Lieferung 274, 109 pp. Berlin: Preußische Geologische Landesanstalt.
- Bartsch, K., & Weyer, D. (1982). Zur Stratigraphie des Untertournai (*Gattendorfia*-Stufe) von Saalfeld im Thüringischen Schiefergebirge. *Berichte und Abhandlungen des Museums für Naturkunde und Vorgeschichte*, 12(4), 3–53 [imprint 1981].
- Bartsch, K., & Weyer, D. (1986). Biostratigraphie der Devon/Karbon-Grenze im Bohlen-Profil bei Saalfeld (Thüringen, DDR). *Zeitschrift für Geologische Wissenschaften*, 14(2), 147–152.
- Basse, M., & Lemke, U. (2011). *Cyrtosymbolina niensis* n. gen. et n. sp., *Tireisiasibole* n. gen. and *Platybole* n. gen. (Trilobita: Cyrtosymbolinae) aus dem deutschen Famennium (Ober-Devon). *Dortmunder Beiträge zur Landeskunde, naturwissenschaftliche Mitteilungen*, 43, 51–93.
- Becker, G. (1993). Verkieselte Ostracoden vom Thüringer Ökotyp aus dem Grenzbereich Devon/Karbon des Steinbruchs Dreher (Rheinisches Schiefergebirge). *Courier Forschungsinstitut Senckenberg*, 160, 1–131.
- Becker, G. (1999). Verkieselte Ostracoden vom Thüringer Ökotyp aus den Devon/Karbon-Grenzschichten (Top Wocklumer Kalk und Basis Hangenberg-Kalk) im Steinbruch Dreher (Rheinisches Schiefergebirge). Die natürliche D/C-Grenze. *Courier Forschungsinstitut Senckenberg*, 218, 1–159.
- Becker, R. T. (1985). Devonische Ammonoideen aus dem Raum Hohenlimburg-Letmathe (Geologisches Blatt 4611 Hohenlimburg). *Dortmunder Beiträge zur Landeskunde, naturwissenschaftliche Mitteilungen*, 19, 19–34.
- Becker, R. T. (1988). Ammonoids from the Devonian-Carboniferous Boundary in the Hasselbach Valley (northern Rhenish Slate Mountains). *Courier Forschungsinstitut Senckenberg*, 100, 193–213.
- Becker, R. T. (1996). New faunal records and chronostratigraphical correlation of the Hasselbachtal D/C Boundary Auxiliary Stratotype (Germany). *Annales de la Société Géologique de Belgique*, 117(1), 19–45.
- Becker, R. T. (1997). Eine neue und älteste *Glatziella* (Clymeniida) aus dem höheren Oberdevon des Nordsauerlandes (Rheinisches Schiefergebirge). *Berliner geowissenschaftliche Abhandlungen*, E25, 31–41.
- Becker, R. T. (2000). Taxonomy, evolutionary history, and distribution of the middle to late Famennian Wocklumeriina (Ammonoidea, Clymeniida). *Mitteilungen aus dem Museum für Naturkunde in Berlin, Geowissenschaftliche Reihe*, 3, 27–75.
- Becker, R. T. (2002). *Alpinites* and other Posttornoceratidae (Goniatitida, Famennian). *Mitteilungen aus dem Museum für Naturkunde Berlin, Geowissenschaftliche Reihe*, 5, 51–73.
- Becker, R. T., & Hartenfels, S. (2017). In pursuit for a revised Devonian-Carboniferous boundary – new data from the Rhenish Massif, Ardennes, southern Morocco, and South China. *Münstersche Forschungen zur Geologie und Paläontologie*, 109, 29.
- Becker, R. T., & Paproth, E. (1993). Auxiliary stratotype sections for the Global Stratotype Section and Point (GSSP) for the Devonian-Carboniferous Boundary: Hasselbachtal. *Annales de la Société Géologique de Belgique*, 115(2), 703–706.
- Becker, R. T., & Weber, H. M. (2016). Review of the Devonian-Carboniferous transition in the Aachen region (western Rhenish Massif). *Münstersche Forschungen zur Geologie und Paläontologie*, 108, 29–35.
- Becker, R. T., & Weyer, D. (2004). *Bartzschiceras* n. gen. (Ammonoidea) from the Lower Tournaisian of Southern France. *Mitteilungen aus dem Geologisch-Paläontologischen Institut der Universität Hamburg*, 88, 11–36.
- Becker, R. T., Bless, M. J. M., Brauckmann, C., Friman, L., Higgs, K., Keupp, H., Korn, D., Langer, W., Paproth, E., Rachebeuf, P., Stoppel, D., Strel, M., & Zakowa, H. (1984). Hasselbachtal, the section best displaying the Devonian-Carboniferous Boundary beds in the Rhenish Massif (Rheinisches Schiefergebirge). *Courier Forschungsinstitut Senckenberg*, 67, 181–191.
- Becker, R. T., Korn, D., Paproth, E., & Strel, M. (1993). Beds near the Devonian-Carboniferous Boundary in the Rhenish Massif, Germany. In *Guidebook, IUGS Subcommission on Carboniferous Stratigraphy (SCCS)* 86 pp. Liège: Services associés de paléontologie de l'ULg.
- Becker, R. T., House, M. R., Bockwinkel, J., Ebbighausen, V., & Aboussalam, Z. S. (2002). Famennian ammonoid zones of the eastern Anti-Atlas (southern Morocco). *Münstersche Forschungen zur Geologie und Paläontologie*, 93, 159–2005.
- Becker, R. T., Hartenfels, S., Aboussalam, Z. S., Tragelehn, H., Brice, D., & El Hassani, A. (2013). The Devonian – Carboniferous boundary at Lalla Mimouna (northern Maider) – a progress report. In R. T. Becker, A. El Hassani, & A. Tahiri (Eds.) *International Field Symposium "The Devonian and Lower Carboniferous of northern Gondwana"*, 22nd to 29th March 2013, Field Guidebook (pp. 109–120). Documents de l'Institut Scientifique, Rabat, 27.

- Becker, R. T., Kaiser, S. I., & Aretz, M. (2016a). Review of chrono-, litho- and biostratigraphy across the global Hangenberg Crisis and Devonian-Carboniferous Boundary. In R. T. Becker, P. Königshof, & C. E. Brett (Eds.) *Devonian Climate, Sea Level and Evolutionary Events* (pp. 355–386). London: Geological Society Special Publications, 423.
- Becker, R. T., Hartenfels, S., Weyer, D., & Kumpan, T. (2016b). The Famennian to lower Viséan at Dreher (northern Rhenish Massif). *Münstersche Forschungen zur Geologie und Paläontologie*, 108, 158–178.
- Bischoff, G. (1957). Die Conodonten-Stratigraphie des rheno-herznischen Unterkarbons mit Berücksichtigung der *Wocklumeria*-Stufe und der Devon/Karbon-Grenze. *Abhandlungen des Hessischen Landesamtes für Bodenforschung*, 19, 1–64 + 6 pls.
- Bless, M. J. M., & Groos-Uffenorde, H. (1984). Ostracodes at the Devonian-Carboniferous Boundary. *Courier Forschungsinstitut Senckenberg*, 67, 23–28.
- Bless, M. J. M., Bouckaert, J., Bouzet, P., Conil, R., Cornet, P., Fairon-Demaret, M., Groessens, E., Longerstaey, P. J., Meessen, J. P. M. T., Paproth, E., Pirlet, H., Strel, M., van Amerom, H. W. J., & Wolf, M. (1976). Dinantian rocks in the subsurface North of the Brabant and Ardenno-Rhenish massifs in Belgium, the Netherlands and the Federal Republic of Germany. *Mededelingen Rijks Geologische Dienst, Nieuwe Serie*, 27(3), 81–195.
- Bless, M. J. M., Becker, R. T., Higgs, K., Paproth, E., & Strel, M. (1993). Eustatic cycles around the Devonian-Carboniferous boundary and the sedimentary and fossil record in Sauerland (Federal Republic of Germany). *Annales de la Société Géologique de Belgique*, 115(2), 689–702.
- Bless, M. J. M., Brauckmann, C., Conil, R., Herbig, H.-G., Poty, E., Ribbert, K.-H., Strel, M., & Weber, H. (1998). Ein Devon/Karbon-Grenzprofil im Untergrund der Niederrheinischen Bucht bei Krefeld. *Fortschritte in der Geologie von Rheinland und Westfalen*, 37, 55–79.
- Böger, H. (1962). Zur Stratigraphie des Unterkarbons im Velberter Sattel. *Decheniana*, 114(2), 133–170.
- Bomfleur, B. (2005). *Geologische Neukartierung des Raumes Hemer im Bereich der Deutschen Grundkarten 4228–4230 (Landhausen, Urbecke, Hüingsen-West), Märkischer Kreis*. – Unpublished Diplom Thesis, WWU Münster, 63 pp. + 1 map.
- Bouckaert, J., & Groessens, E. (1976). *Polygnathus paprothae, Pseudopolygnathus conili, Pseudopolygnathus graulichi*: espèces nouvelles à la limite Dévonien-Carbonifère. *Annales de la Société Géologique de Belgique*, 99, 587–599.
- Branson, E. B., & Mehl, M. G. (1934). Conodonts from the Bushberg sandstone and equivalent formations of Missouri. *University of Missouri Studies*, 8(4), 265–299 + pls. 22–24.
- Brauckmann, C. (1990). Oberdevon und Unterkarbon von Ratingen. In K. Weidert (Ed.) *Klassische Fundstellen der Paläontologie, II*, 49–58. Korb: Goldschnecke.
- Brauckmann, C., & Hahn, G. (1984). Trilobites as index fossils at the Devonian-Carboniferous Boundary. *Courier Forschungsinstitut Senckenberg*, 67, 11–14.
- Brauckmann, C., Chluápc, I., & Feist, R. (1993). Trilobites at the Devonian-Carboniferous Boundary. *Annales de la Société géologique du Belgique*, 115(2), 507–518.
- Bultynck, P., & Dejonghe, L. (2002). Devonian lithostratigraphic units (Belgium). *Geologica Belgica*, 4(1/2), 39–69 (imprint 2001).
- Byvsheva, T. V., Higgs, K., & Strel, M. (1984). Spore correlation between the Rhenish Slate Mountains and the Russian platform near the Devonian-Carboniferous Boundary. *Courier Forschungsinstitut Senckenberg*, 67, 37–45.
- Claoué-Long, J., Jones, P. J., & Roberts, J. (1993). The age of the Devonian-Carboniferous boundary. *Annales de la Société Géologique de Belgique*, 115(2), 531–549.
- Clausen, C.-D. (2008). Bohrungen im Lippstädter Gewölbe. *Schriftenreihe der Deutschen Gesellschaft für Geowissenschaften*, 52, 564–568.
- Clausen, C.-D., & Korn, D. (2008). Höheres Mitteldevon und Oberdevon des nördlichen Rheinischen Schiefergebirges (mit Velberter Sattel und Kellerwald). *Schriftenreihe der Deutschen Gesellschaft für Geowissenschaften*, 52, 439–481.
- Clausen, C.-D., & Leuteritz, K. (1979a). Übersicht über die Geologie des Warsteiner Sattels und seiner näheren Umgebung. *Aufschluss, Sonderband*, 29, 1–32.
- Clausen, C.-D., & Leuteritz, K. (1979b). Lohnende Exkursionsziele im Warsteiner Raum. *Aufschluss, Sonderband*, 29, 253–266.
- Clausen, C.-D., Korn, D., & Uffenorde, H. (1979). Das Devon/Karbon-Profil am alten Schießstand bei der Bilstein-Höhle (Blatt 4515 Hirschberg, Warsteiner Sattel, Rheinisches Schiefergebirge). *Aufschluss, Sonderband*, 29, 47–68.
- Clausen, C.-D., mit Beiträgen von Erkwoh, F. D., Grünhage, H., Kamp, V., Rehagen, H.-W., & Wolf, M. (1984a). Erläuterungen zu Blatt 4515 Hirschberg. In *Geologische Karte von Nordrhein-Westfalen 1 : 25 000, 115 pp., 1 map*. Krefeld: Geologisches Landesamt NRW.
- Clausen, C.-D., Leuteritz, K., mit Beiträgen von Erkwo, F. D., Kamp, H. V., Rehagen, H.-W., Weber, P., & Wolf, M. (1984b). Erläuterungen zu Blatt 4516 Warstein. In *Geologische Karte von Nordrhein-Westfalen 1 : 25 000, 155 pp., 3 pls*. Krefeld: Geologisches Landesamt NRW.
- Clausen, C.-D., Korn, D., Leuteritz, K., Paproth, E., & Stoppel, D. (1987). *Die Devon-Karbon-Grenze im nördlichen Sauerland*. Unpublished field guide “Bestwig 1987”, Subkommission für Karbonstratigraphie in der DUGW, 35 pp.; Olsberg.
- Clausen, C.-D., Leuteritz, L., Ziegler, W., & Korn, D. (1989a). Ausgewählte Profile an der Devon/Karbon-Grenze im Sauerland (Rheinisches Schiefergebirge). *Fortschritte in der Geologie von Rheinland und Westfalen*, 35, 161–226.
- Clausen, C.-D., Korn, D., Luppold, F. W., & Stoppel, D. (1989b). Untersuchungen zur Devon/Karbon-Grenze auf dem Müssemburg (nördliches Rheinisches Schiefergebirge). *Bulletin de la Société belge de Géologie*, 98(3/4), 353–369.
- Clausen, C.-D., Korn, D., Feist, R., Leuschner, K., Groos-Uffenorde, H., Luppold, F. W., Stoppel, D., Higgs, K., & Strel, M. (1994). Die Devon/Karbon-Grenze bei Stockum (Rheinisches Schiefergebirge). *Geologie und Paläontologie in Westfalen*, 29, 71–95.
- Conil, R., & Paproth, E. (1968). Mit Foraminiferen gegliederte Profile aus dem nordwest-deutschen Kohlenkalk und Kulm. *Decheniana*, 119(1/2), 51–94.
- Conil, R., Lys, M., & Paproth, E. (1964). Localités et coupes types pour l'étude du Tournaisien inférieur (Révision des limites sous l'aspect micropaléontologique). *Mémoirs de l'Academie Royal de Belgique, CI, Sciences*, 15(4), 1–87.
- Corradini, C., & Spalletta, C. (2018). Continuity of fossil record and biozonation schemes: an example across the Devonian/Carboniferous boundary. In *5th International Palaeontological Congress, “The Fossil Week”, July 9th to 13th 2018, France, Abstract Book*, 789; Paris.
- Corradini, C., Barca, S., & Spalletta, C. (2003). Late Devonian-Early Carboniferous conodonts from the “Clymeniae limestones” of SE Sardinia (Italy). *Courier Forschungsinstitut Senckenberg*, 245, 227–253.
- Corradini, C., Spalletta, C., Mossoni, A., Matyja, H., & Over, D. J. (2016). Conodonts across the Devonian/Carboniferous boundary: a review and implications for the redefinition of the boundary and a proposal for an updated conodont zonation. *Geological Magazine*, 154(4), 888–902.
- Corradini, C., Schönlau, H.-P., & Kaiser, S. I. (2017). The Devonian/Carboniferous boundary in the Grüne Schneid section. *Berichte des Institutes für Erdwissenschaften, Karl-Franzenz-Universität Graz*, 23, 271–275.

- Crônier, C., & Feist, R. (2000). Evolution et systématique du groupe *Cryphops* (Phacopinae, Trilobita) du Dévonien supérieur. *Senckenbergiana lethaea*, 79(2), 501–515.
- Denayer, J., Poty, E., & Aretz, M. (2011). Uppermost Devonian and Dinantian rugose corals from Southern Belgium and surrounding areas. *Kölner Forum für Geologie und Paläontologie*, 20, 151–201.
- Denayer, J., Prestianni, C., Mottequin, B., Hance, L., & Poty, E. (2019). Revision of the Devonian-Carboniferous Boundary in Belgium and surrounding areas: a scenario. In S. Hartenfels, H.-G. Herbig, M. R. W. Amler, & M. Aretz (Eds.) *19th International Congress on the Carboniferous and Permian, Cologne, July 29 – August 2, 2019, Abstracts* (pp. 75–76). Kölner Forum für Geologie und Paläontologie, 23.
- Denckmann, A. (1901). Ueber das Oberdevon auf Blatt Balve (Sauerland). *Jahrbuch der Preußischen Geologischen Landesanstalt*, 21(for 1900), 1–19.
- Denckmann, A. (1902). Einige weniger bekannte Clymenien aus dem Dasberger Kalke von Braunaub im Kellerwalde bezw. vom Dasberge im Sauerlande. *Zeitschrift der deutschen geologischen Gesellschaft, Verhandlungen*, 54, 53–54.
- Denckmann, A., & Lotz, H. (1900). Ueber einige Fortschritte in der Stratigraphie des Sauerlandes. *Zeitschrift der Deutschen Geologischen Gesellschaft*, 52, 564–567.
- Di Pasquo, M. M., Warren, A., Rice, B., Isaacs, P., & Grader, G. W. (2016). Palynological delineation of the Devonian-Carboniferous Boundary, west-central Montana. *GSA, 68th Annual Meeting, Moscow, 18–19 May 2016, Rocky Mountain Section, Abstract 275796*, 1 p.
- Dölling, B., & Piecha, M. (2010). Die Kernbohrung Anröchte 4415/1001 – neue Erkenntnisse über das Paläozoikum im Lippstädter Gewölbe. *Schriftenreihe der Deutschen Gesellschaft für Geowissenschaften*, 73(1/2), 45–52.
- Drevermann, F. (1902). Ueber eine Vertretung der Étroeungt-Stufe auf der rechten Rheinseite. *Zeitschrift der deutschen Geologischen Gesellschaft*, 54, 480–524 + pl. 14.
- Ebbighausen, V., & Bockwinkel, J. (2007). Tournaisian (Early Carboniferous/Mississippian) ammonoids from the Ma'der Basin (Anti-Atlas, Morocco). *Fossil Record*, 10(2), 125–163.
- Ebbighausen, V., & Korn, D. (2007). Conch geometry and ontogenetic trajectories in the triangularly coiled Late Devonian ammonoid *Wocklumeria* and related genera. *Neues Jahrbuch für Geologie und Paläontologie, Abhandlungen*, 244(1), 9–41.
- Ebbighausen, V., Bockwinkel, J., Korn, D., & Weyer, D. (2004). Early Tournaisian ammonoids from Timimimoun (Gourara, Algeria). *Mitteilungen aus dem Museum für Naturkunde Berlin, Geowissenschaftliche Reihe*, 7, 133–152.
- Ebert, A., & Müller, H., with contributions by v. Kamp, H., Wolf, M., Weber, P., & Wirth, W. (1973). *Erläuterungen zu Blatt 4715 Eslohe*. Geologische Karte von Nordrhein-Westfalen 1 : 25 000, 298 pp., 5 pls. Krefeld: Geologisches Landesamt NRW.
- Eickhoff, G. (1970). Foraminiferen aus dem Wocklumer Kalk am Borkewehr bei Balve (Oberdevon, Rheinisches Schiefergebirge). *Neues Jahrbuch für Geologie und Paläontologie, Abhandlungen*, 135, 227–267, pls. 30–32.
- Eickhoff, G. (1973). Das hohe Oberdevon und das tiefe Unterkarbon im Bahneinschnitt Oberrödinghausen bei Menden (Rheinisches Schiefergebirge). *Compte Rendu Septième Congrès International de Stratigraphie et de Géologie du Carbonifère, Krefeld, 23.–28. August 1971*, 2, 418–434.
- Ernst, A., Tolokonnikova, Z., & Herbig, H.-G. (2015). Uppermost Famennian bryozoans from Ratingen (Velbert Anticline, Rhenish Massif/Germany) – taxonomy, facies dependencies and palaeobiogeographic implications. *Geologica Belgica*, 18(1), 37–47.
- Evans, S. D., Over, F. J., Day, J. E., & Hasenmueller, N. R. (2013). The Devonian/Carboniferous boundary and the holotype of *Siphonodella sulcata* (Huddle, 1934) in the upper New Albany Shale, Illinois Basin, southern Indiana. In A. El Hassani, R. T. Becker, & A. Tahiri (Eds.) *International Field Symposium “The Devonian and Lower Carboniferous of northern Gondwana”, Abstract Book* (pp. 42–43). Rabat: Documents de l’Institut Scientifique 26.
- Feist, R., & Weyer, D. (2018). The proetid trilobite *Perliproetus*, a marker of the late Famennian in Central Europe and North Africa. *Neues Jahrbuch für Geologie und Paläontologie, Abhandlungen*, 287(2), 195–206.
- Feist, R., Lemke, U., & Korn, D. (2000). Trilobiten aus der Wocklumeria-Stufe des höchsten Oberdevon von Apricke, Sauerland. *Senckenbergiana lethaea*, 79(2), 517–539.
- Feist, R., Cornée, J.-J., Corradini, C., Hartenfels, S., Aretz, M., & Girard, C. (2020). The Devonian-Carboniferous boundary in the stratotype area (SE Montagne Noire, France). *Palaeodiversity and Palaeoenvironments*, 17. <https://doi.org/10.1007/s12549-019-00402-6>.
- Franke, W., Eder, W., & Engel, W. (1975). Sedimentology of a Lower Carboniferous shelf-margin (Velbert anticline, Rheinisches Schiefergebirge, W-Germany). *Neues Jahrbuch für Geologie und Paläontologie, Abhandlungen*, 150(3), 314–353.
- Frech, F. (1902). Über devonische Ammonien. *Beiträge zur Paläontologie und Geologie Österreich-Ungarns und des Orients*, 14(I-II), 27–111 + 4 pls.
- Fuchs, A., & Paekelmann, W. (1928). *Blatt Barmen, Nr. 2721. Erläuterungen zur Geologischen Karte von Preußen und benachbarten deutschen Ländern, Lieferung 263* (99 pp.), 1 pl.). Berlin: Preußische Geologische Landesanstalt.
- Gallwitz, H. (1928). Stratigraphische und tektonische Untersuchungen an der Devon-Karbongrenze des Sauerlandes. *Jahrbuch der Preußischen Geologischen Landesanstalt*, 48(for 1927), 487–527 + pl. 23.
- Gallwitz, H. (1932). Die Fauna des deutschen Unterkarbons. 3. Teil: Die Brachiopoden, 3. Teil: Die Orthiden, Strophomeniden und Choneten des Unteren Unterkarbons (Etroeungt). *Abhandlungen der Preußischen Geologischen Landesanstalt, Neue Folge*, 141, 75–131 + pls. 6–8.
- Greifelt, T. (2008). *Agglutinierende Foraminiferen aus dem Oberdevon des Nordsauerlandes*. Unpublished B.Sc. Thesis, WWU Münster, 39 pp.
- Groos-Uffenorde, H., & Uffenorde, H. (1974). Zur Mikrofauna im höchsten Oberdevon und tiefen Unterkarbon im nördlichen Sauerland. *Notizblätter des hessischen Landesamtes für Bodenforschung*, 102, 58–87 pls. 2–6.
- Hahn, G., Hahn, E., & Wolf, C. (1990). *Belgibole abruptirhachis*, Leit-Trilobit an der Devon/Karbon-Grenze. *Senckenbergiana Lethaea*, 70(1/3), 89–103.
- Hartenfels, S. (2011). Die globalen *Annulata*-Events und die Dasberg-Krise (Famennium, Oberdevon) in Europa und Nord-Afrika – hochauflösende Conodonten-Stratigraphie, Karbonat-Mikrofazies, Paläökologie und Paläodiversität. *Münstersche Forschungen zur Geologie und Paläontologie*, 105, 17–527.
- Hartenfels, S., & Becker, R. T. (2009). Timing of the global Dasberg Crisis – implications for Famennian eustasy and chronostratigraphy. *Palaeontographica Americana*, 63, 71–97.
- Hartenfels, S., & Becker, R. T. (2016). Age and correlation of the transgressive *Gonioclymenia* limestone (Famennian, Tafilalt, eastern Anti-Atlas, Morocco). *Geological Magazine*, 153(3), 566–629.
- Hartenfels, S., & Becker, R. T. (2018). Borkewehr near Wocklum (northern Rhenish Massif), a possible future Devonian/Carboniferous boundary GSSP section. In *GeoBonn 2018, 2–6 September 2018, Bonn, Germany, Abstracts*, 252; Bonn.
- Hartenfels, S., & Becker, R. T. (2019). The Devonian/Carboniferous transition in the Rhenish Massif – Borkewehr, a potential GSSP section. In S. Hartenfels, H.-G. Herbig, M. R. W. Amler, & M.

- Aretz (Eds.) 19th International Congress on the Carboniferous and Permian, Cologne, July 29–August 2, 2019, Abstracts (pp. 140–141). Kölner Forum für Geologie und Paläontologie 23.
- Hartenfels, S., Hartkopf-Fröder, C., Herbig, H.-G., Becker, R. T., & Esteban Lopez, S. (2016). Middle Famennian to Viséan stratigraphy at Riescheid (Herzkamp Syncline, Rhenish Massif). *Münstersche Forschungen zur Geologie und Paläontologie*, 108, 102–125.
- Hartenfels, S., Becker, R. T., & Kumpan, T. (2017a). Uppermost Famennian to Lower Tournaisian stratigraphy at Borkewehr near Wocklum (northern Rhenish Massif, Germany). In J.-C. Liao & J. I. Valenzuela-Ríos (Eds.) *Fourth International Conodont Symposium “Progress on Conodont Investigation”* (pp. 195–197). Cuadernos del Museo Geominero 22.
- Hartenfels, S., Becker, R. T., & Kumpan, T. (2017b). A possible new Devonian-Carboniferous Boundary stratotype section: Borkewehr near Wocklum (Northern Rhenish Massif, Germany). In G. Yang, J. Reitner, Y.-D. Wang, & M. Reich (Eds.) *2nd joint conference of the Palaeontological Society of China and the Paläontologische Gesellschaft, “critical intervals in earth history: Palaeobiological innovations”, abstract volume* (pp. 79–81). Beijing: University of Science and Technology of China Press.
- Hass, W. H. (1959). Conodonts from the Chappel limestone of Texas. *United States Geological Survey, Professional Paper*, 294-J, 365–399.
- Haude, R., & Thomas, E. (1989). Ein Oberdevon-/Unterkarbon-Profil im Velberter Sattel (nördliches Rheinisches Schiefergebirge) mit neuen Arten von (?) *Sostroñocrinus* (Echinodermata). *Bulletin de l’Société Belge de Géologie*, 98(3/4), 373–383.
- Henke, W. (1924). *Blatt Endorf. Erläuterungen zur Geologischen Karte von Preußen und benachbarten Bundesstaaten, Lieferung 236*. 44 pp. Berlin: Preußische Geologische Landesanstalt.
- Henningsen, D. (1972). Die Sandsteine in den Devon/Karbon-Grenzschichten des rechtsrheinischen Schiefergebirges. *Neues Jahrbuch für Geologie und Paläontologie, Monatshefte*, 1972(1), 1–15.
- Herbig, H.-G. (2016). Mississippian (Early Carboniferous) sequence stratigraphy of the Rhenish Kulm Basin, Germany. *Geologica Belgica*, 19(1/2), 81–110.
- Herbig, H.-K., Tragelehn, H., Ampler, M. W. (2001). *Höchstes Oberdevon und Mississippium im Niederbergischen Land zwischen Ratingen und Wuppertal (Velberter Sattel, Herzkämper Mulde) – Der Übergang vom Kohlenkalkschild in das Kulmbecken*. Unpublished Field Guide, Subkommission für Karbonstratigraphie in der Deutschen Stratigraphischen Kommission, 27. April 2001, (11 pp., 1 map) Cologne.
- Herbig, H.-G., Lobova, D., & Seekamp, V. (2014). Sea-level history during the birth of a Foreland Basin: the Famennian-Visean of “Velbert 4”, Westernmost Rhenish Massif, Germany. In R. Rocha, J. Pais, J. C. Kullberg, & S. Finney (Eds.) *STRATI 2013, first international congress on stratigraphy, at the cutting edge of stratigraphy* (pp. 397–402). Zürich: Springer.
- Herbig, H.-G., Salamon, M., Ampler, M. R. W., Buchholz, P., Korn, D., Lupold, F.-W., Menning, M., Nesbor, H.-D., Schneider, J. W., Schultka, S., Weller, H., Weyer, D., & Wrede, V. (2018). The Carboniferous in the stratigraphic table of Germany 2016. *Zeitschrift der Deutschen Gesellschaft für Geowissenschaften*, 168(4), 483–502.
- Herbig, H.-G., Korn, D., Ampler, M. R. W., Hartenfels, S., & Jäger, H. (2019). The Mississippian Kulm Basin of the Rhenish Mountains, western Germany – fauna, facies, and stratigraphy of a mixed carbonate-siliciclastic foreland basin. In H.-G. Herbig, M. Aretz, M. R. W. Ampler, & S. Hartenfels (Eds.) *19th International Congress on the Carboniferous and Permian, Cologne, July 29–August 2, 2019, Field Guides* (pp. 143–216). Kölner Forum für Geologie und Paläontologie, 24.
- Heuser, H., Krebs, W., Schäfer, W., Uffenorde, H., Stoppel, D. (1977). *Exkursionen in das nordöstliche Sauerland, Warstein-Hirschberg*, 1977. Unpublished field guide (27 pp.). Hannover.
- Higgs, K. T., & Streel, M. (1984). Spore stratigraphy at the Devonian-Carboniferous boundary in the northern “Rheinisches Schiefergebirge”, Germany. *Courier Forschungsinstitut Senckenberg*, 67, 157–179.
- Higgs, K. T., & Streel, M. (1994). Palynological age for the lower part of the Hangenberg Shales in Sauerland, Germany. *Annales de la Société Géologique de Belgique*, 116, 243–247.
- Higgs, K. T., Streel, M., Korn, D., & Paproth, E. (1993). Palynological data from the Devonian-Carboniferous boundary beds in the new Stockum trench II and the Hasselbachatal borehole, northern Rhenish Massif, Germany. *Annales de la Société Géologique de Belgique*, 115(2), 551–557.
- House, M. R. (1993). Earliest Carboniferous goniatite recovery after the Hangenberg Event. *Annales de la Société Géologique de Belgique*, 155(2), 559–579.
- Hu, K., Qi, Y., Qie, W., & Wang, Q. (2019). Carboniferous conodont zonation of China. *Newsletters on Stratigraphy*, 50 pp. <https://doi.org/10.1127/nos/2019/0498>.
- Ji, Q. (1985). Study on the phylogeny, taxonomy, zonation and biofacies of *Siphonodella* (Conodontata). *Bulletin of the Institute of Geology, Chinese Academy of Geological Sciences*, 1985(11), 51–75 + 3 pls (in Chinese with extended English summary).
- Ji, Q., Xiong, J.-F., & Wu, X.-H. (1985). Conodonts. In H.-F. Hou (Ed.) *Muhua Sections of Devonian-Carboniferous Boundary Beds* (pp. 99–145, 190–195, pls. 13–41). Beijing: Geological Publishing House.
- Ji, Q., Wang, Z.-J., Sheng, H.-B., Hou, J.-P., Feng, R.-L., Wie, J.-Y., Wang, S.-T., Wang, H.-D., Xiang, L.-W., & Fu, G.-M. (1989). *The Dapouchang Section. An excellent section for the Devonian-Carboniferous Boundary Stratotype in China*. 165 pp. + 43 pls. Beijing: Science Press.
- Kaiser, S. I. (2005). *Mass extinctions, climatic and oceanographic changes at the Devonian/Carboniferous boundary*. Ph. D. Thesis, Ruhr University Bochum, 156 pp.
- Kaiser, S. I. (2009). The Devonian/Carboniferous boundary stratotype section (La Serre, France) revisited. *Newsletters on Stratigraphy*, 43(2), 195–205.
- Kaiser, S. I., & Corradini, C. (2011). The early siphonodellids (Conodontata, Late Devonian-Early Carboniferous): overview and taxonomic state. *Neues Jahrbuch für Geologie und Paläontologie, Abhandlungen*, 261(1), 19–35.
- Kaiser, S. I., Steuber, T., Becker, R. T., & Joachimski, M. M. (2006). Geochemical evidence for major environmental change at the Devonian-Carboniferous boundary in the Carnic Alps and the Rhenish Massif. *Palaeogeography, Palaeoclimatology, Palaeoecology*, 240, 146–160.
- Kaiser, S. I., Becker, R. T., Spalletta, C., & Steuber, T. (2009). High-resolution conodont stratigraphy, biofacies, and extinctions around the Hangenberg Event in pelagic successions from Austria, Italy, and France. *Palaeontographica Americana*, 63, 97–139.
- Kaiser, S. I., Becker, R. T., Steuber, T., & Aboussalam, Z. S. (2011). Climate-controlled mass extinctions, facies, and sea-level changes around the Devonian-Carboniferous boundary in the eastern Anti-Atlas (SE Morocco). *Palaeogeography, Palaeoclimatology, Palaeoecology*, 310, 340–364.
- Kaiser, S. I., Aretz, M., & Becker, R. T. (2015). The global Hangenberg Crisis (Devonian-Carboniferous transition): review of a first-order mass extinction. In R. T. Becker, P. Königshof, & C. E. Brett (Eds.) *Devonian Climate, Sea Level and Evolutionary Events*. Geological Society, London, Special Publications, 423, 387–437.
- Kaiser, S. I., Kumpan, T., & Cigler, V. (2017). New unornamented siphonodellids (Conodontata) of the lower Tournaisian from the Rhenish Massif and Moravian Karst (Germany and Czech Republic).

- Neues Jahrbuch für Geologie und Paläontologie, Abhandlungen*, 286(1), 1–33.
- Kaiser, S. I., Kumpan, T., & Rasser, M. W. (2019). High-resolution conodont biostratigraphy in two key sections from the Carnic Alps (Grüne Schneid) and Graz Paleozoic (Trolp) – implications for the biozonation concept at the Devonian-Carboniferous boundary. *Newsletters on Stratigraphy*, 53, 26 pp. <https://doi.org/10.1127/nos/2019/0520>.
- Kasig, W., & Reissner, B. (2008). Aachen – Hohes Venn. *Schriftenreihe der Deutschen Gesellschaft für Geowissenschaften*, 52, 267–286.
- Kasig, W., Katsch, A., & Kollenberg, W. (1984). Geochemische Untersuchungen im Profil Stockum II (Grenze Devon/Karbon) im rechtsrheinischen Schiefergebirge (Sauerland/Deutschland). *Courier Forschungsinstitut Senckenberg*, 67, 143–155.
- Keupp, H., & Kompa, R. (1984). Mikrofazielle und sedimentologische Untersuchungen an Devon/Karbon Profilen am Nordrand des rechtsrheinischen Schiefergebirges. *Courier Forschungsinstitut Senckenberg*, 67, 139–142.
- Klapper, G. (1966). Upper Devonian and Lower Mississippian conodont zones in Montana, Wyoming, and South Dakota. *The University of Kansas Paleontological Contributions*, 3, 1–43.
- Klapper, G., & Ziegler, W. (1979). Devonian conodont biostratigraphy. *Special Papers in Palaeontology*, 23, 199–224.
- Klein, C., & Korn, D. (2016). Quantitative analysis of the late Famennian and early Tournaisian ammonoid stratigraphy. *Newsletters on Stratigraphy*, 49(1), 1–26.
- Klug, C., Frey, L., Korn, D., Jattiot, R., & Rücklin, M. (2016). The oldest Gondwanan cephalopod mandibles (Hangenberg Black Shale, Late Devonian) and the mid-Palaeozoic rise of jaws. *Palaeontology*, 59(5), 1–19.
- Koch, M., Leuteritz, K., & Ziegler, W. (1970). Alter, Fazies und Paläogeographie der Oberdevon/Unterkarbon-Schichtenfolge an der Seiler bei Iserlohn. *Fortschritte in der Geologie von Rheinland und Westfalen*, 17, 679–732.
- Koch, L., Gröning, E., & Brauckmann, C. (2003). Sutropcarididae n. fam. (Phyllocarida, Crustacea) from the Upper Devonian of the Sauerland (Rhenish Massif, Germany). *Neues Jahrbuch für Geologie und Paläontologie, Monatshefte*, 2003, 415–427.
- Koltonik, K., Pisarowska, A., Paszkowski, M., Slama, J., Becker, R. T., Szczera, M., Krawczynski, W., Hartenfels, S., & Marynowski, L. (2018). Baltic provenance of top-Famennian siliciclastic material of the northern Rhenish Massif, Rhenohercynian zone of the Variscan orogen. *International Journal of Earth Sciences*, 107, 2645–2669.
- Korn, D. (1981a). *Cymaclymenia* – eine besonders langlebige Clymenien-Gattung (Ammonoidea, Cephalopoda). *Neues Jahrbuch für Geologie und Paläontologie, Abhandlungen*, 161(2), 172–208.
- Korn, D. (1981b). Ein neues, Ammonoideen-führendes Profil an der Devon-Karbon-Grenze im Sauerland (Rhein. Schiefergebirge). *Neues Jahrbuch für Geologie und Paläontologie, Monatshefte*, 1981(9), 513–526.
- Korn, D. (1984). Die Goniatiten der Stockumer *Imitoceras*-Kalklinsen (Ammonoidea; Devon-Karbon-Grenze). *Courier Forschungsinstitut Senckenberg*, 67, 71–89.
- Korn, D. (1988a). Goniatites from the *Gattendorfia*-Stufe of Hoppecke (Lower Carboniferous, Northeastern Rhenish Massif). *Courier Forschungsinstitut Senckenberg*, 100, 217–218.
- Korn, D. (1988b). Oberdevonische Goniatiten mit dreieckigen Innenwindungen. *Neues Jahrbuch für Geologie und Paläontologie, Monatshefte*, 1988(10), 605–610.
- Korn, D. (1989). *Cymaclymenia* aus der Acutimitoceras-Fauna (prorsum-Zone) vom Müssemburg (Devon/Karbon-Grenze; Rheinisches Schiefergebirge). *Bulletin de la Société belge de Géologie*, 98(3/4), 371–372.
- Korn, D. (1991). Threedimensionally preserved clymeniids from the Hangenberg Black Shale of Dreher (Cephalopoda, Ammonoidea; Devonian-Carboniferous boundary; Rhenish Massif). *Neues Jahrbuch für Geologie und Paläontologie, Monatshefte*, 1991(9), 553–563.
- Korn, D. (1992a). Heterochrony in the evolution of Late Devonian Ammonoids. *Acta Palaeontologica Polonica*, 37(1), 21–36.
- Korn, D. (1992b). Ammonoideen aus dem Oberdevon und Unterkarbon von Aprath, Schurf Steinbergerbach und Straßeneinschnitt Kohleiche. In E. Thomas (Ed.) *Oberdevon und Unterkarbon von Aprath im Bergischen Land (Nördliches Rheinisches Schiefergebirge). Ein Symposium zum Neubau der Bundesstraße 224* (pp. 169–182). Cologne: Sven von Loga.
- Korn, D. (1993). The ammonoid faunal change near the Devonian-Carboniferous Boundary. *Annales de la Société Géologique de Belgique*, 115(2), 581–593.
- Korn, D. (1994). Devonische und karbonische Prionoceraten (Cephalopoda, Ammonoidea) aus dem Rheinischen Schiefergebirge. *Geologie und Paläontologie in Westfalen*, 30, 1–85.
- Korn, D. (2000). Morphospace occupation of ammonoids over the Devonian-Carboniferous boundary. *Paläontologische Zeitschrift*, 74(3), 247–257.
- Korn, D. (2002). *Faziesbereiche im Unterkarbon am Nordrand des Rheinischen Schiefergebirges. Exkursionsführer, Tagung der Subkommission für Karbon-Stratigraphie in der DUGW, Warstein, 26. – 28. April 2002* (26 pp.). Tübingen: Institut und Museum für Geologie und Paläontologie.
- Korn, D. (2004). The mid-Famennian ammonoid succession in the Rhenish Mountains: the “annulata Event” reconsidered. *Geological Quarterly*, 48(3), 245–252.
- Korn, D. (2006). Ammonoideen. *Schriftenreihe der Deutschen Gesellschaft für Geowissenschaften*, 41, 147–170.
- Korn, D. (2010). Lithostratigraphy and biostratigraphy of the Kulum succession in the Rhenish Mountains. *Zeitschrift der Deutschen Gesellschaft für Geowissenschaften*, 161(4), 431–453.
- Korn, D. (2017). The genus *Gonioclymenia* (Ammonoidea; Late Devonian) in Central Europe. *Neues Jahrbuch für Geologie und Paläontologie, Abhandlungen*, 284(3), 259–287.
- Korn, D., & Lippold, F. W. (1987). Nach Clymenien und Conodonten gegliederte Profile des oberen Famennium im Rheinischen Schiefergebirge. *Courier Forschungsinstitut Senckenberg*, 92, 199–223.
- Korn, D., & Price, J. D. (1987). Taxonomy and phylogeny of the Kosmoclymeniinae subfam. nov. (Cephalopoda, Ammonoidea, Clymeniida). *Courier Forschungsinstitut Senckenberg*, 92, 5–75.
- Korn, D., & Price, J. D. (2018). The genus *Sellacymenia* in Europe (Ammonoidea; Late Devonian). *Neues Jahrbuch für Geologie und Paläontologie, Abhandlungen*, 287(3), 227–233.
- Korn, D., & Price, J. D. (2019). Advanced gonioclymeniid ammonoids from Central Europe. *Neues Jahrbuch für Geologie und Paläontologie, Abhandlungen*, 294(2), 157–176.
- Korn, D., & Thomas, E. (1988). Ammonoids from the Devonian-Carboniferous Boundary of Aprath (Velbert Anticline, Northern Rhenish Massif). *Courier Forschungsinstitut Senckenberg*, 100, 219–220.
- Korn, D., & Vöhringer, E. (2004). Allometric growth and intraspecific variability in the basal Carboniferous ammonoid *Gattendorfia crassa* Schmidt, 1924. *Paläontologische Zeitschrift*, 78(2), 425–432.
- Korn, D., & Weyer, D. (2003). High resolution stratigraphy of the Devonian-Carboniferous transitional beds in the Rhenish Mountains. *Mitteilungen aus dem Museum für Naturkunde Berlin, Geowissenschaftliche Reihe*, 6, 79–124.
- Korn, D., Clausen, C.-D., & Lippold, F. W. (1994a). Die Devon/Karbon-Grenze im Rheinischen Schiefergebirge. *Geologie und Paläontologie in Westfalen*, 29, 1–221.
- Korn, D., Clausen, C.-D., Belka, Z., Leuteritz, K., Lippold, F. W., Feist, R., & Weyer, D. (1994b). Die Devon/Karbon-Grenze bei Dreher

- (Rheinisches Schiefergebirge). *Geologie und Paläontologie in Westfalen*, 29, 97–147.
- Korn, D., Piecha, M., & Wrede, V. (2010). The Hasselbachtal section – an auxiliary stratotype for the Devonian-Carboniferous Boundary. *Schriftenreihe der Deutschen Geologischen Gesellschaft*, 66, 66.
- Korn, D., Bartzsch, K., & Weyer, D. (2016). The last representatives of the late Famennian posttornoceratid ammonoids in Central Europe. *Neues Jahrbuch für Geologie und Paläontologie, Abhandlungen*, 281(2), 183–200.
- Korn, D., Price, J. D., & Weyer, D. (2018). The genus *Costaclymenia* in Europe Ammonoidea, Late Devonian. *Neues Jahrbuch für Geologie und Paläontologie, Abhandlungen*, 287(3), 249–260.
- Kramm, U., Lork, A., & Paproth, E. (1991). Datierung der Grenze Devon-Karbon. *Zentralblatt für Geologie und Paläontologie, Teil I*, 1991(5), 1336–1338.
- Kronberg, P., Pilger, A., Scherp, S., & Ziegler, W. (1960). Spuren alvariszischer Bewegungen im nordöstlichen Teil des Rheinischen Schiefergebirges. *Fortschritte in der Geologie von Rheinland und Westfalen*, 3(1), 1–46.
- Kühne, F. (1938). Erläuterungen zu Blatt Arnsberg-Süd, Nr. 2616 (neue Nr. 4614). In *Geologische Karte von Preußen und benachbarten deutschen Ländern, Lieferung 349* (52 pp.), Tabs. 3–10, 1 map. Berlin: Preußische Geologische Landesanstalt.
- Kumpan, T., Bábek, O., Kalvoda, J., Grygar, T. M., Frýda, J., Becker, R. T., & Hartenfels, S. (2015). Petrophysical and geochemical signature of the Hangenberg Events: an integrated stratigraphy of the Devonian-Carboniferous Boundary Interval in the Northern Rhenish Massif (Avalonia, Germany). *Bulletin of Geosciences*, 90(3), 667–694.
- Kürschner, W., Becker, R. T., Buhl, D., & Veizer, J. (1993). Strontium isotopes in conodonts: Devonian–Carboniferous transition, the northern Rhenish Slate Mountains, Germany. *Annales de la Société Géologique de Belgique*, 115, 595–621.
- Lange, W. (1929). Zur Kenntnis des Oberdevons am Enkeberg und bei Balve (Sauerland). *Abhandlungen der Preußischen Geologischen Landesanstalt, neue Folge*, 119, 1–132 + 3 pls.
- Leuschner, K. (1994). Trilobiten aus Devon/Karbon-Grenzbereich und aus der *Gattendorfia*-Stufe des Profiles NF/G von Drewer (Rheinisches Schiefergebirge). *Geologie und Paläontologie in Westfalen*, 29, 149–175.
- Liebus, A. (1932). Die Fauna des deutschen Unterkarbons. 3. Teil: Die Foraminiferen. *Abhandlungen der Preußischen Geologischen Landesanstalt, Neue Folge*, 141, 133–173 + pls. 9–10.
- Luppold, F. W., Hahn, G., & Korn, D. (1984). Trilobiten-, Ammonoideen- und Conodonten-Stratigraphie des Devon/Karbon-Grenzprofiles auf dem Müszenberg (Rheinisches Schiefergebirge). *Courier Forschungsinstitut Senckenberg*, 67, 91–121.
- Luppold, F. W., Clausen, C.-D., Korn, D., & Stoppel, D. (1994). Devon/Karbon-Grenzprofile im Bereich von Remscheid-Altenaer Sattel, Warsteiner Sattel, Briloner Sattel und Attendorn-Elsper Doppelmulde (Rheinisches Schiefergebirge). *Geologie und Paläontologie in Westfalen*, 29, 7–69.
- Matern, H. (1929). Die Ostracoden des Oberdevons. 1. Teil: Aparchitidae, Primitiidae, Zygobolbidae, Beyrichiidae, Kloedenellidae, Entomidae. *Abhandlungen der Preußischen Geologischen Landesanstalt, Neue Folge*, 118, 100 pp. + 5 pls.
- Michels, D. (1986). Ökologie und Fazies des jüngsten Ober-Devon von Velbert (Rheinisches Schiefergebirge). *Göttinger Arbeiten zur Geologie und Paläontologie*, 29, 1–86.
- Mottequin, B., & Poty, E. (2014). The uppermost Famennian Hangenberg Event in the Namur-Dinant Basin (southern Belgium). *Berichte des Institutes für Erdwissenschaften, Karl-Franzenz-Universität Graz*, 19, 36–37.
- Mottequin, B., Bartzsch, K., Simon, E., & Weyer, D. (2019). Brachiopod faunas from the basinal facies of southeastern Thuringia (Germany) before and after the Hangenberg Crisis (Devonian-Carboniferous boundary). *Palaeontologia Electronica*, 22(1, 16A), 1–54.
- Nekhoroshev, B. (1932). Die Fauna des deutschen Unterkarbons. 3. Teil: Die Bryozoen des deutschen Unterkarbons. *Abhandlungen der Preußischen Geologischen Landesanstalt, Neue Folge*, 141, 4–74 + pls. 1–5.
- Nowak, H. (2008). *Stratigraphie des höchsten Famenniums bei Hemer-Oese (Nordsauerland)*. Unpublished B.Sc. Thesis, WWU Münster, 26 pp.
- Paeckelmann, W. (1913). Das Oberdevon des Bergischen Landes. *Abhandlungen der Preußischen Geologischen Landesanstalt, neue Folge*, 70, 1–356 + 1 map, 6 pls.
- Paeckelmann, W. (1922a). Oberdevon und Untercarbon der Gegend von Barmen. *Jahrbuch der Preußischen Geologischen Landesanstalt*, 41, 52–147 (imprint 1921).
- Paeckelmann, W. (1922b). Bemerkungen zu O. H. Schindewolf's "Versuch einer Paläogeographie des Europäischen Oberdevonmeeres". *Zentralblatt für Mineralogie, Geologie und Paläontologie*, 1922, 578–587.
- Paeckelmann, W. (1923). Über das Oberdevon und Untercarbon des Südfügels der Herzkammer Mulde auf Blatt Elberfeld. *Jahrbuch der Preußischen Geologischen Landesanstalt*, 42, 257–306 pl. 2. (imprint 1922).
- Paeckelmann, W. (1924). Das Devon und Carbon der Umgebung von Balve i. Westf. *Jahrbuch der Preußischen Geologischen Landesanstalt*, 44, 51–97 pls. 4–5.
- Paeckelmann, W. (1928). *Blatt Elberfeld*, Nr. 2720. *Erläuterungen zur Geologischen Karte von Preußen und benachbarten deutschen Ländern, Lieferung 263*, 91 pp., 2 pl. Berlin: Preußische Geologische Landesanstalt.
- Paeckelmann, W., & Kühne, F. (1936, mit Beiträgen von P. Pfeffer). *Erläuterungen zu Blatt Alme*, Nr. 2585. Geologische Karte von Preußen und benachbarten Deutschen Ländern, 61 pp., 1 pl; Berlin: Preußische Geologische Landesanstalt.
- Paeckelmann, W., & Kühne, F. (1938). *Erläuterungen zu Blatt Balve*, Nr. 2655 (Neue Nr. 4613). Geologische Karte von Preußen und benachbarten Deutschen Ländern, Lieferung 349, 70 pp. + 8 tabs. Berlin: Preußische Geologische Landesanstalt.
- Paeckelmann, W., & Schindewolf, O. H. (1937). Die Devon-Karbon-Grenze. In W. J. Jongmans (Ed.) *Compte Rendu Deuxième Congrès pour l'Avancement des Etudes de Stratigraphie Carbonifère*, 1935 (Vol. 2, pp. 704–714). Heerlen.
- Paproth, E. (1986). An introduction to a field trip to the Late Devonian outcrops in the northern Rheinisches Schiefergebirge (Federal Republic of Germany). *Annales de la Société Géologique de Belgique*, 109, 275–284.
- Paproth, E., & Strel, M. (1970). Corrélations biostratigraphiques près de la limite Dévonien/Carbonifère entre les faciès littoraux ardennais et les faciès bathyaux rhénans. *Les Congrès et Colloques de l'Université de Liège*, 5, 365–398.
- Paproth, E., & Strel, M. (1982). Devonian – Carboniferous transitional beds of the northern "Rheinisches Schiefergebirge". *Guidebook, IUGS Working Group on the Devonian/Carboniferous Boundary*, 33 pp. Liège.
- Paproth, E., & Strel, M. Eds., (1984). The Devonian-Carboniferous Boundary. *Courier Forschungsinstitut Senckenberg*, 67, 1–258.
- Paproth, E., Stoppel, D., & Conil, R. (1976). Révision micro-paléontologique des sites dinantiens de Zippenhaus et de Cromford (Allemagne). *Bulletin de la Société belge de Géologie, de Paléontologie et d'Hydrologie*, 82(1), 51–139.
- Paproth, E., Dreesen, R., & Thorez, J. (1986a). Famennian paleogeography and event stratigraphy of northwestern Europe. *Annales de la Société Géologique de Belgique*, 109, 175–186.
- Paproth, E., Becker, R. T., Clausen, C.-D., Kompa, R., Korn, D., & Stoppel, D. (1986b). *Field Trip to the Late Devonian outcrops in the northern Rheinisches Schiefergebirge (Federal Republic of*

- Germany).* Guidebook, Aachen 1986, “Late Devonian Events around the Old Red Continent”, 12 pp., 4 tabs, 27 figs.; Aachen.
- Paul, H. (1937a). Die Transgression der Visé-Stufe am Nordrande des Rheinischen Schiefergebirges. *Abhandlungen der Preußischen Geologischen Landesanstalt, Neue Folge*, 179, 1–117 + 3 pls.
- Paul, H. (1937b). Vergleich des nordwestdeutschen Unterkarbon mit dem belgischen. In W. J. Jongmans (Ed.) *Compte Rendu Deuxième Congrès pour l’Avancement des Etudes de Stratigraphie Carbonifère 1935* (Vol. 2, pp. 745–764). Heerlen.
- Paul, H. (1938a). Das Unterkarbon der Gegend von Lintorf. *Decheniana*, 97A, 25–42.
- Paul, H. (1938b). Die *Dibunophyllum*-Zone des Bergischen Unterkarbons. *Neues Jahrbuch für Mineralogie, Geologie und Paläontologie, Beilage-Band*, 79, 187–242.
- Paul, H. (1939a). Zur Kenntnis der Viséstufe bei Ratingen. *Decheniana*, 98(2), 185–190.
- Paul, H. (1939b). Revision einiger Muscheln des Wocklumer und Dasberger-Kalkes (Oberdevon). *Jahrbuch der Preußischen Geologischen Landesanstalt*, 59(for 1938), 42–44.
- Poty, E., Hance, L., Lees, A., & Hennebert, M. (2002). Dinantian lithostratigraphic units (Belgium). *Geologica Belgica*, 4(1/2), 69–94.
- Price, J. D. (1982). *Some Famennian (Upper Devonian) ammonoids from north western Europe*. Unpublished Ph.D. Thesis, The University of Hull, 554 pp.
- Price, J. D., & Korn, D. (1989). Stratigraphically important Clymeniids (Ammonoidea) from the Famennian (Late Devonian) of the Rhenish Massif, West Germany. *Courier Forschungsinstitut Senckenberg*, 110, 257–294.
- Rabien, A. (1954). Zur Taxionomie und Chronologie der Oberdevonischen Ostracoden. *Abhandlungen des Hessischen Landesamtes für Bodenforschung*, 9, pp. 268 + 5 pls.
- Rabien, A. (1960). Zur Ostracoden-Stratigraphie an der Devon/Karbon-Grenze im Rheinischen Schiefergebirge. *Fortschritte in der Geologie von Rheinland und Westfalen*, 3(1), 61–106.
- Reissner, B. (1990). *Stratigraphische und faciale Untersuchungen im Mittel- und Oberdevon des Aachener Raumes, Nordeifel, Rheinisches Schiefergebirge*. – Unpublished Ph.D. Thesis, RWTH Aachen, 179 pp.
- Ribbert, K.-H. (1998). Devonische Schichtenfolgen im Untergrund der Niederrheinischen Bucht. *Fortschritte in der Geologie von Rheinland und Westfalen*, 37, 9–47.
- Ribbert, K.-H. (2008). Untergrund der Niederrheinische Bucht und des Velberter Sattels. *Schriftenreihe der Deutschen Gesellschaft für Geowissenschaften*, 52, 555–563.
- Rice, B., Grader, G. W., Doughty, P. T., di Pasquo, M. M., & Isaacson, P. (2017). Revision of the type *Siphonodella praesulcata* conodont locality at Lick Creek, Montana. *GSA Annual Meeting*, 2017, 22–25.
- Richter, R. (1948). *Einführung in die Zoologische Nomenklatur durch Erläuterung der Internationalen Regeln Regeln*, 2nd Edition, 252 pp. Frankfurt a.M.: Waldemar Kramer.
- Richter, E. (1992). *Zur Geologie an der Nord-West-Flanke des Velberter Sattels (nördliches Rheinisches Schiefergebirge)*. Unpublished Diplom Thesis, Phillips University Marburg, 65 pp. + 2 pls., 2 appendices.
- Richter, R., & Richter, E. (1926). Die Trilobiten des Oberdevons. Beiträge zur Kenntnis devonischer Trilobiten IV. *Abhandlungen der Preußischen Geologischen Landesanstalt, Neue Folge*, 99, 1–314 + 12 pls.
- Richter, R., & Richter, E. (1949). Die Trilobiten der Erdbach-Zone (Kulm) im Rheinischen Schiefergebirge und im Harz. 1. Die Gattung *Phillibole*. *Senckenbergiana*, 30(1/3), 63–94 pls. 1–5.
- Richter, R., & Richter, E. (1951). Der Beginn des Karbons im Wechsel der Trilobiten. *Senckenbergiana*, 32(1/4), 219–266.
- Sacher, M. (2016). *Conodonten-Stratigraphie, Karbonat-Mikrofazies und Schwarzschiefer-Events im Famennium von Oberrödinghausen (nördliches Rheinisches Schiefergebirge)*. Unpublished M.Sc. Thesis, WWU Münster, 107 pp.
- Sacher, M., Hartenfels, S., & Becker, R. T. (2016). Middle Famennian to Lower Tournaisian conodont stratigraphy at Oberrödinghausen (northern Rhenish Massif) – a progress report. In *87th Annual Conference of the Paläontologische Gesellschaft e. V., Dresden, September 11–15, 2016, “Fossils: Key to evolution, stratigraphy and palaeoenvironments”, Programme, abstracts, field trip guides*, 133. Dresden: Saxoprint.
- Sandberg, C. A., Ziegler, W., Leuteritz, K., & Brill, S. M. (1978). Phylogeny, speciation, and zonation of *Siphonodella* (Conodonts, Upper Devonian and Lower Carboniferous). *Newsletters on Stratigraphy*, 7(2), 102–120.
- Sandberger, G. (1853). Einige Beobachtungen über Clymenien, mit besonderer Berücksichtigung auf die westphälischen Arten. *Verhandlungen des naturhistorischen Vereins des Rheinlandes*, 10, 171–216.
- Sartenaer, P. (1997). *Novaplatirostrum*, late Famennian rhynchonellid brachiopod genus from Sauerland and Thuringia (Germany). *Bulletin de l’Institut royal des Sciences naturelles de Belgique, Sciences de la Terre*, 67, 25–37.
- Schäfer, W. (1976). Einige neue Conodonten aus dem höheren Oberdevon des Sauerlandes (Rheinisches Schiefergebirge). *Geologica et Palaeontologica*, 10, 141–152.
- Schindewolf, O. H. (1921). Versuch einer Paläogeographie des europäischen Oberdevonmeeres. *Zeitschrift der Deutschen Geologischen Gesellschaft*, 73, 137–223.
- Schindewolf, O. H. (1923a). Beiträge zur Kenntnis des Paläozoikums in Oberfranken, Ostthüringen und dem Sächsischen Vogtlande. 1. Stratigraphie und Ammonienfauna des Oberdevons von Hof a. Saale. *Neues Jahrbuch für Mineralogie, Geologie und Paläontologie, Beilage-Band*, 49, 250–357 393–509 + pls. 14–18.
- Schindewolf, O. H. (1923b). Über Fossley, Étroeung und verwandte Fragen. Eine Erwiederung an Herrn W. Paeckelmann. *Centralblatt für Mineralogie, (not.) Geologie und Paläontologie*, 1923, 214–221 246–254.
- Schindewolf, O. H. (1924). Bemerkungen zur Stratigraphie und Ammonienfauna des Saalfelder Oberdevons. *Senckenbergiana*, 6, 95–113.
- Schindewolf, O. H. (1926). Zur Kenntnis der Devon-Karbon-Grenze in Deutschland. *Zeitschrift der Deutschen Geologischen Gesellschaft*, 78, 88–133 + 1 tab.
- Schindewolf, O. H. (1937). Zur Stratigraphie und Paläontologie der Wocklumer Schichten. *Abhandlungen der Preußischen Geologischen Landesanstalt, Neue Folge*, 178, 132 + 4 pls.
- Schindewolf, O. H. (1952). Über das Oberdevon und Unterkarbon von Saalfeld in Ostthüringen. Eine Nachlese zur Stratigraphie und Ammonien-Fauna. *Senckenbergiana*, 32(5/6), 281–306.
- Schmidt, H. (1922). Das Oberdevon-Culm-Gebiet von Warstein i.W. und Belecke. *Jahrbuch der Preussischen Geologischen Landesanstalt*, 41, 254–339.
- Schmidt, H. (1924a). Zwei Cephalopodenfaunen an der Devon-Carbon-Grenze im Sauerland. *Jahrbuch der Preussischen Geologischen Landesanstalt*, 44, 98–170.
- Schmidt, W. E. (1924b). *Blatt Plettenberg. Erläuterungen zur Geologischen Karte von Preußen und benachbarten Bundesstaaten, Lieferung 236*, 63 pp. Berlin: Preußische Geologische Landesanstalt.
- Schmidt, H. (1925). Die carbonischen Goniatiten Deutschlands. *Jahrbuch der Preußischen Geologischen Landesanstalt*, 45(for 1924), 489–609 + pls. 19–26.
- Schmidt, H., & Pleßmann, W. (1961). *Sauerland. Sammlung Geologischer Führer* (Vol. 39, 151 pp.). Berlin: Bornträger.

- Schönlau, H.-P. (2018). Review of the Devonian/Carboniferous boundary in the Carnic Alps. *Jahrbuch der Geologischen Bundesanstalt*, 158(1/4), 29–47.
- Slotta, F., Korn, D., Klug, C., Kröger, B., & Keupp, H. (2011). Sublethal injuries in Late Devonian ammonoids (Cephalopoda) from Kattensiepen (Rhenish Mountains). *Neues Jahrbuch für Geologie und Paläontologie, Abhandlungen*, 261(3), 321–336.
- Söte, T., Harternfels, S., & Becker, R. T. (2017). Uppermost Famennian stratigraphy and facies development of the Reigern Quarry near Hachen (northern Rhenish Massif, Germany). *Palaeodiversity and Palaeoenvironments*, 97(3), 633–654.
- Spalletta, C., Perri, M. C., Over, D. J., & Corradini, C. (2017). Famennian (Upper Devonian) conodont zonation: revised global standard. *Bulletin of Geosciences*, 92(1), 31–57.
- Staschen, D. (1968). Zur Geologie des Warsteiner und Belecker Sattels (Rheinisches Schiefergebirge, Deutschland). *Münstersche Forschungen zur Geologie und Paläontologie*, 5, 1–119.
- Steenwinkel, M. van (1984). Sedimentology of the Devonian-Carboniferous boundary sediments in the Oberrödinghausen 1 bore-hole (Germany). *Courier Forschungsinstitut Senckenberg*, 67, 123–137.
- Steenwinkel, M. van (1993). The D/C boundary: comparison between the Dinant synclinorium and the northern border of the Rhenish Slate Mountains, a sequence stratigraphic view. *Annales de la Société Géologique de Belgique*, 115(2), 665–681.
- Stoppe, D. (1977). *Exkursionen in das nordöstliche Sauerland, Warstein-Hirschberg, 19.-21. Mai 1977*. Subkommission für Karbonstratigraphie in der D. U. G. W., 27 pp.; Hannover.
- Streel, M. (1966). Critères palynologiques pour une stratigraphie détaillée du Tn1a dans le bassins Ardenno-Rhénans. *Annales de la Société géologique de Belgique*, 89, B65-B96 + 2 pls.
- Streel, M. (1969). Corrélations palynologiques entre les sédiments de transition Dévonien/Dinantien dans les bassins Ardenno-Rhénans. *Compte Rendu 6è Congrès International de Stratigraphie et de Géologie Carbonifère, Sheffield 1967*, 1, 3–18.
- Streel, M., & Korn, D. (2016). Pleading for a new DCB in the historical German deep facies of Sauerland near Stockum. *SDS Newsletter*, 31, 45–46.
- Streel, M., Sevastopulo, G., & Paproth, E. (1993). Devonian-Carboniferous Boundary. *Annales de la Société Géologique de Belgique*, 115(2), 405–708.
- Struckmeier, W. (1974). *Der Horizont der „Liegenden Alaunschiefer“ (cu IIa) des Warsteiner und Belecker Sattels (Nördl. Rheinisches Schiefergebirge)*. Unpublished Diplom Thesis, University Braunschweig, 81 pp.
- Struve, W. (1989). *Rabienops evae* aus dem späten Ober-Devon des Rheinischen Schiefergebirges. *Bulletin de l'Association belge de Géologie*, 98(3/4), 335–342.
- Thomas, E. (Ed.). (1992). *Oberdevon und Unterkarbon von Aprath im Bergischen Land (Nördliches Rheinisches Schiefergebirge). Ein Symposium zum Neubau der Bundesstraße 224* (468 pp. + 12 pls.). Cologne: Sven von Loga.
- Thompson, T. L., & Fellows, L. D. (1970). Stratigraphy and conodont biostratigraphy of Kinderhookian and Osagean (lower Mississippian) rocks of southwestern Missouri and adjacent states. *Missouri Geological Survey and Water Resources, Report of Investigations*, 45, 1–263.
- Tragelehn, H. (2010). Short note on the origin of the conodont genus *Siphonodella* in the Uppermost Famennian. *SDS Newsletter*, 25, 41–43.
- Trapp, E., Kaufmann, B., Mezger, K., Korn, D., & Weyer, D. (2004). Numerical calibration of the Devonian-Carboniferous boundary: two new U-Pb isotope dilution-thermal ionization mass spectrometry single-zircon ages from Hasselbachtal (Sauerland, Germany). *Geology*, 32(10), 857–860.
- Voges, A. (1959). Conodonten aus dem Untercarbon I und II (*Gattendorfia-* und *Pericyclus*-Stufe) des Sauerlandes. *Paläontologische Zeitschrift*, 33(4), 266–314.
- Voges, A. (1960). Die Bedeutung der Conodonten für die Stratigraphie des Unterkarbons I und II (*Gattendorfia-* und *Pericyclus*-Stufe) im Sauerland. *Fortschritte in der Geologie von Rheinland und Westfalen*, 3(1), 197–228.
- Vöhringer, E. (1960). Die Goniatiten der unterkarbonischen *Gattendorfia*-Stufe im Hönnetal (Sauerland). *Fortschritte in der Geologie von Rheinland und Westfalen*, 3(1), 107–196.
- Walter, R. (2010). Aachen und südliche Umgebung, Nordeifel und Nordost-Ardennen. *Sammlung Geologischer Führer*, 100, 1–360.
- Walliser, O. H. (1984). Pleading for a natural D/C-Boundary. *Courier Forschungsinstitut Senckenberg*, 67, 241–246.
- Weber, H. (1934). Das Oberdevon der Attendorn-Elsper Doppelmulde. *Zeitschrift der deutschen geologischen Gesellschaft*, 86, 537–574 pl. 40.
- Wedekind, R. (1914). Monographie der Clymenien des Rheinischen Gebirges. *Abhandlungen der Königlichen Gesellschaft der Wissenschaften zu Göttingen, mathematisch-naturwissenschaftliche Klasse, Neue Folge*, 10(1), 1–73 + 7 pls.
- Wedekind, R. (1918). Die Genera der Palaeoammonoidea (Goniatiten). *Palaeontographica*, 62, 85–184 + pls. 14–22 (imprint 1917).
- Weyer, D. (1965a). Zur Ammonoideen-Fauna der *Gattendorfia*-Stufe von Dzikowiec (Ebersdorf) in Dolny Ślask (Niederschlesien), Polen. *Berichte der geologischen Gesellschaft in der DDR*, 10(4), 443–464.
- Weyer, D. (1965b). Etroeungt im Morvan (Zentralfrankreich). *Mitteilungen des Zentralen Geologischen Institutes*, 1, 289–302.
- Weyer, D. (1972). Zum Alter der Ammonoideen-Faunen des Marshall-Sandsteins (Unterkarbon, Michigan, USA). *Berichte der deutschen Gesellschaft für geologische Wissenschaften, Reihe A, Geologie, Paläontologie*, 17(3), 325–350.
- Weyer, D. (1977). Ammonoideen aus dem Untertournai von Schleiz (Osthüringisches Schiefergebirge). *Zeitschrift für Geologische Wissenschaften*, 5(2), 167–185.
- Weyer, D. (2000). Korallen im Unterkarbon Deutschlands. *Abhandlungen und Berichte für Naturkunde, Museum für Naturkunde Magdeburg*, 23, 57–91.
- Winkler-Prins, C. F., & Amler, M. R. W. (2006). Brachiopoden. *Schriftenreihe der Deutschen Gesellschaft für Geowissenschaften*, 41, 89–100.
- Winter, J. (1993). Identification of a bentonic ash layer by crystal morphology of its zircon population (Bed 79, Hasselbachtal, Rheinisches Schiefergebirge). *Annales de la Société Géologique de Belgique*, 115(2), 683–687.
- Zhang, M.-Q., Becker, R.T., Ma, X.-P., Zhang, Y., & Zong, P. (2019). Hangenberg Black Shale with cymaclymeniid ammonoids in the terminal Devonian of South China. In W. Qie, K. Liang, P. Königshof (Eds.) *Devonian palaeoecosystems and palaeoenvironments of South China. Palaeobiodiversity and Palaeoenvironments*, 99(1), 129–142.
- Zhuravlev, A. V., & Plotitsyn, A. N. (2018). Taxonomical reassignment of some siphonodellids (Conodonts, Early Carboniferous) from W. Hass's collection. *Newsletters on Carboniferous Stratigraphy*, 34, 31–34.
- Zhuravlev, A. V., Plotitsyn, A. N., Vevel, Y. A., & Erofeevskiy, A. V. (2018). Devonian-Carboniferous Boundary Beds in the Vorkuta Transverse Uplift (Bolshaya Us River). *Proceedings of Kazan University, Natural Sciences Series*, 160(3), 467–483. [in Russian with English abstract]
- Ziegler, W. (1962). Taxonomie und Phylogenie Oberdevonischer Conodonten und ihre stratigraphische Bedeutung. *Abhandlungen des hessischen Landesamtes für Bodenforschung*, 38, 1–166.
- Ziegler, W. (1969). Eine neue Conodontenfauna aus dem höchsten Oberdevon. *Fortschritte in der Geologie von Rheinland und Westfalen*, 17, 343–360.

- Ziegler, W. (1970). Erläuterungen zu Blatt 4713 Plettenberg (2. Auflage). In *Geologische Karte von Nordrhein-Westfalen 1: 25 000, 179 pp., pls. 1–3*. Krefeld: Geologisches Landesamt NRW.
- Ziegler, W. (1971). Post-Symposium Excursion, Sept. 15–18, 1971 to Rhenish Slate Mountains and Hartz Mountains. Symposium on Conodont Taxonomy. In *Marburg/Lahn, September 4 to 18, 1971, A Field Trip Guidebook*, 47 pp. Marburg.
- Ziegler, W., & Sandberg, C. A. (1984a). Important candidate sections for stratotype of conodont based Devonian-Carboniferous Boundary. *Courier Forschungsinstitut Senckenberg*, 67, 231–239.
- Ziegler, W., & Sandberg, C. A. (1984b). *Palmatolepis*-based revision of upper part of standard Late Devonian conodont zonation. *Geological Society of America, Special Paper*, 196, 179–194.
- Zimmerle, W., Gaida, K.-H., Gedenk, R., Koch, R., & Paproth, E. (1980). Sedimentological, mineralogical, and organic-geochemical analyses of Upper Devonian and Lower Carboniferous strata of Riescheid, Federal Republic of Germany. *Mededelingen Rijks Geologische Dienst*, 32(5), 34–43.

Publisher's note Springer Nature remains neutral with regard to jurisdictional claims in published maps and institutional affiliations.